uOttawa

L'Université canadienne
Canada's university

FACULTÉ DES ÉTUDES SUPÉRIEURES ET POSTOCTORALES

uOttawa

L'Université canadienne
Canada's university

FACULTY OF GRADUATE AND POSDOCTORAL STUDIES

Sara Jirari

AUTEUR DE LA THÈSE / AUTHOR OF THESIS

M.Sc. (Biology)

GRADE / DEGREE

Faculty of Science – Department of Biology

FACULTÉ, ÉCOLE, DÉPARTEMENT / FACULTY, SCHOOL, DEPARTMENT

Functional Analysis of the Nclear Membrane Protein MANI in Zebrafish Adults and Embryos

TITRE DE LA THÈSE / TITLE OF THESIS

Marc Ekker

DIRECTEUR (DIRECTRICE) DE LA THÈSE / THESIS SUPERVISOR

CO-DIRECTEUR (CO-DIRECTRICE) DE LA THÈSE / THESIS CO-SUPERVISOR

Kathleen Gilmour

Patrick Walsh

John Vierula

Gary W. Slater

Le Doyen de la Faculte des études superieures et postdoctorales / Dean of the Faculty of Graduate and Postdoctoral Studies

Functional Analysis of the Inner Nuclear Membrane Protein MAN1 in Zebrafish Adults and Embryos

Sara Jirari

Thesis submitted to the
Faculty of Graduate and Postdoctoral Studies
University of Ottawa
In partial fulfillment of the requirements for the
M.Sc. degree in the
Ottawa-Carleton Institute of Biology

Your file Votre référence
ISBN: 978-0-494-73765-1
Our file Notre référence
ISBN: 978-0-494-73765-1

TABLE OF CONTENTS

ACKNOWLEDGEMENTS

I would like to thank my supervisors Dr. Paulin-Levasseur and Dr. Ekker for their support and guidance throughout my whole project, for providing me with the tools to complete my work, for reading my thesis and for giving me valuable criticism. The completion of this thesis would not have been possible without them. My thanks also go to my committee members: Dr. Gilmour, Dr. Akimenko and Dr. Willmore for their interesting comments. I owe my deepest gratitude to Dr. Basso for his readiness to help and for mentoring and guiding me throughout all these years, as well as, correcting my work. Many thanks to my colleague Steve Levesque who has taken the time to alert me of technical errors and who has always offered valuable advice, to Jennifer Kasbary and Mathieu Duchiron for providing technical help, to Vishal Saxena for advice on zebrafish breeding and for explaining protocols and to Ihab for proof-reading my references. I also thank the rest of the Ekker lab for their help throughout the molecular part of my project. Moreover, my thanks go to Mustafa and Goran from the Perry lab for teaching me how to isolate RNA from zebrafish.

I would like to show my gratitude to my parents for helping me with my education, for being always willing to provide for me, for teaching me determination and for their love and support. I would like to thank my sisters, Meriem and Sonia, and my cousin, Mia, for their enthusiasm and their love. I would like to thank my boyfriend Shahrouz for his love and moral support and his inspiring advice. He has made available his support in a number of ways. I am heartily thankful to Dr. Moriarty for her understanding and her teachings. Last but not least, I would like to thank all people who knowingly or unknowingly helped me throughout my project.

RÉSUMÉ

La protéine ZMAN1 a été identifiée dans les tissus du poisson zèbre suivants : le cerveau, les branchies, le foie, le rein et le muscle. La microscopie immunofluorescente des cellules somatiques et embryonnaires a permis de visualiser la protéine ZMAN1 autour de l'enveloppe nucléaire. De plus, cette protéine a aussi été localisée dans le cytoplasme durant les phases de la mitose ce qui indiquerait que ZMAN1 ne s'associe pas aux chromosomes mitotiques. On retrouve cette protéine, au début du réassemblage nucléaire, à la surface de l'enveloppe nouvellement reconstituée. ZMAN1 a aussi été examinée durant la mitose des embryons, durant le stade embryonnaire de la blastula, où elle est présente principalement dans le cytoplasme sauf dans le cas de l'interphase, la télophase et la cytocinèse où elle a été localisée à la surface de l'enveloppe nucléaire. Cette protéine est synthétisée et transmise maternellement et apparait notamment dans la région de la queue des embryons pendant la mi-pharyngula. Par contre, l'expression de ZMAN1 est très faible dans le tissu musculaire ce qui suggère une sous-régulation de cette protéine dans le muscle des poissons zèbres adultes. Finalement, j'ai détecté des anomalies phénotypiques dans les morphants ZMAN1 qui révèlent une malformation des vaisseaux sanguins et de la cavité péricardique ainsi qu'une queue tordue. Ceci démontre que ZMAN1 pourrait jouer un rôle durant la morphogénèse du cœur et des vaisseaux sanguins. En conclusion, l'ensemble de mes données semblent indiquer une fonction importante de ZMAN1 durant les processus du développement embryonnaire du poisson zèbre ainsi que durant sa vie adulte.

ABSTRACT

ZMAN1 protein was identified in the brain, the gills, the liver, the kidney and the muscle tissue of the adult zebrafish. It is ubiquitously present in the brain and gill tissues. Using immunofluorescence on adult and embryonic cell lines, ZMAN1 was observed at the nuclear periphery. Moreover, cytoplasmic localization of ZMAN1 during mitotic phases indicates that ZMAN1 is not associated to mitotic chromosomes. ZMAN1 appeared at the surface of the new nuclear envelope at the beginning of nuclear reassembly. ZMAN1 distribution in blastula embryos was in the cytoplasm at different mitotic stages except for interphase, telophase and cytokinesis where it was targeted to the nuclear envelope. The maternally synthesized ZMAN1 was localized to the tail/posterior trunk of mid-pharyngula embryos and showed a very low expression and distribution patterns in the muscle tissue suggesting down-regulation of ZMAN1 at the adult stage. I also detected phenotypical abnormalities in ZMAN1 morphants, displayed a curved tail, dysfunctional tail vasculature and an enlarged pericadium, suggesting a possible function of ZMAN1 in blood vessels and heart morphogenesis. Altogether, my data suggest that ZMAN plays a role in early developmental processes and during the adult life of zebrafish.

LIST OF FIGURES

1- INTRODUCTION

1.1 The nuclear envelope and its major components

The nuclear envelope (NE) is the essential physical border that confers protection as well as architectural structure to the eukaryote nucleus. Surrounding major cellular components, the NE sets the boundary between the nucleoplasm and the cytoplasm (Vlcek *et al.,* 2001). Apart from the structural support that it provides, it is also involved in numerous key cellular processes such as gene expression, chromatin organization, cell division, and others (Somech *et al.*, 2005).

Exhibiting a unique structure that allows for dynamism and stability, the NE comprises three main compartments: the outer membrane (ONM), the inner nuclear membrane (INM) and the nuclear pore complexes (NPCs). Underlying the INM, the nuclear lamina is a mesh-like structure of nuclear proteins called the lamins, which display interaction sites with the INM and the chromatin. Though distinct in structure, the ONM is similar in composition and is continuous with the endoplasmic reticulum (ER). Moreover, it possesses a set of unique proteins and a series of ribosomes on its surface (Ishimura *et al.*, 2008).

1.1.1 The outer nuclear membrane

The ONM is involved in several cellular functions and one of its most essential roles is the proper localization of the nucleus inside the cell (Starr, 2007; Wilhelmsen *et al.*, 2005). Two main families of nuclear proteins are implicated in nuclear positioning: 1) - the KASH proteins, containing a KASH (Klarsicht, ANC-1, Syne homology) domain at

their C terminal region; and, 2) - the SUN proteins, which share a conserved SUN (Sad1, UNC-84 homology) segment (Starr, 2007). Recent findings have shown that KASH proteins are ONM proteins that bind from one side to the SUN proteins, which are INM proteins, and, from another side to cytoskeletal structures, such as microfilaments, intermediate filaments or microtubules (Kvam & Goldfarb, 2006). Thus SUN proteins maintain KASH proteins anchored in the ONM (Kvam & Goldfarb, 2006), while remaining in the INM due to their interactions with the lamins (Wu *et al.*, 2002). Indeed, the KASH proteins collaborate with INM proteins to interact with the NE and the cytoskeleton establishing a direct connection that is fundamental to nuclear positioning. Both the ONM and the INM share sites of interaction with another important domain; the nuclear pore (Caputo *et al.*, 2006).

1.1.2 The nuclear pore complex

The nuclear pore complex (NPC) is a large structure, perfectly symmetrical and of high molecular weight (~60 to 125 MDa in mammals), comprising a total of 50 different proteins called the nucleoporins (Nups) (Tzfira & Citovsky, 2005). The NPC plays a critical role in facilitating the transport of metabolites in and out of the nucleus. Smaller molecules, such as ions, can easily circulate from the nucleoplasm to the cytoplasm and vice versa. However, molecules with a molecular weight over 60 kDa must be bound to a carrier protein to be transported through the NPC (D'Angelo & Hetzer, 2008). Despite its fundamental cellular functions, the NPC is composed only of several repeated nucleoporins and, therefore, does not exhibit a much diversified structure (D'Angelo & Hetzer, 2008). Consequently, while many Nups seem to only have a structural role, others possess phenylalanine glycine (FG) enriched domains and are

Figure 1.1: General networking of the nuclear envelope. The nuclear pore complex, the outer nuclear membrane and inner nuclear membrane are shown within the nuclear envelope. The cytoskeleton components including actin, intermediate filaments, microtubules, SUN proteins (yellow) and KASH proteins (purple) are depicted in the red rectangle.

NPC: nuclear pore complex, ER: endoplasmic reticulum, ONM: outer nuclear membrane, INM: inner nuclear membrane. Orange: nuclear lamina; green: integral proteins of the INM; brown: integral proteins of the ONM and the ER.

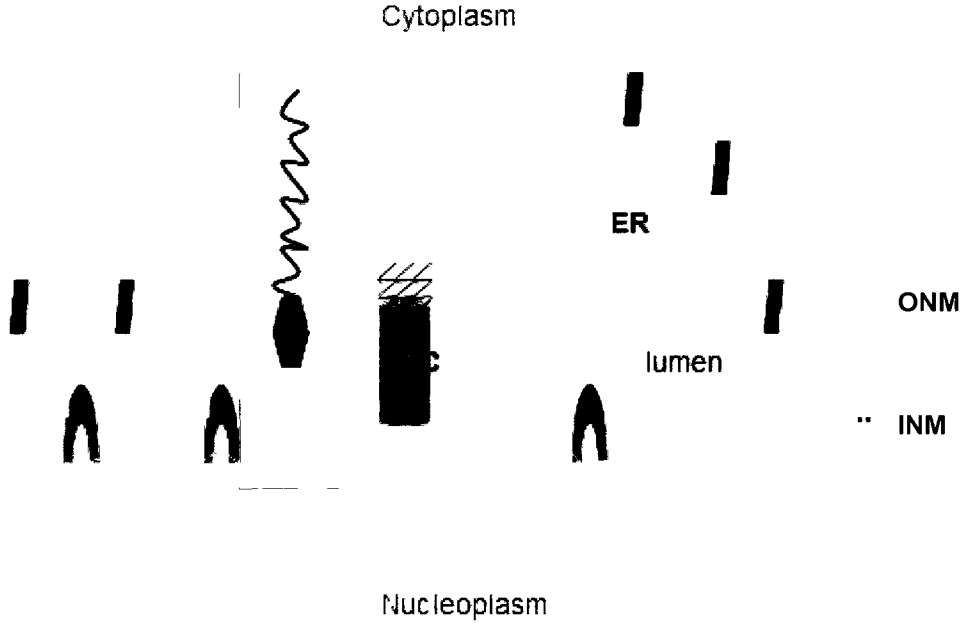
Cytoplasm
ER
ONM
lumen
INM
Nucleoplasm

crucial for translocation mechanisms (Salina *et al.*, 2001). Another important component of the NE that binds with fundamental cellular structures, such as the NPC and the INM, is the nuclear lamina (Salina *et al.*, 2001).

1.1.3 The nuclear lamina

The nuclear lamina is a framework of nuclear filamentous proteins called the lamins. These filamentous lamins are the major components of the nuclear lamina and are shaped into a meshwork like structure underlining the INM on its nucleoplasmic surface. Lamins are type V intermediate filament proteins and show a structure very similar to keratins, neurofilaments and other cytoplasmic intermediate filaments (Somech *et al.*, 2005). They share a conserved α-helical rod domain with cytoplasmic intermediate filaments though the amino-terminal domain and the carboxyl-terminal end vary among all intermediate filaments (Ostlund & Worman, 2003). Another characteristic unique to lamins is their C-terminal tail, which exhibits a nuclear localization signal (NLS) that has not been detected in other cytoplasmic intermediate filaments (Ostlund & Worman, 2003).

Typically, there are two main classes of lamins: A-type and B-type lamins, which differ from each other in terms of their biochemical attributes and cellular functions (Somech *et al.,* 2005). The LMNA gene encodes the A-type lamin transcripts from which two splicing variants derive, lamin A and lamin C. In contrast, B-type lamins do not originate from a single gene. In fact, the LMNB1 gene encodes for lamin B1 whereas the LMNB2 gene is responsible for lamin B2 (Worman & Courvalin, 2000).

One of the primary functions of the nuclear lamina is the mechanical support that it provides to the NE, therefore controlling nuclear shaping and architecture. Bridging the INM and the chromatin, the nuclear lamina is a playground for the numerous interactions

between these two structures ranging from gene regulation and chromatin organization to nuclear envelope assembly/disassembly (Cohen *et al.*, 2007).

Moreover, the nuclear lamina and its binding partners have been linked to human inherited bone and skin diseases such as muscular dystrophy and premature aging, further emphasizing the critical functions of the lamina within the cell (Cohen *et al.*, 2007). The nuclear lamina displays close interactions between the lamins and their binding partners: the integral proteins of the INM (Somech *et al.*, 2005).

1.1.4 The inner nuclear membrane

The INM faces the nucleoplasm and is the inner compartment of the NE. Despite the fact that they connect at the NPC, the INM and the ONM have distinct structures and do not share the same integral proteins (Tsuchiya, 2008). The discovery of an impressive diversity of integral proteins in the INM has made it the most investigated nuclear membrane (Ishimura *et al.*, 2008).

Although quite different from each other, these integral proteins share common characteristics such as their transmembrane domains and their nucleoplasmic segment (Ishimura *et al.*, 2008). Radioisotope labelling allowed identification of the first integral protein of the INM, which binds exclusively to the B-type lamins, specifically lamin B (Holmer & Worman, 2001). Purification and sequencing of the lamin B receptor (LBR) revealed that its N-terminal head is the main binding site for chromatin proteins and lamin B. Many other integral proteins have been identified since then, such as emerin, otefin and lamin associated proteins (LAPs) and there is evidence that a total of eighty integral proteins reside in the INM (Ishimura *et al.*, 2008).

An issue that the discovery of these INM integral proteins has brought up is the way that these proteins are synthesized and transported to the INM. Current theories agree that the synthesis is carried out in the endoplasmic reticulum (ER). The newly synthesized proteins diffuse freely from the ER along the ONM passing via the NPC site to reach the INM (Worman, 2005). The passage through the NPC requires a maximum molecular mass of 60 kDa and major size restriction applies if this mass is exceeded (Worman & Courvalin, 2000). Once the proteins reach the INM, retention occurs as a consequence of the associations of their nucleoplasmic domain with chromatin and other nuclear components, or/and interactions between their transmembrane segments (Worman, 2005). Once these integral proteins reach the targeted INM site, they do not seem to slip back to the ER and thus remain anchored at their specified location (Salina *et al.*, 2001).

1.1.5 The LEM domain

Analysis of several integral proteins of the INM has discerned that some of them share a small molecular segment of approximately 40 amino acids at their amino-terminal tail. It is a helix-loop-helix motif that faces the nucleoplasm (Worman, 2005). This domain was localized in the integral inner nuclear protein **M**AN1 and it has also been found in other integral proteins such as lamina associated polypeptide 2 (**L**AP2) and **E**merin, thus the acronym "**LEM** domain" (Gruenbaum *et al.*, 2005). However, the LEM domain was also identified in proteins from other species, such as Otefin and Bocksbeutel in *Drosophila melanogaster* and LEM3 in *Caenorhabditis elegans* (Brachner *et al.*, 2005).

The LEM proteins share common binding partners suggesting that they might have overlapping roles. It was demonstrated that all LEM proteins interact either directly or

indirectly with the chromatin and the nuclear lamins (Hirano *et al.*, 2009) Moreover, the LEM domain binds to a small protein called barrier-to-autointegration factor (BAF), which in turn, associates with DNA (Ostlund & Worman, 2003) So far, BAF and LEM proteins have only been identified in multicellular organisms; they seem to be absent from yeast and plants (Mansharamani & Wilson, 2005). The roles of BAF within the cell remain uncertain However, recent studies showed the importance of the LEM proteins-BAF interactions in the reassembly of the NE during mitosis (Tokuko *et al.*, 2001).

LEM proteins are involved in key cellular mechanisms such as chromatin organisation, DNA replication and mitosis and it would be interesting to review some of the known functions of the main LEM proteins. LAP2, emerin and MAN1.

1.1.6 LAP2

The lamina-associated polypeptide 2 (LAP2) was first identified as a binding partner of chromatin and lamin B1 and was extracted from rat somatic cells using a monoclonal antibody (Foisner & Gerace, 1993) Though both LAP2 and LAP1 display an affinity for the nuclear lamina, their protein sequences are very different (Worman & Courvalin, 2000). The LAP2 gene produces several splice variants through RNA alternative splicing and a specific set of isoforms has been identified in each species examined. In mammals, the LAP2 protein is represented by six isoforms α, β, δ, ε, γ, ζ. (Prüfert *et al.*, 2004). Apart from LAP2 α and LAP2 ζ, all LAP2 isoforms are integral proteins of the INM (Wagner & Krohne, 2007). Typically, the LAP2 protein amino-terminal head possess a LEM domain and another closely related segment called the LEM-like domain, which can directly bind DNA without the intervention of BAF (Cai *et al* , 2001) The carboxylic tail is responsible for the localization of LAP2 in the INM and

comprises a putative transmembrane domain and a lamin/lamina binding region (Prufert *et al*, 2004)

LAP2α is a unique isoform characterized by its distinctive carboxylic end, which lacks a transmembrane domain but instead possesses an additional nuclear/chromatin binding region (Schoft *et al*, 2003) As a result of its missing transmembrane segment, LAP2α cannot anchor in the INM and is observed dispersed throughout the nucleus (Georgatos *et al*, 2001) Several theories suggested that the α-isoform is a mammalian innovation (Prufert *et al*, 2004)

LAP2β is another isoform that caught the interest of the research community and is one of the most studied LAP2 variants LAP2β has a crucial function in DNA replication by interacting with HA95, a nuclear protein (Martin *et al*, 2003) In addition, LAP2β seems to be involved in transcription repression via its close association with the germ-cell-less (GCL), as well as in chromatin organisation by binding to the A-type and B-type lamins (Prufert *et al*, 2004)

1.1.7 Emerin

Emerin is another inner nuclear protein made by the EMD gene and it is also a member of the LEM family The importance of emerin comes from the fact that its mutant form is the direct cause of the Emery-Dreifuss muscular dystrophy (EDMD) (Mansharamani & Wilson, 2005) EDMD disease is an inherited X-linked recessive trait, which exhibits various degrees of severity and ultimately results in the breakdown of the muscle cell integrity (Fairley *et al*, 2002) Emerin is present in most tissues tested so far (Wagner & Krohne, 2007) and though essential for humans, it is not an essential protein for cell survival (Bengtsson & Wilson, 2004) Just like any other LEM protein, emerin

interacts with the nuclear lamina and has a special affinity with lamin A (Lee *et al*, 2001). It also binds the transcriptional repressor GCL and therefore appears to occupy overlapping functions with LAP2β. Moreover, GCL competes with BAF to bind the amino terminal domain of emerin (Holaska *et al.,* 2003). Surprisingly, emerin is able to associate with the nuclear actin thus suggesting a role in nuclear organization and shaping (Vlcek *et al.*, 2001). Interestingly, this protein is also able to interact *in vitro* with another LEM protein, MAN1 (Mansharamani & Wilson, 2005).

1.1.8 MAN1

MAN1, also known as LEM-domain containing protein 3 (LEMD3), is an integral protein that was isolated from the serum containing polypeptides recognized by the autoantibodies of a patient suffering from collagenosis (Paulin-Levasseur *et al.*, 1996). MAN1 displays many key binding sites with the nuclear lamina, the chromatin and other nuclear proteins, which confirms its influence on gene transcription; on early development as well as on later tissue functions (Bengtsson, 2007). My project focuses on understanding the functions of MAN1 and its expression patterns. Therefore, a general overview of publications involving MAN1 is necessary to understand its important functions at the cellular and at the physiological levels.

Figure 1.2: Cellular interactions of the LEM proteins within the nuclear envelope. Some LEM proteins (LAP2 and MAN1) interact directly with DNA and others form indirect associations with chromatin (emerin and MAN1).

NPC: nuclear pore complex, ER: endoplasmic reticulum, ONM: outer nuclear membrane, INM: inner nuclear membrane, C: carboxyl-terminal, N: amino terminal.

Orange filament: nuclear lamina; blue filament: chromatin; brown: integral proteins of the ONM and the ER; red rectangle: LEM domain; pink oval: BAF protein.

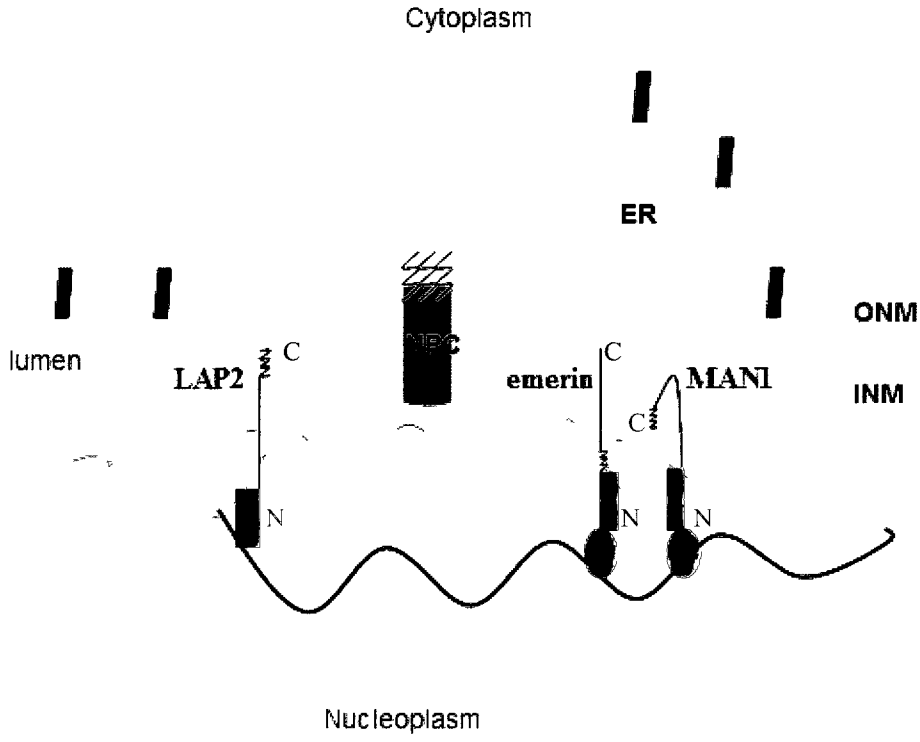
Cytoplasm
ER
ONM
lumen
LAP2
C
NPC
emerin
C
MAN1
INM
C
N
N
N
Nucleoplasm

1.2. The structure and functions of MAN1

1.2.1 MAN1 structure and binding partners

"MAN polypeptides" were first detected as auto-antigens in the serum of a patient suffering from a collagen vascular disease (Paulin-levasseur *et al.,* 1996). One of them was identified as the LAP2 antigen and had a mass of approximately 60 kDa (Lang *et al.*, 1999). Characterization and isolation of the actual MAN1 antigen from the serum was performed in later screening experiments of expression libraries (Lin *et al.*, 2000). With a molecular mass close to 100 kDa, MAN1 possesses two transmembrane domains embedded in the INM, an amino terminal head of 476 amino acids (a.a.), and a nucleoplasmic C-terminal region of 252 a.a (Wu *et al.*, 2002). Both the N-terminal and the C-terminal domains are nucleoplasmic and serve as anchors for the numerous interactions between MAN1 and other proteins. The gene coding for MAN1 is localized on the human chromosome 12q14 (Lin *et al.*, 2000). Moreover, sequence analysis of MAN1 transcript in human cell lines estimated its molecular mass to 97 kDa.

Exhibiting a great affinity with other nuclear proteins, the amino-terminal head is an essential domain. This site displays key interaction sites for emerin, lamin A and lamin B1 (Mansharamani & Wilson, 2005). The LEM domain is located in the first 50 amino-acid of MAN1 and is necessary for MAN1-BAF interactions (Mansharamani & Wilson, 2005). Several suggestions have arisen from the interactions between emerin and MAN1, such as an overlapping function between the two proteins, or even a regulatory role of MAN1 towards emerin (Bengtsson, 2007). The targeting of MAN1 to the INM is largely attributed to the close interactions between its N-terminal domain and the nuclear lamina (Wu et al., 2002). However, its carboxylic end does not play any role in its

Figure 1.3: Schematic representation of the nuclear localization of the MAN1 protein. MAN1 spans the inner nuclear membrane twice and has its carboxylic (C-term) and amino (N-term) ends facing the nucleoplasm. The main domains of MAN1 are the LEM (LAP2-Emerin-MAN1) domain, the winged-helix (WH), the U2AF homology domain (UHM) and the RNA-recognition motif (RRM). The binding partners of MAN1 are also depicted including barrier auto-integration factor (BAF), germ cell-less (GCL), BCL2-associated transcription factor (Btf) and the MH2domain of Smads binding at the carboxylic end and BAF, lamin A/B1 and emerin at the amino-terminal.

INM: inner nuclear membrane; T1, T2: transmembrane domains 1 and 2.

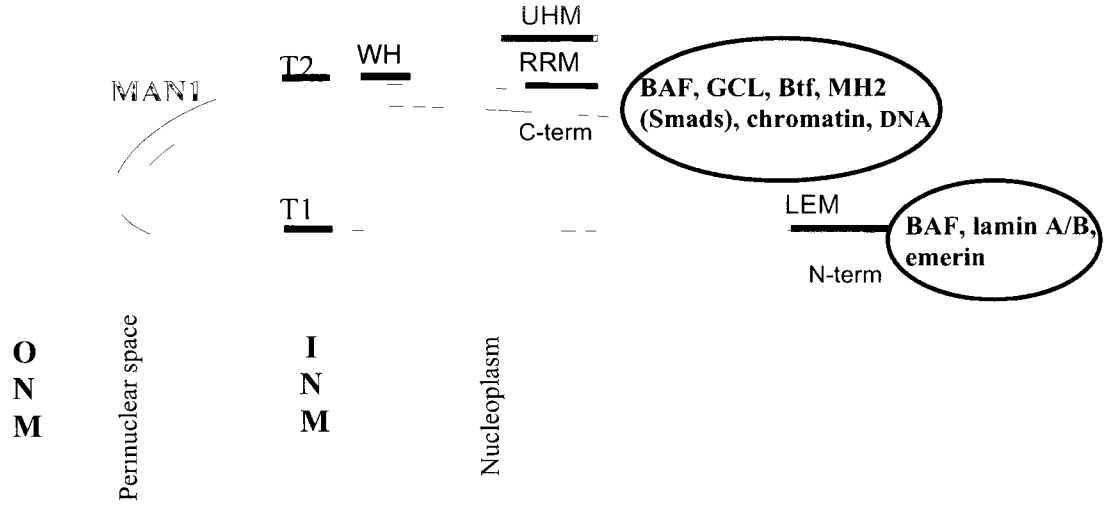
UHM
RRM
T2
WH
MAN1
BAF, GCL, Btf, MH2
(Smads), chromatin, DNA
C-term
T1
LEM
BAF, lamin A/B,
emerin
N-term
O
N
M
Perinuclear space
I
N
M
Nucleoplasm

targeting given that it does not localize to the nucleus (Osada *et al*, 2003) This C-terminal tail is a binding site for GCL and Btf (Bcl-2-associated transcription factor), two proteins involved in transcription regulation (Mansharamani & Wilson, 2005) Surprisingly, the carboxylic terminal region of MAN1 is a binding site for BAF and has shown higher affinity for this latter protein than the LEM region itself Further sequence analysis of MAN1 brought into light the structure of the carboxylic end It comprises a RRM (RNA-recognition motif) segment within a U2 auxilliary factor homology motif (UHM), and a MAN1-Src1p C-terminal domain (MSC), which forms a winged-helix (WH) DNA-binding domain (Caputo *et al*, 2006) The RRM region of MAN1 is the interaction site for the MH2 region of Smads, mediator proteins in the cytokine signalling pathway, which happens as a protein-protein bond (Bengtsson, 2007)

As with other INM proteins, the process governing the synthesis and the targeting of MAN1 to the INM follows the "diffusion-retention" model (Wu *et al*, 2002) MAN1 is first synthesized within the ER and is allowed to laterally diffuse to reach the nuclear pore membrane MAN1 is then translocated through the NPC and its diffusion rate slows down in the INM (Wu *et al*, 2002) Once it reaches its appropriate location within the nuclear envelope it will be retained through its interactions with the nuclear lamina and chromatin and will remain at a specific location in the INM (Wu *et al*, 2002)

1.2.2 MAN1 in the TGFβ signalling pathway

In order to understand the involvement of MAN1 as a key regulatory protein of the transforming growth factor-β (TGF- β) super family signalling, it is necessary to provide a brief overview of the TGF-β proteins and their interacting partners within the cell The TGF-β superfamily is constituted of two main classes of ligands assembled as the TGF-β

/ activin on one side, and the bone morphogenic proteins (BMPs) / growth differentiation factor (GDF) on the other side (Xiao & Zhang, 2008). BMPs were originally isolated as proteins that induce bone and cartilage formation *in vivo* (Wozney *et al.*, 1988).

When a TGF-β ligand binds to a TGF-β type II receptor, it phosphorylates and activates the type I receptor kinase, which then phosphorylates the downstream Smad proteins (Pan *et al.,* 2005). The Smad proteins are critical mediators of the TGF-β superfamily signalling. There are three classes of Smad proteins; the receptor-regulated R-Smads (Smad1, 2 3, 5, and 8), the co-Smad (Smad4) and the inhibitory I-Smads (Smad6 and 7) (Xiao & Zhang, 2008). The R-Smads are selected differently depending on the ligand. Indeed, Smad2 and Smad3 respond to the signalling by TGF-β and activins; Smad1, Smad5 and Smad8 respond to BMPs and GDFs. Once the R-Smad is phosphorylated, it couples with the co-Smad, Smad4, and translocates into the nucleus to interact with transcription factors (Pan *et al.*, 2005). The TGF-β ligands are implicated in many cellular processes including cardiac hypertrophy, collagen synthesis, and apoptosis (Xiao & Zhang, 2008).

In the past few years, several studies have linked MAN1 to antagonizing effects on the TGF-β signalling pathway. Interestingly, the TGFβ/BMP pathway was found to be regulated by the MAN1 protein. Besides, several studies elucidated the influence of MAN1 on this cascade and demonstrated the major players involved are also binding partners of this protein. Experiments in human cell lines demonstrated that MAN1 is able to interact with all the R-Smads; Smad1, 2, 3, and 5, but does not associate with the co-Smad (Smad4) (Lin *et al.*, 2005; Pan *et al.,* 2005). Furthermore, this binding is mediated by the RRM region localized to the carboxylic end of MAN1 and occurs at the MH2 site

of the Smad protein (Lin *et al.*, 2003; Pan *et al.,* 2005; Caputo *et al.* 2006). Soon after, overexpression experiments of MAN1 in mammalian cells confirmed the suspected inhibitory effect of MAN1on the BMP/TGFβ pathway (Pan *et al.*, 2005; Lin *et al.* 2005). Somewhere along the signalling cascade, the R-Smad/co-Smad complex interacts with MAN1 at the nuclear border and, as a result, is sequestered and dissolved. Hence, the BMP/TGFβ signalling pathway is blocked at this step, and the Smad modulator never reaches the targeted gene (Pan *et al.*, 2005).

The acknowledged influence of the BMP/TGF-β pathway on a multitude of cellular events as well as the evidence of its inhibition by MAN1 have brought up questions, yet unanswered, as to what other functions are occupied by this protein. In the past few years, several studies have tried to identify ortholog proteins of MAN1 in other species, considering this to be a key to the better understanding of its functions.

1.2.3 MAN1 in developmental and clinical studies

1.2.3.1 *Xenopus laevis*

The earliest experiments that recognized the implications of MAN1 and its fundamental functions in embryogenesis were conducted in *Xenopus*. The *Xenopus* ortholog of MAN1 was isolated by two independent research teams. Raju *et al.* (2003) characterized the *Xenopus* MAN1 ortholog and named it Smad1 Antagonistic Effector (SANE). Subsequent analysis of SANE demonstrated its ability to bind Smad1 and its blocking effects on the BMP signalling pathway. The same protein was also characterized by Osada *et al.* (2003) and called XMAN1. Subsequent comparison of XMAN1 mRNA with the SANE sequence confirmed their exact match (Bengtsson,

2007). XMAN1 associates with Smad1 (Raju *et al.,* 2003; Osada *et al.*, 2003) and this interaction, mediated by its carboxylic tail (Osada *et al.*, 2003), will consequently inhibits the downstream expression of BMP gene targets (Raju *et al.*, 2003; Osada *et al.*, 2003).

As discussed above, MAN1 is a strong antagonist of the BMP pathway; and consequently it is an inhibitor of the BMP downstream target genes. MAN1 acts as a neuralization factor of the ectoderm by preventing gene expression of BMP targets, namely Msx1 (an epidermal inductor) and Xhox3 (regulator of the anterior/posterior cellular fate). In addition, the over-expression of XMAN1 in the ventral mesoderm induces a secondary axis and the expression of dorsal markers. In *Xenopus* embryos, XMAN1/SANE directs dorsal-ventral axis determination by associating with Smad1 or Smad5, consequently antagonizing BMP signalling.

1.2.3.2 *Caenorhabditis elegans* and *Drosophila melanogaster*

The emerin and MAN1 orthologs in *C. Elegans* were named Ce-emerin and Ce-MAN1, respectively (Liu *et al.*, 2003). Ce-MAN1 was detected ubiquitously during development and it seems to be an essential protein for viability (Liu *et al.*, 2003).

A study involving *Drosophila melanogaster* conducted by Pinto *et al.* (2008) showed the importance of MAN1 in the early development of the fly tissues. The generation of mutant flies lacking DMAN1, the ortholog of MAN1 characterized in *Drosophila,* has permitted a thorough study of fly embryogenesis. This study also showed that the loss of DMAN1 had a negative impact on viability compared to the wild-type. Furthermore, Pinto *et al.* (2008) observed that a large number flies died during the metamorphosis process going from the pupal to the adult stage. Moreover, mutant flies displayed several phenotypic defects including wing-patterning abnormalities,

locomotion problems, and sterility amongst males with a reduced fertility amongst female (Pinto *et al.,* 2005).

1.2.3.3 *Mus musculus*

Two recently published papers studied the MAN1 protein in mice models and characterized several tissue defects associated with the loss of MAN1 in mutant mice. Analysis of wild-type mice tissues showed a ubiquitously expressed MAN1 protein with a predominant presence in the brain, testes and placenta. The MAN1 homozygous mutants were developmentally delayed and showed an enlarged pericardium, and, they did not survive after stage E10.5 (Ishimura *et al.*, 2006; Cohen *et al.*, 2007). Moreover, the loss of MAN1 caused vasculogenesis and angiogenesis defects due to the failure to develop large blood vessels, which results from improper recruitment of smooth muscle cells and of endothelial cells to the vascular wall (Ishimura *et al.*, 2006; Cohen *et al.*, 2007). Finally, these two groups demonstrated that the TGF-ß1 signalling pathway, a critical down-regulator of endothelial cells and smooth muscle cells, is upregulated and that the Smad proteins are abnormally elevated in the cellular nucleus of the mutant mice (Ishimura *et al.*, 2006; Cohen *et al.*, 2007). The two teams concluded that the death of mutant mice at midgestation is a product of a highly disorganized vascular system leading to the defective formation of the yolk sac (Ishimura *et al.*, 2006; Cohen *et al.*, 2007). Ishimura *et al.* (2008) observed abnormal shaping of the heart in mutant mice, and several types of looping defects. Besides, this research group elucidated a novel role of MAN1 in the early formation of the left-right axis. Indeed, due to the lack of Smad-interacting domain in the MAN1 mutant mice, the essential regulator genes of left-right axis formation -such as Nodal, Lefty1, and Lefty2 - are abnormally expressed.

These studies collectively imply the importance of MAN1 during mice vasculogenesis, and during the formation of the heart.

1.2.4 MAN1 in human diseases

In addition to the essential roles played by MAN1, the discovery of a connection between MAN1 and several inherited human diseases has piqued the interest of the scientific community. Previous experiments had demonstrated that mutated forms of certain integral proteins were causing genetic illnesses; for example, absence of emerin was connected to the X-linked Emery–Dreifuss muscular dystrophy (EDMD) myopathy (Bione *et al.*, 1994); and, mutations in the LMNA, which encodes for the A-type lamins, were linked to limb-girdle muscular dystrophy and dilated cardiomyopathy (Somech *et al.*, 2005). Hellemans *et al.* (2004) demonstrated that a mutation in the MAN1 gene induces an increase in bone density, which in turn provokes severe bone dysfunctions such as osteopoikilosis, Buschke-Ollendorff syndrome and melorheostosis. These autosomal dominant diseases are the result of a heterozygous loss-of-function of MAN1. Osteopoikilosis is an inherited autosomal dominant disease characterized by sclerotic lesions in different areas of the skeleton. Buschke–Ollendorff syndrome is a rare autosomal dominant disorder related to osteopoikilosis that affects the skin and the bone. Melorheostosis patients display a thickening of the bone cortex in addition to skin lesions and other soft tissue abnormalities. These disorders are degenerative and painful and induce long term physical limitations (Lin *et al.*, 2005).

1.3. *Danio rerio* in developmental studies

1.3.1 Zebrafish, a model organism

Danio rerio, commonly called zebrafish, is a tropical freshwater fish inhabiting the Ganges River in East India and Burma (Sprague *et al.*, 2006). It has become a popular tool amongst the research community for understanding signalling pathways in developmental, physiological and behavioural studies (Sprague *et al.*, 2003). The zebrafish was introduced as an inexpensive way to detect early developmental problems occurring in vertebrates, to understand the cellular pathways involved in many diseases. The zebrafish possesses several interesting characteristics, making them an ideal candidate for developmental studies. Firstly, *D. rerio* is a vertebrate; therefore, it is easier to relate the processes occurring in this fish to human cellular pathways. Moreover this fish is small in size, thus easy to hold, breed and manipulate. Breeding is facilitated by sexual maturity around the age of three months and a healthy female can lay up to 200 eggs per week (Nusslein-Volhard & Dahm, 2002). The embryo is also transparent, a unique feature that has been widely used to monitor developmental changes induced by molecular techniques. Finally, the strong resemblance discovered between a zebrafish embryonic heart and a three-week old human heart (Dooley & Zon, 2000) has made *D. rerio* an important model for human heart diseases research (Stainier, 2001).

Over the past decade, establishing *D. rerio* as a reliable model organism was an important step forward in developmental, molecular and cellular biology. Since then, an expanding number of methods and genetics approaches have been developed to provide the research community with strong molecular tools. These include microinjection

techniques, the generation of transgenic fish, cell lineage tracing experiments and tissue transplantation among others (Dooley & Zon, 2000)

1.3.2 The early development of zebrafish

1.3.2.1 The zygote

When the egg is fertilized, the zygotic period is the first stage post-fertilization of the embryo and lasts until the first cellular division (Kimmel *et al* , 1995) Following egg fertilization, the animal-vegetal axis of the newly formed embryo becomes visible At the one-cell stage, the embryonic yolk is an integral part of the transparent membrane surrounding the embryo, the chorion, and cannot be distinguished from this envelope Nevertheless, just a few minutes after fertilization, the formation of the blastodisc takes place (Jesuthasan & Strahle, 1996) This phenomenon is triggered by separation and migration of the cytoplasm towards the animal pole while the yolk remains at the vegetal pole (Nusslein-Volhard & Dahm, 2002) At the time the zygote undergoes its first mitotic cellular division, a series of events is activated and sets the scene for the next developmental period, cleavage (Nusslein-Volhard & Dahm, 2002)

1.3.2.2 Cleavage

Cleavage is the second developmental stage that follows the zygotic period It is characterized by a high rate of cellular division, from which the word cleavage originates, and lasts approximately 2 and a half hour The importance of this stage is accentuated by the accelerated and synchronized cellular divisions (Nusslein-Volhard & Dahm, 2002) The rapidly dividing mitotic cells, also known as blastomeres, exhibit an incomplete cleavage during which the cells remain attached and connected to each other through

their cytoplasmic junctions (Kimmel *et al.,* 1995). Typically, cleavage starts at the 2-cell stage (30 minutes) and lasts until the 64-cell stage (2hpf) (Kimmel *et al.,* 1995).

1.3.2.3 The blastula

If the cleavage stage was defined by regular synchronous cell divisions, the blastula, however, begins at the 128-cell stage during which the first irregular cleavage emerges. It is important to mention that, although the beginning of this stage is characterized by irregular and undefined cleavage planes, the cellular divisions remain synchronous (Kimmel *et al.*, 1995).

In itself, the blastula period is divided into three continuous key stages: the mid-blastula transition (MBT), the yolk syncytial layer (YSL) and epiboly. Around the 512-cell stage, the cell cycles slowly lengthen and divisions become less and less synchronous resulting in distinctive mitotic phases. It is also around this time of development that the first cellular motility is observed, defining the beginning of the MBT phase (Kimmel *et al.,* 1995). Concomitantly, the fragile marginal blastomeres of the blastoderm collapse and spill their contents into the yolk cell. Blastomeric spill induces the breaking of connection channels initially linking the marginal blastomeres and the yolk. This phenomenon triggers formation of the YSL (Yojiro *et al.*, 1998). A distinctive embryonic shape is characteristic of the late blastula and is a consequence of three delimited cellular layers: the enveloping layer of the blastoderm, the deep layer cells (DEL) of the blastoderm and the yolk cell (Kane *et al.*, 1992).

At the end of the blastula period, the three cellular domains mentioned above become thinner and thinner and the blastoderm that was once displayed a three-layered structure takes on a cup-shaped appearance and spreads to cover the yolk (Wilson *et al.*,

1995). Expansion of the blastoderm towards the animal pole takes place marking the onset of epiboly. This migration of the blastoderm is also a literal definition of the epiboly stage; in fact, at 30% epiboly, the expanding blastoderm covers 30% of the distance from the vegetal to the animal pole. Epiboly represents more than the migration of the blastoderm towards the animal pole. This event is also the trigger for the following developmental phase: the gastrula (Solnica-Krezel & Driever, 1994).

1.3.2.4 The gastrula

An hour after the onset of epiboly, the embryo enters a new stage, the gastrula period, which is responsible for major changes observed in the blastoderm. The gastrulation events occur from approximately 5 ¼ hour-post-fertilization (hpf) to 10 hpf. Concomitantly with gastrulation, cell involution occurs and triggers the thickening of a uniform band at the margin of the blastoderm termed the germ-ring. On the other hand, cells involved under the margin, move towards the animal pole and induce the rearrangement of the blastoderm into two germ layers; an outer epiblast and an inner hypoblast. At this point of embryogenesis, the previously formed germ-ring plays an important role within which cells converge to one side and accumulate to produce the embryonic shield (Warga & Kimmel, 1990). As gastrulation progresses, cells of the epiblast align themselves with the hypoblast layer and converge dorsally. Consequently, at 70% epiboly, the ventral side of the blastoderm typically becomes thinner than its dorsal side (Kimmel *et al.,* 1995). Soon afterwards, cell movements expand and the shield lengthens along the anterior-posterior (AP) axis of the embryo. The dorsal-ventral (DV) axis can be easily observed at this stage (Jesuthasan & Strähle, 1996). The neural plate emerges from the thickening of the dorsal epiblast. At 100% epiboly, the bud stage

begins with the blastoderm covering the entire yolk. Extension movements and dorsal convergence give rise to a bulge at the vegetal pole of the embryonic axis, the tailbud. Meanwhile, the neural plate at the animal pole thickens and forms a distinct swelling, the polster (Kimmel *et al.,* 1995).

Thickening of the neural plate triggers the onset of the segmentation period, which starts at approximately the 2-somite stage and continues to 24hpf (Schmitz & Campos-Ortega, 1994). At the end of the gastrula period, a rudimental zebrafish body can be observed. The epiblast germ layer is the precursor for the ectoderm (i.e. the central nervous system and the epidermis) while the hypoblast give rise to endodermal and mesodermal structures (Warga & Nüsslein-Volhard, 1999).

1.4. Objectives

When I first initiated my project, the expression of MAN1 in *D. rerio* during developmental processes had not yet been reported. Two groups Raju *et al.* (2003) and Osada *et al.* (2003) had almost concomitantly published data on a homologous protein of MAN1 found in *Xenopus.* Interestingly, these two studies were not only the first ones to analyze the *in vivo* functions of MAN1 in a vertebrate species, but also the only ones to directly implicate this protein in the early development of the frog. Since there was so little information on the expression of MAN1 during development, my project was intended to complement *Xenopus* findings and, therefore, further characterize MAN1 in the development of vertebrates. Previous results collected from studies published on the roles of MAN1 at the developmental level and in the BMP/TGFß pathway were utilized as a basis for my objectives. As a model organism, *D. rerio* offers unique features and

seemed to be a perfect candidate to facilitate my analyses. I was aiming to functionally characterize the MAN1 protein in zebrafish in order to further investigate developmental processes in this vertebrate. I had several molecular and cellular tools at my disposal and I was able to define several aspects of MAN1 expression to be examined. Therefore, my objectives for this project can be summarized into three headings:

- The quantification of MAN1 protein and RNA expression levels at different stages of development, in cultured cells and in different adult tissues;
- The localization of the MAN1 protein and its transcripts in the adult tissues and in zebrafish embryos at different stages;
- The knock-down of the MAN1 protein in early embryogenesis using morpholino oligos (MO) to observe the subsequent changes at the morphological and molecular levels.

Relying on molecular and cellular techniques such as immunofluorescence staining, microinjection, RT-PCR, Western immunoblotting and others, I proceeded with the functional analysis of the inner nuclear membrane protein MAN1 in zebrafish adults and embryos.

2. MATERIALS AND METHODS

To characterize MAN1 in zebrafish, it was necessary to determine the expression levels of this protein and its transcripts in several embryonic stages and in tissues originating from three different germ layers formed during zebrafish embryogenesis These expression patterns were verified by Western immunoblotting to resolve protein expression, along with reverse transcriptase (RT)-PCR experiments to determine RNA expression Moreover, the MAN1 protein was also localized in embryonic and adult cell lines as well as in tissues and in embryos by indirect immunofluorescence microscopy Finally, in order to elucidate the possible roles played by MAN1 in zebrafish, morpholino oligonucleotides (MO) were microinjected during early embryogenesis to knockdown the MAN1 protein This microinjection strategy was further utilized to visualize the subsequent knockdown effects on vasculogenesis in the transgenic fli fish line A thorough description of the techniques and methodology used during this study is exposed below

2.1. Cell culture

Two zebrafish cell lines, AB9 and ZF4, were used to visualize ZMAN1 protein distribution during the cell cycle AB9 and ZF4 cell lines were provided by Dr Ekker (University of Ottawa, Ontario) ZF4 is a somatic embryonic cell line, while AB9 is a somatic cell line isolated from the caudal fin of one-day-old embryos AB9 cells were cultured in Dulbecco's Modified Eagle Medium (DMEM, Gibco BRL, Burlington, Ontario) and supplemented with 15% fetal bovine serum (FBS, Gibco BRL) and antibiotics (50 µg/mL streptomycin, Gibco BRL) ZF4 were also cultured in Dulbecco's

Modified Eagle Medium (DMEM; Gibco BRL, Burlington, Ontario) mixed with nutrient F-12 (DMEM/F12) which contains 15 mM N-[2-hydroxyethyl] piperazine-N1-[2-ehanesulfonic acid] (HEPES) buffer, L-glutamine and pyridoxine hydrochloride. ZF4 cells were also treated with 15% fetal bovine serum (FBS; Gibco BRL) and antibiotics (50 µg/mL streptomycin; Gibco BRL).

The cell lines were cultured and grown in a humid chamber held at 27.5°C in 5% CO2 atmosphere.

2.2. Antibodies

In order to carry out indirect immunofluorescence and Western immunoblotting, several primary and secondary antisera were selected to assess ZMAN1 protein distribution and expression patterns in the cells, tissues and embryos. The primary antibodies utilized were the guinea-pig polyclonal ZMAN1 serum 1, which was raised by Dr. Paulin-Levasseur and other colleagues (Germany, 2006) against a peptide of the homologous zebrafish MAN1 protein (ZMAN1). ZMAN1 serum 1 was used at a concentration of 1:2000 for the immunoblots and of 1:1000 for immunofluorescence stainings. The other primary serum in immunoblotting experiments is a monoclonal mouse anti-GAPDH at a dilution of 1:40000 (Sigma, Oakville, ON, Canada). Moreover, anti-tubulin (DM1A, Sigma Aldrich, St Louis, MO, USA) was used to detect tubulin in immunostaining assays at a concentration of 1:2000. Also used for immunofluorescence, the MAN antiserum (Paulin-Levasseur et al., 1996) was used at a dilution of 1:5000 and the polyclonal ZLAP2 serum 1, generated in guinea-pig to react specifically to zebrafish LAP2 isoforms, at a dilution of 1:500.

The following horseradish peroxidase-coupled secondary antisera were used for blotting: donkey anti-guinea pig IgG (Jackson Immunoresearch, West Grove, Pa.) at a dilution of 1:10000, goat anti-mouse IgG (AMersham Canada) diluted to 1:2000. Secondary sera used for immunostaining: donkey anti-mouse conjugated to indocarbocyanine (CY3) (Jackson ImmunoResearch) diluted to 1:2000, donkey anti-guinea pig coupled with CY3 (Jackson ImmunoResearch) at a concentration of 1:2000, goat anti-human IgG conjugated with CY3 (Jackson ImmunoResearch) at a dilution of 1:1000, and goat anti-guinea pig IgG conjugated with Alexa Fluor 488 (Molecular Probes, Invitrogen).

2.3. SDS-PAGE and Western immunoblotting

Protein expression profiles were investigated in four different embryonic stages and in adult tissues, as well as in morpholino injected embryos. These protein patterns are useful to determine in which embryonic stages and tissues ZMAN1 is expressed, and to assess the knockdown of this protein, in the case of morpholino injections. After scrapping cells from their Petri dishes using a rubber policeman, I collected them in centrifuge tubes. Centrifugation for 5 min at 15000 rpm (revolutions per minute) followed and the cell pellets were washed in Tris acetate-EGTA pH 7.5 [10mM Tris-acetate, 150 mM NaCl, and 1mM ethylene glycol tetraacetic acid (EGTA)]. Protein extraction was carried out by diluting the pellets with an SDS (Sodium dodecyl sulphate- polyacrylamide) sample buffer (SB) 2X to obtain a final concentration of $2.0x10^6$cells/ml. 12 µl was then loaded on a polyacrylamide SDS-PAGE gel [5% Acrylamide (Bio Rad) stacking, 12% Acrylamide (Bio Rad) resolving].

Brain, gill, muscle, liver and kidney tissues were collected from 10 adult zebrafish and were placed in sterile centrifuge tubes, and were flash-frozen in liquid nitrogen. Using a mortar and pestle, previously kept in liquid nitrogen, the tissues were separately crushed in liquid nitrogen and approximately 100 mg of each tissue were transferred to sterile plastic screw-cap centrifuge tubes containing 1 ml of Trizol reagent (Gibco-BRL). Homogenization of the tissues in Trizol was followed by the addition of 200 µl of chloroform for phase separation. The tissues were then centrifuged at 12000 rpm for 15 min at 4°C. The solution separates in two phases. The clear upper phase contains RNA and was kept at -80°C for further RNA isolation, while the lower organic phase was used for protein extraction. Solutions were then homogenized in acetone to precipitate the proteins and sedimented by centrifugation for 10 min at 12000rpm at 4°C. Supernatants were discarded and pellets were washed, incubated and centrifuged three times in a solution of 0.3 M guanidine hydrochloride in 95% ethanol and 2.5% glycerol at 10000rpm. The pellets were finally washed in 75% ethanol containing 2.5% glycerol. The extracted proteins were then allowed to dry for 10 min at room temperature and they were solubilised in 200 µl of 1% SDS and heated at 50°C.

Zebrafish embryos were collected at specific developmental stages. Fish were directly homogenized in SB2X at a concentration of 10 embryos/40 µl and 10 µl was loaded on the SDS polyacrylamide gel for embryos at the gastrula stage or younger, and 5 µl for older embryos.

Profiles of cells, tissues and embryos were analyzed by Coomassie Blue staining or were electrophoretically transferred to nitrocellulose membranes (Whatman – GE

Healthcare, Baie d'Urfe, Québec) to visualize protein expression by Western immunoblotting.

Transfer onto nitrocellulose membranes was carried out at 40V overnight at 4°C. Proteins were visualized the next morning in a solution of Ponceau red (0.2% Ponceau red in 3% trichloroacetic acid) for 8 min. Subsequently, membranes were washed with phosphate-buffered saline 1X (PBS 1X; 130mM NaCl, 5mM Na_2HPO_4, 1.5mM KH_2PO_4) solution and incubated in milk diluted in PBS-Tween 20 (PBST) at a concentration of 1:200 for one hour. They were then incubated for two hours with the appropriate primary antibody (see section 2.2) diluted in 0.5% milk/PBS. The membranes were rinsed afterwards in PBST (3X10 min each wash) and exposed to secondary antibodies (see section 2.2) for detection of antigen-antibody complexes. Three 10 min washes with PBS T and two 10 min washes with PBS1X followed incubation. The blots were developed using the enhanced chemiluminescence (ECL) kit (Amersham, Canada) and reactivity was visualized on Hyperfilm ECL (Amersham, Canada). The resulting signals were quantified using the program Image J.

2.4. Indirect immunofluorescence staining

To observe ZMAN1 protein distribution in cells, embryos and tissues indirect immunofluorescence staining was carried out using different protocols for each system. Zebrafish AB9 and ZF4 cells were transferred onto sterile coverslips and allowed to recover and multiply for approximately 22 hours. Cells were then fixed in a solution of 3% paraformaldehyde (PFA) (MERCK KGaA, Darmstadt, Germany) for 5 min, and were then exposed to sodium borohydride/PBS (1mg/ml in PBS 1X) three consecutive times for 4 min. Cell permabilization was carried out in a solution of 0.2% Triton X-100/PBS

for 20 min Next, the cells were rinsed in PBS1X (3X4 min) and exposed to the primary antibodies (see section 2 2) for 1 hour at room temperature Cells were washed again with PBS 1X prior to incubation with the secondary antisera for another hour Cells were then counterstained with a DNA dye, Hoechst 33258 (diluted 1µg/mL in PBS from a stock of 1mg/mL, Sigma Aldrich) in order to visualize the chromatin, and were mounted on microscope slides using 10µL of mounting medium (MM, P-Phenylenediamine 1% in ddH_2O) per slide Slides were stored at 4°C for one or two days prior to observation, which was carried out on a Zeiss Axiophot equipped for epifluorescence illumination

Zebrafish embryos were collected at specific stages of development, deposited in 4 well slides, and fixed in a solution of 4% PFA (MERCK KGaA, Germany) for 10 min to stop intrinsic enzymes from digesting the sample and to prevent external bacterial contamination Three consecutive washes for 10 min each followed to eliminate aldehyde residues Embryos were then dehydrated with 100% ice-cold ethanol for 10 min at -20°C Dechorionation of each embryo was then performed manually using forceps and exposure to 3% bovine serum albumin (BSA), fraction V (MERCK KGaA) for 30 min BSA is used to block non-specific binding of the antibody sera Embryos were then incubated in primary antibodies (see section 2 2) for the night The next morning, embryos were washed with PBS1X (2X10 min) and exposed to the appropriate secondary antibodies Washes follow incubations (PBS, 3X10 min each wash) and slides were mounted with 10µL of mounting medium (MM, P-Phenylenediamine 1% in ddH_2O) per slide and observed using a Zeiss Axiophot equipped for epifluorescence illumination

Brain, gill and muscle tissues were collected from two adult zebrafish and were directly fixed in fresh ice-cold 4% PFA (paraformaldehyde) They were then cryo-

protected with sucrose solutions and thinly sliced using a Cryostat slicer (see section 2 5) The tissues were then either stored at -20°C or immunostained Slides are taken out of the freezer 20 min prior to staining to allow them to be at room temperature Tissue slides were then washed in PBS1X (2X10 min each) and blocked using 3%BSA for 2 hours The slides were then incubated with the appropriate primary antisera (see section 2 2) for 2 hours and with the secondary antibodies to detect the proteins tested for 1 hour, and this was performed in a humidity chamber Slides were washed three consecutive times for 15 min each time with 3%BSA between antibody incubations Finally, slides were rinsed in PBS1X and mounted with 20µl of mounting media

2.5. Cryostat Slicing

Brain, gill and muscle tissues were collected from adult zebrafish and were directly fixed in fresh ice cold 4% PFA in 0 1M phosphate buffer (PB), pH 7 4, and they were then left for the night in the fridge at 4°C To cryo-protect the tissues, 15% sucrose (in PBS1X) solution was added and tissues were kept at 4°C for 2 hours and this was followed by an additional 2-hour-incubation period in 30% sucrose at 4°C Slides were embedded in OCT (Tissue-Tek) frozen on liquid N2, and cut on a cryostat (Leica (Nussloch, Germany) CM3050 S) as 20 µm sections at -20°C and mounted on Superfrost slides

2.6. RNA isolation and RT-PCR

Expression patterns of ZMAN1 RNA were also verified in three tissues originating from the three embryonic germ layers Brain (ectoderm origin), gill (endoderm origin) and muscle (mesoderm origin) tissues were collected from 20-25 adult zebrafish, were placed carefully in sterile centrifuge tubes, and were flash-frozen in liquid nitrogen Using a mortar and pestle, previously kept in liquid nitrogen, the tissues were separately crushed

in liquid nitrogen and approximately 100mg of each tissue were transferred to sterile plastic screw-cap centrifuge tubes containing 1ml of Trizol reagent (Gibco-BRL). Homogenization of the tissues in Trizol was followed by the addition of 200 µl of chloroform for phase separation. The tissues were then centrifuged at 12000 rpm for 15 min at 4°C. The solution separates into two phases and the clear upper phase contains RNA. The RNA phase was transferred into a fresh sterile centrifuge tube and precipitation of RNA was accomplished with isopropanol followed by centrifugation for 10 min at 12000 rpm at 4°C. The supernatant was discarded and the remaining RNA was washed with 75% ethanol and centrifuged again for 5 min at 8000 rpm at 4°C. Finally, the pellets were allowed to dry for few minutes and were then diluted in nuclease-free water. RNA was then quantified using a NanoDrop (model ND-1000, NanoDrop, Wilmington, DE). 2 µg of RNA were used for cDNA synthesis and total RNA was treated with DNase I Amplification Grade (Invitrogen), to eliminate any DNA residues, before reverse transcription.

First strand cDNA synthesis was performed in a 20 µl reaction mixture at 42°C for 1 hour. Reverse transcription (RT) reagents used for cDNA synthesis were: 1 µL (50 units/µL) of Stratascript reverse transcriptase (StrataScript RT, Stratagene), 2 µL of 10x Stratascript RT buffer, 3 µL of random primers (0.1µg/nl), 2 µL of dNTP (10 mM stock; Invitrogen), and 11 µL of DNase- and RNase-free water.

The PCR reaction mixture (25µl) consisted of 2µl cDNA, 20 pmol each of 5′ and 3′ primers, 0.16 mM dNTP, 5µl PCR reaction buffer (10XPCR buffer: 100mM TrisHCl, pH 8.3, 500mM KCl, 15mM $MgCl_2$) and 1 µl of Taq polymerase diluted in 8µl of DNAse and RNAse free water. The PCR cycle consisted of 30 cycles at 95°C for 30s, 60°C for

30s, and 72°C for 1 min for each cycle, with a final step at 72°C for 5 min at the end of the reaction.

The forward primer for elongation factor 1-α (EF1-α) was ordered from Invitrogen and its sequence was: 5'CTCTTGGTCGCTTTGCTGT3'; and, the reverse sequence for the control gene EF1- α was: 5'TTTGGAACGGTGTGATTGAG3'. These primers were tested before by the Ekker lab (University of Ottawa, Ontario). The forward sequence of ZMAN1 was: 5'CTATCAACAACAACGGCAGCG3' and its reverse sequence was: 5'GCTTCCGCTAAACTCGCTAGG3'. I designed these ZMAN1 primers and checked their specificity using NCBI. After performing RT-PCR, the identity of the resulting products amplified by these ZMAN1 and EF1- α primers were verified by sequencing.

2.7. Antisense morpholinos

Microinjecting morpholino oligonucleotides in zebrafish embryos allowed me to determine which structures and organs are affected by ZMAN1 loss by observing the phenotypes engendered by the knockdown. Morpholino antisense oligonucleotides were designed and manufactured by Gene Tools (Philomath, OR). The ZMAN1 morpholino 1 (MO1) was designed to target the ZMAN1 mRNA sequence (NCBI, NM_001044864.1) at the initiation codon. MO1 sequence was 5'GCAGACGCCATCTTTGCACGAAAAA 3'. This morpholino overlaps the start codon (see Fig.3.14 in Results section) and acts as a translational blocker. Another morpholino was also designed later on to confirm results, ZMAN1 morpholino 2 (MO2) (Gene Tools) and was targeted to the 5' untranslated region (UTR) at approximately 50 bp upstream of the start methionine (see Fig.3.14): 5'-AAAGTAAGCGGACAGACGGCCAACT-3'. Moreover, another morpholino was

injected in parallel to our experimental injections and was used as a control. This morpholino was also ordered from Gene Tools and is the company's standard control morpholino (cont. MO: 5′-CCTCTTACCTCAGTTACAATTTATA-3′). Morpholinos were reconstituted in RNase free water at stock concentrations of 2 mM. Morpholinos were then diluted in a solution of 1X Danieau buffer (58 mM NaCl, 0.7 mM KCl, 04 mM $MgSO_4$, 0.6 mM $Ca(NO_3)_2$, 5 mM HEPES pH 7.6) and phenol red was added to a final working concentration of 1mM. Working injection stocks were maintained at -20°C.

2.8. Zebrafish maintenance and breeding

Adult zebrafish were ordered from Big Al's Aquarium Services (Ottawa, ON, Canada) and 20-25 fish were kept together in 10-liter tanks in multirack aquatic housing systems (Aquatic Habitats, Apopka, FL). Tanks were maintained under a 14h to 10h light-dark cycle. All fish handling was carried out in accordance with institutional animal care guidelines and those of the Canadian Council of Animal Care. Moreover, experimental protocols were preapproved by the University of Ottawa Animal Care and Veterinary Service. The breeding occurred at the beginning of the light cycle and embryos were collected right away. 100- 200 embryos were collected at a time during the earliest stages of development (one to two-cell embryos) and 25-30 embryos were placed in the rows of an agar solution solidified in a Petri plate.

Microinjection needles were borosilicate glass capillaries made by using a COPF needle puller model 730 machine. The needle was filled with 1ul of MO (morpholino) solution and each embryo was injected with 1-2nl of MO solution at a concentration of 1mM. The microinjection system consisted of microinjector/micromanipulator (Narishige International USA, Inc., New York, NY) and a Nikon SMZ-1500 microscope

(Nikon Instruments Inc., Lewisville, TX) equipped with OCC illumination base and epifluorescence illuminator. A total of 50-60 embryos were microinjected for each microinjection experiment. The embryos were allowed to recover in an incubator at 27.5°C and were collected at different developmental times for phenotypical analysis or Western immunoblotting. Fish used in immunofluorescence experiments, in RT-PCR and Western analysis were kept under the same conditions. When tissue isolation was performed for RNA or protein extraction, adult zebrafish were euthanized by injecting benzocaine (catalog no. E1501, Sigma).

3. RESULTS

3.1. Distribution of ZMAN1 *in vitro* during the embryonic and adult mitosis

The protein ZLAP2 is a nuclear protein that associates with mitotic chromosomes (Schoft *et al.,* 2003). Several other inner nuclear proteins were found to interact with the chromosomes during mitosis. Consequently, the behaviour of ZMAN1 during the cell cycle was investigated by indirect immunofluorescence stainings using a cultured embryonic fibroblast cell line, ZF4, and an adult cell line from the zebrafish caudal region, AB9, to see if ZMAN1 interacts with mitotic chromosomes. The primary polyclonal antibody α-ZMAN1 and the secondary antibodies labelled with CY3 and Alexa Fluor 488 were used for ZF4 and AB9 respectively. Cells were collected at different non-consecutive days for immunostaining purposes and these experiments were performed at least six times for each cell line, each time yielding the same results.

At interphase, the ZMAN1 protein was localized in the entire nucleoplasm and more intensely at the periphery of the nucleus of the somatic (AB9) cells with some traces in the cytoplasm (Fig.3.1, panel A). In order to detect the mitotic phases during the cell cycle and to distinguish nuclei from the cell, it was necessary to stain DNA with a DNA dye, Hoechst 33258 (Fig.3.1, panels B, E, H, K, N and Q). Omissions of the primary antibodies were also used as negative control experiments to visualize background residue from secondary serums. No immunolabelling is observed in any of these negative controls (Fig.3.1, panels C, F, I, L, O and R; and Fig.3.2 panels C, F and I).

Figure 3.1: Distribution of ZMAN1 during the cell cycle in the AB9 zebrafish somatic cell line. Immunofluorescence localization of ZMAN1 was performed by indirectly immunostaining AB9 cells with the polyclonal ZMAN1 serum (**A, D, G, J, M,** and **P**). Counterlabelling using the DNA dye Hoechst 33258 was also done (**B, E, H, K, N** and **Q**). A negative control omitting the primary antibody was performed to assess non specific binding of the detection system (**C, F, I, L, O** and **R**). Cells are shown at different mitotic stages: interphase (A-C), prophase (D-F), prometaphase (G-I), anaphase (J-L), telophase (M-O), and cytokinesis (P-R). The arrows in **A** indicate immunostaining at the nuclear periphery and some traces in the cytoplasm. The arrows in **M** and **P** point to the immunolabelling of newly reformed nuclear envelopes at the periphery of the daughter cells. Digital images were taken using a Zeiss Axiophot. Bars, 10μm.

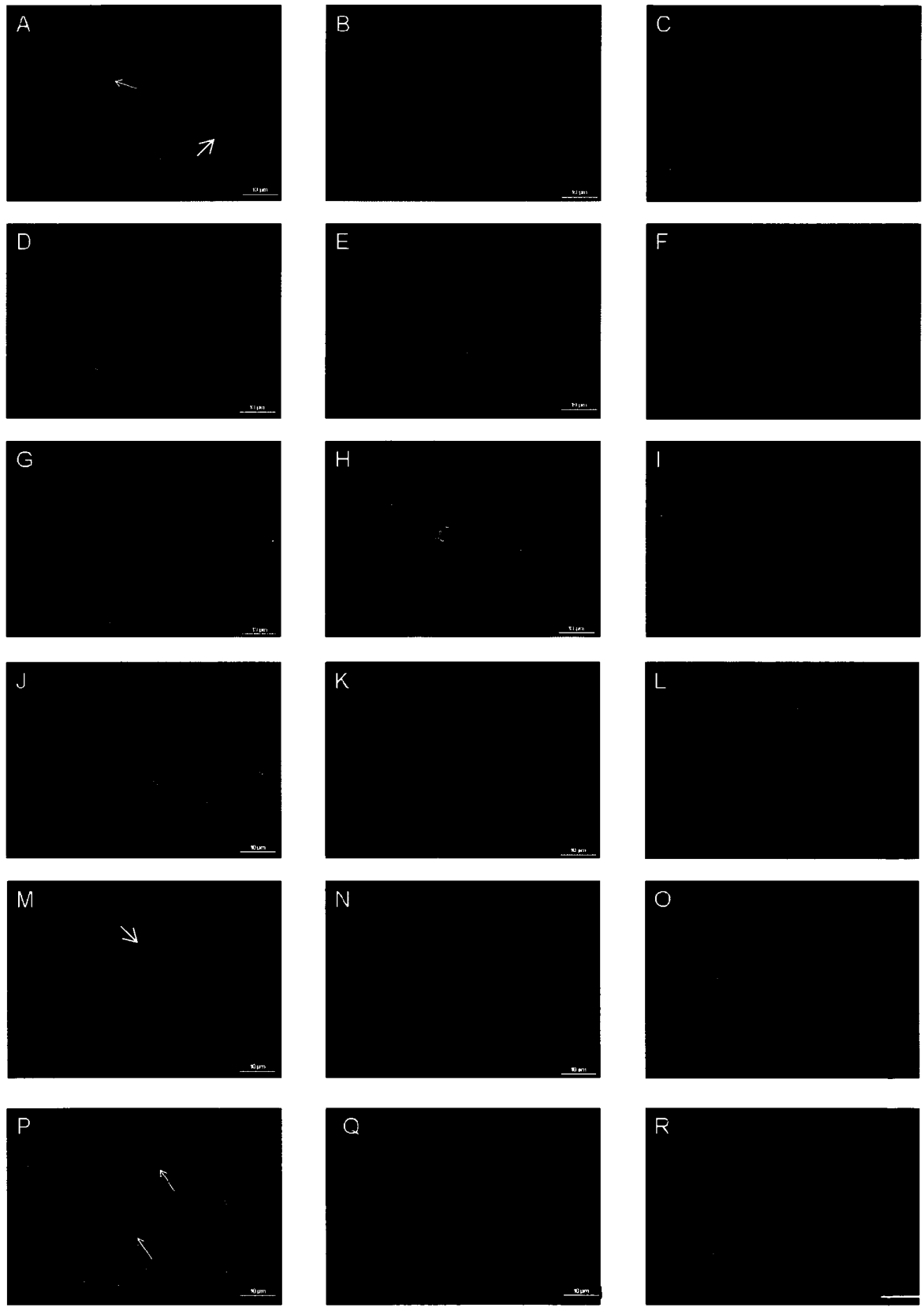
A
B
C
D
E
F
G
H
I
J
K
L
M
N
O
P
Q
R

As a way of verifying the protocols of my immunostaining experiments, the human serum of MAN1 (hMAN1) (Fig.3.2, panel A) and the zebrafish LAP2 (ZLAP2) antibodies (Fig.3.2, panel D) were used as positive controls. These serums were extensively used in previous studies making them ideal controls. An anti-tubulin antiserum qualified as an internal control to verify that the immunofluorescence experiments were done properly (Fig.3.2, panel G). Further analysis of another cell line originating from 24-hour old embryos demonstrated a localization of ZMAN1 at the nuclear periphery and in the nuclear interior in interphasic cells (Fig.3.3, panel A). This embryonic cell line was also counterstained with a DNA dye to visualize chromosomes during mitotis (Fig.3.3, panels B, E, H, K, N, Q and T). The arrow in Fig.3.3 (panel A) indicates intranuclear staining of the invaginated ZF4 nuclei. This invagination is a characteristic of nuclei formed by the assembly of karyomeres. Karyomeric formation occurs at late telophase with the initial assembly of small nuclear envelopes around few chromosomes resulting in the merge of a single nuclear envelope (Schoft *et al.,* 2003). Another experiment was performed in parallel to ZMAN1 staining was the immunolabelling of hMAN1, ZLAP2, tubulin for the same reasons mentioned above (Fig.3.4, panels A, D and G). As a mean of verifying non specific staining originating from secondary sera, another parallel immunostaining was done by omitting the primary antibody. I observed no background staining related to secondary staining (Fig.3.3, panels C, F, I, L, O, R and U; and Fig.3.4 panels C, F and I). Note that in the positive controls intranuclear staining is also present in the embryonic invaginated nuclei (indicated by arrows in Fig.3.4, panels A and D).

Figure 3.2: Distribution of hMAN1, ZLAP2 and tubulin in the AB9 zebrafish somatic cell line. Indirect immunofluorescence experiments were performed on somatic cells using the human MAN1 serum (**A**), polyclonal antibodies against ZLAP2 (**D**), and anti-tubulin antibodies (**G**). Cells were counterstained with the DNA dye Hoechst 33258 and visualized by immunofluorescence microscopy (**B, E** and **H**). A negative control omitting the primary antibody was performed to assess non specific binding of the detection system (**C, F** and **I**). Digital images were taken using a Zeiss Axiophot. Bars, 10μm.

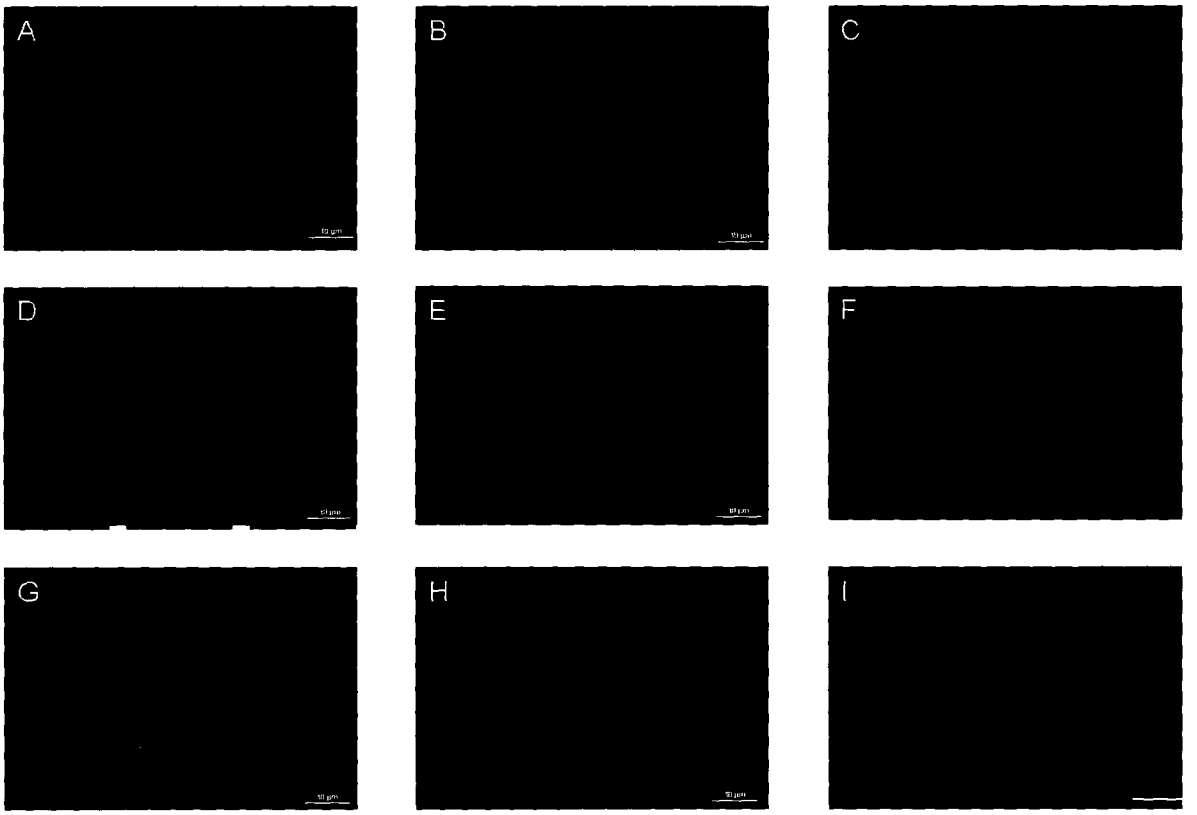
A
B
C
D
E
F
G
H
I

In cells entering prophase, ZMAN1 was still detected at the nuclear envelope but was also observed in the nuclear interior and cytoplasm This cytoplasmic migration of ZMAN1 indicates an early nuclear disassembly, which starts approximately at late prophase (Fig.3.3, panel D). At prometaphase, ZMAN1 seems to be present all over the cytoplasm and nuclear interior At this point of mitosis, the nuclear breakdown is advanced and ZMAN1 is dispersed within the cytoplasm and does not anchor in the dissembled envelope (Fig.3.1 and Fig.3.3, panel G). An unexpected observation was the lack of immunolabelling of metaphasic cells (Fig 3 3, panel J) This phenomenon is unusual and may have several implications, which will be discussed in chapter IV (Discussion). During anaphase, staining was detectable mostly in the cytoplasmic interior but part of ZMAN1 protein wass also distributed around the newly forming nuclear membrane (Fig.3 1 and Fig.3.3, panel J and M respectively) Coinciding with an accelerated nuclear reassembly, immunolabelling was observed at the nuclear periphery during telophase (Fig 3.1 and Fig 3 3, panels M and P) and cytokinesis (Fig.3.1 and Fig 3 3, panels P and S) of the two daughter cells It is also important to mention that ZMAN1 was present around the small vesicles of telophasic embryonic cells (indicated by arrows in Fig 3.3, panel P) and this may indicate an active role of this protein in nuclear reassembly. However, no vesicles were observed at late telophase in the somatic cells (Fig 3.1, panel M). These results indicate that the ZMAN1 protein displays a similar localization pattern in embryonic and somatic adult cells and is mainly distributed within the cytoplasm during late prophase, prometaphase and anaphase. However, ZF4 cell staining diverges from the AB9 cell line at metaphase where no immunolabelling was detected

Figure 3.3: Distribution of ZMAN1 during the cell cycle in the ZF4 zebrafish embryonic fibroblast cells. Immunofluorescence localization of ZMAN1 was performed by indirectly immunostaining ZF4 cells with the polyclonal ZMAN1 serum (**A, D, G, J, M, P** and **S**). Counterlabelling using the DNA dye Hoechst 33258 was also done (**B, E, H, K, N, Q** and **T**). A negative control omitting the primary antibody was performed to assess non specific binding of the detection system (**C, F, I, L, O, R** and **U**). Cells are shown at different mitotic stages: interphase (A-C), prophase (D-F), prometaphase (G-I), metaphase (J-L), anaphase (M-O), telophase (P-R) and cytokinesis (S-U). The arrows in **A** show traces of immunolabelling in the cytoplasm and intranuclear staining in the invaginated nucleus. The arrow in **D** indicates immunostaining of the cytoplasm at the beginning of nuclear breakdown. The arrow in **P** points to the staining at the chromosomal periphery. The arrows in **M** and **S** designate the immunolabelling of newly reassembled nuclear envelopes at the periphery of the daughter cells. Digital images were taken using a Zeiss Axiophot. Bars, 10μm.

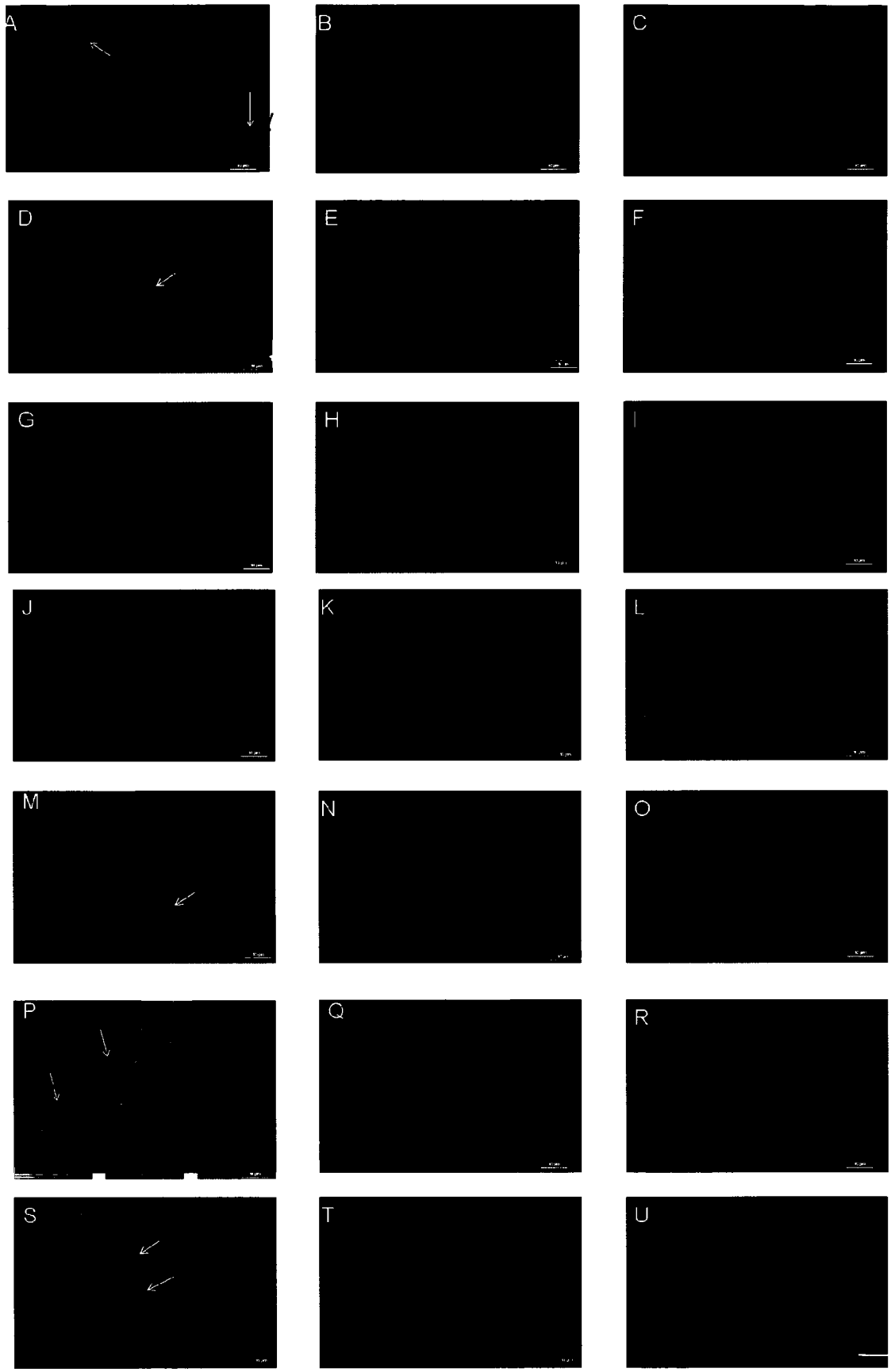
A
B
C
D
E
F
G
H
I
J
K
L
M
N
O
P
Q
R
S
T
U

Figure 3.4: Indirect immunostaining of the ZF4 zebrafish embryonic cells. Immunofluorescence experiments were performed on embryonic cells using the human MAN1 serum (**A**), the polyclonal antibodies against ZLAP2 (**D**), and an anti-tubulin serum (**G**). Cells were counterstained with the DNA dye Hoechst 33258 and analyzed by immunofluorescence microscopy (**B, E** and **H**). A negative control omitting the primary antibody was performed to assess non specific binding of the detection system (**C, F** and **I**). The arrows in A and D indicate the intranuclear immunostaining of the invaginated ZF4 nuclei. Digital images were taken using a Zeiss Axiophot. Bars, 10μm.

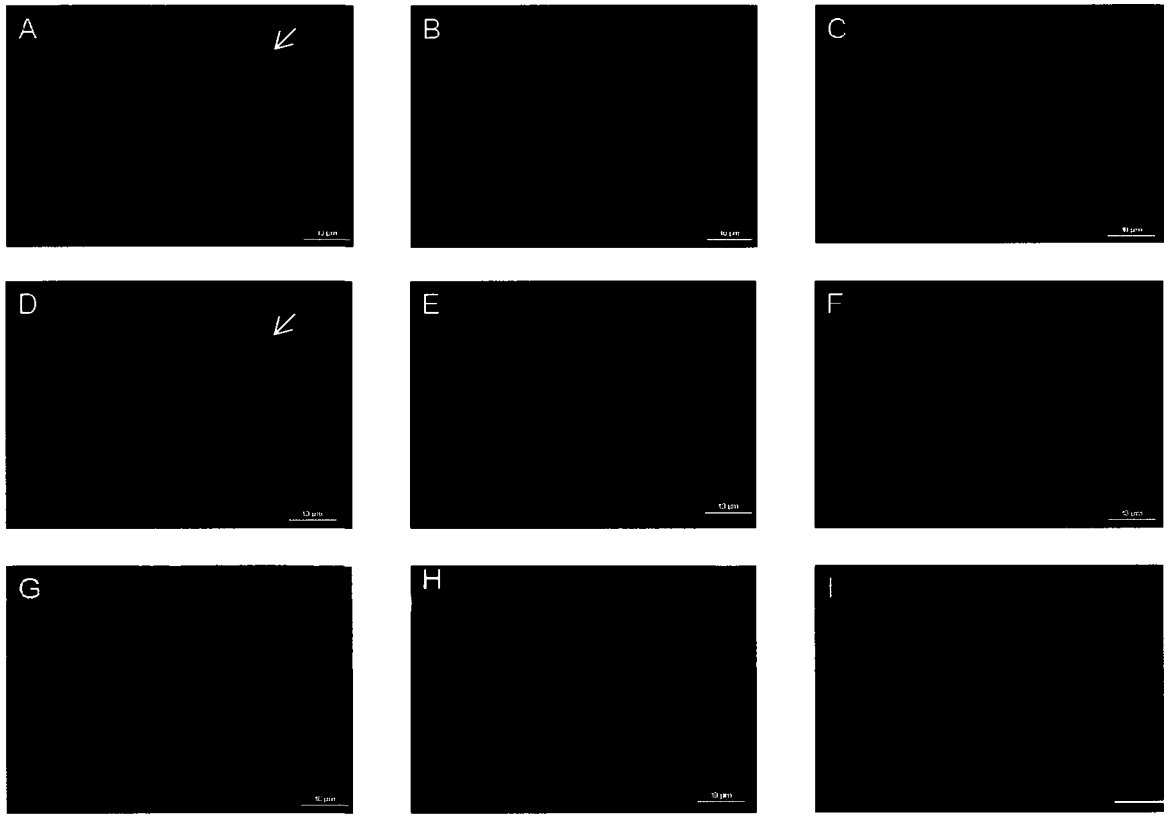
A
B
C
D
E
F
G
H
I

and, at late telophase, during which nuclear reassembly results from karyomeric formation.

3.2. ZMAN1 protein expression during zebrafish early development

The study published by Osada *et al.* (2003) showed that the transcripts of XMAN1, the *Xenopus* ortholog of ZMAN1, are maternally transmitted to *Xenopus* embryos. By RT-PCR, they also looked at mRNA levels throughout development, and it appeared that XMAN1 transcripts remain relatively constant throughout early embryogenesis but their expression drops around stage 45, which is a late embryogenesis stage, occurring after hatching of the larvae (Denver *et al.*, 1997). Furthermore, an independent study of ZLAP2 demonstrated that the ω isoform is also inherited maternally (Schoft *et al.*, 2003). Therefore, the inspection of ZMAN1 protein expression profile in young embryos was the next step to better understand ZMAN1 behaviour during early zebrafish development. Embryos were collected during key developmental stages: the end of the cleavage period at 2 hours post-fertilization (hpf); the dome stage during blastula (4hpf); the mid-gastrula (at 75% epiboly, 8hpf); and, the end of segmentation/ early pharyngula stage (24hpf). Western blot analysis was performed on the membrane using ZMAN1 as a primary antibody and an anti-guinea pig IgG coupled to horseradish peroxidise (HRP) as a secondary marker (Fig.3.5 panel A). Anti-GAPDH serum was used as an internal control to verify the validity of the experimental design. The GAPDH protein is highly expressed in most zebrafish tissues and serves as a protein loading control. Moreover, a Coomassie blue staining was also performed on these samples for loading control purposes (Fig.3.5 panel B). In addition to these experiments, a negative control immunoblot where the primary antibody was omitted was also run in parallel to the experimental immunoblots.

No signal was detected in the negative control blots (data not shown). These Western immunoblotting experiments were done at least three times using three different batches of tissues collected on different days.

Initially, it was thought that the expression patterns of ZMAN1 would follow the same profiles as XMAN1 and ZLAP2. Therefore, I hypothesized that ZMAN1 would be developmentally regulated and that it is maternally inherited. By analysing the Western blots obtained, I detected a high molecular mass polypeptide at 2hpf (Fig.3.5, panel A, lane 4), at 4hpf (Fig.3.5, panel A, lane 3), at 8hpf (Fig.3.5, panel A, lane 2) and at 24hpf (Fig.3.5, panel A, lane 1) at 120kDa corresponding to ZMAN1. A second band of molecular mass 38kDa was detected at steady levels in all stages and represents GAPDH (Fig.3.5 panel A).

The presence of ZMAN1 at the earliest stage of development, the cleavage period, corroborates the prediction that ZMAN1 is maternally transmitted. However, intensity of expression of ZMAN1 seems to be constant throughout the rest of the developmental stages in comparison with the internal protein control GAPDH.

3.3. Distribution of ZMAN1 protein during the cell cycle in zebrafish embryos

To further establish the distribution of ZMAN1 during the cell cycle, a closer examination of this protein during mitotic stages in zebrafish embryos was carried out by immunohistochemistry. Embryos were collected at early blastula (2½hpf), late blastula (4hpf), and mid-pharyngula (36hpf) stages and were subjected to whole-mount indirect immunostaining with ZMAN1 serum as a primary antibody and an anti-guinea pig coupled with CY3 for detection purposes (Fig.3.6, Fig.3.7 and Fig.3.8).

Figure 3.5: Expression of ZMAN1 during the early zebrafish development by Western blot. (**A**) Embryos at the end of the cleavage period, 2 hours postfertilization (hpf) (lane **4**), at the dome stage during blastula (4hpf, lane **3**), at 75% epiboly during gastrula (8hpf, lane **2**), and at the end of segmentation/ early pharyngula stage (24hpf, lane **1**) were deyolked and total proteins of 10 embryos were extracted, loaded in each lane and separated by SDS-PAGE gel electrophoresis. Immunodetection against ZMAN1 and GAPDH antibodies was subsequently performed. (**B**) A coomassie blue staining is also presented to confirm equal protein levels and to show the molecular weight marker (MW, lane **5**). The positions of ZMAN1 (120kDa) and GAPDH (38kDa) are designated by arrows. Note that the ZMAN1 protein is detected at a very early stage of embryogenesis. The molecular masses (in kDa) of two reference proteins are marked in **A** by black dots.

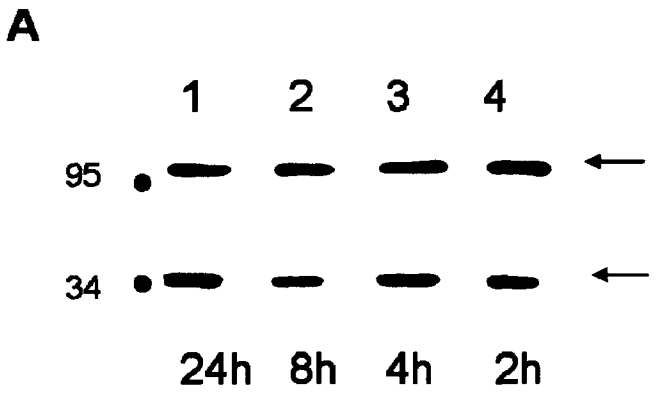
A
1
2
3
4
95
34
24h
8h
4h
2h

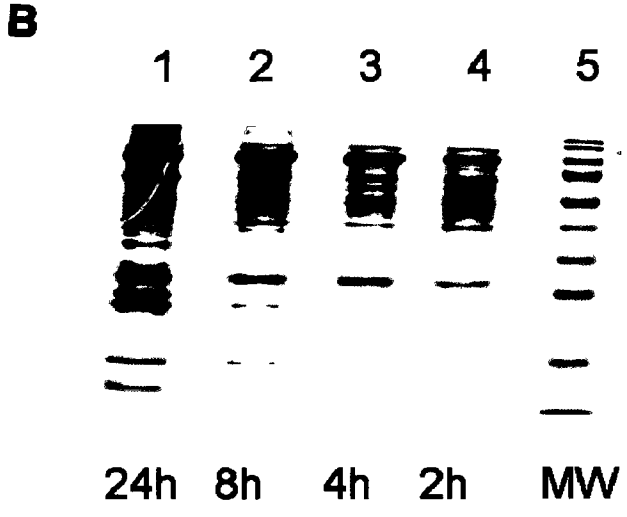
B
1
2
3
4
5
24h
8h
4h
2h
MW

At 2½hpf, maternal genes conduct the early onset of embryogenesis and the proteins expressed are maternally inherited. At mid-blastula, embryonic genome activation takes place and maternal genes are gradually discarded (Schier, 2007). Therefore, it is around early blastula and mid-blastula that it would be interesting to visualize the distribution of the maternally transmitted ZMAN1 protein. Mid-pharyngula is also an interesting stage to identify the presence of ZMAN1 since it is at this stage that one can observe a larva with some primitive tissues already present and visible. Moreover, counterstaining of chromatin was also performed using Hoechst 33258 (Fig.3.7 panels B and D; and Fig.3.8 panels B, D, F, H, J and L). It was also important to use an anti-tubulin serum as an internal control to make sure that immunostaining techniques were performed correctly (Fig.3.6, panel C).

In 36hpf embryos, ZMAN1 was ubiquitously detected throughout the embryo; however, since the intensity of the ZMAN1 signal was much higher in the tail only images obtained from this region are presented. Examination of the tail end showed that ZMAN1 is targeted at the nuclear periphery of the mid-pharyngula cells (Fig.3.6, panel B). Specific labelling of ZMAN1 at the nuclear envelope was also seen in 2hpf and 4hpf embryonic cells during interphase; although, some intranuclear and cytoplasmic staining was also detected in these young embryos (Fig.3.7, panel A, Fig.3.8, panel A). Immunolabelling of early blastula embryonic cells at prophase and anaphase (Fig.3.7, panel C) showed a diffused distribution of ZMAN1 in the cytoplasm and nuclear interior. In fact, it was expected that, during these mitotic stages, ZMAN1 would not localize to the nuclear envelope as prophase and anaphase correspond to the beginning of

Figure 3.6: Distribution of ZMAN1 proteins during interphase in older embryos. Indirect immunofluorescence localization of ZMAN1 was performed in whole-mount embryos at prim-25 stage during pharyngula (36h) by indirect immunostaining with the polyclonal ZMAN1 serum (**A** and **B)** and with anti-tubulin antibodies (**C**). **B** and **C** are close ups of the tail region. Staining is localized to the nuclear envelope in **A** and **B**. Preparations stained with tubulin (**C**) served as a control to confirm the validity of the experiment. A negative control omitting the primary antibody was also performed to assess non specific binding of the detection system (**D**). Digital images were taken using a Zeiss Axiophot. Bar in A represents 1μm. Bars in B, C and D represent 10μm.

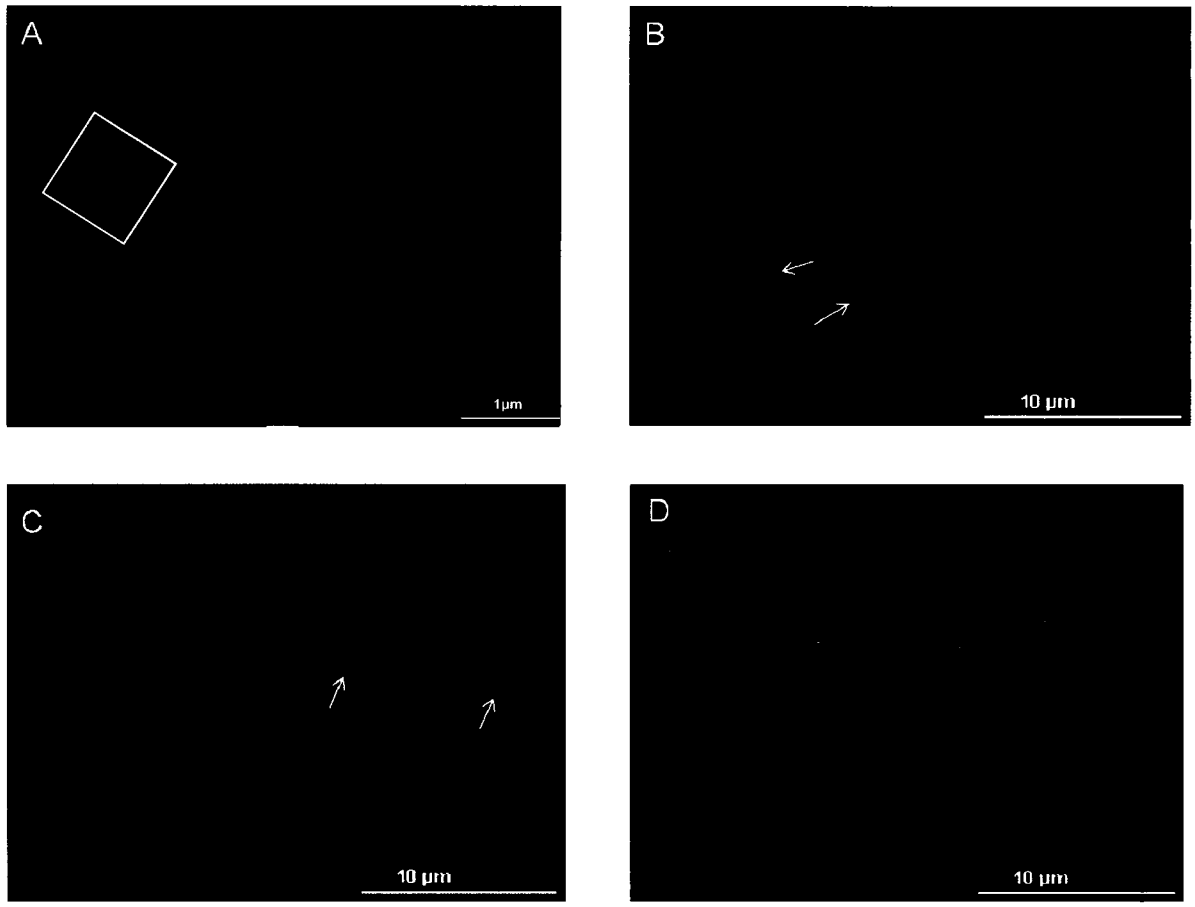
A
1µm
B
10 µm
C
10 µm
D
10 µm

nuclear disassembly and reassembly respectively. I also tried to reconstruct the cell cycle of 4hpf embryonic cells by following ZMAN1 distribution at each mitotic stage. This proved to be a laborious task because some mitotic stages were harder to visualize in these embryos due to the increased cell density and the lengthening of the cell cycle of this embryonic stage. ZMAN1 diffuse immunolabelling is observed during prophase, late anaphase and telophase (Fig.3.8, panels C, I and K). ZMAN1 immunostaining was not detected, however, at late prometaphase and metaphase. These data seem to confirm previous results observed with *in vitro* immunofluorescence microscopy of the AB9 and ZF4 cell lines. The indirect immunostaining experiments were performed at three different times for each developmental stage. Hence, since ZMAN1 labelling was never observed to be associated with mitotic chromosomes, it does not seem to interact with chromatin during mitosis and may have a role at the end of mitosis at the beginning of nuclear reassembly, which will be discussed later on in chapter IV (Discussion).

3.4. Western blot and RT-PCR analysis of ZMAN1 in adult zebrafish tissues

In order to investigate the expression profiles of ZMAN1 protein and transcript, adult zebrafish tissues were collected and analyzed by Western blot and reverse-transcriptase (RT)-PCR.

Total protein extractions of brain, gills, liver, kidney, and muscle were analyzed by SDS-PAGE and immunoblotted with the ZMAN1-serum1 and α-guinea-pig IgG coupled to Horseradish peroxidise (HRP). α-GAPDH antibodies were used as an internal control in these assays to verify even sample loading. Concomitantly to experimental blots, additional experiments were done using secondary serums and omitting the primary antibody. In the experimental blot, a low molecular weight band was detected at 38kDa,

Figure 3.7: Distribution of ZMAN1 in young zebrafish embryos at the early blastula stage. Indirect immunoflorescence localization of ZMAN1 was performed in whole-mount embryos at 2 ½ hpf by indirect immunostaining with the polyclonal ZMAN1 serum (**A** and **C**). Cells are shown during interphase (**A, B**), prophase (**C, D**) and anaphase (**C, D**). Counterstaining using the DNA dye Hoechst 33258 was also done (**B** and **D**). During interphase, staining is detected at the nuclear envelope and in the nuclear interior as indicated by the arrows in **A**. Diffuse nuclear and cytoplasmic staining is observed in mitotic cells as depicted by the arrows in **C**. Digital images were taken using a Zeiss Axiophot. Bars, 10μm.

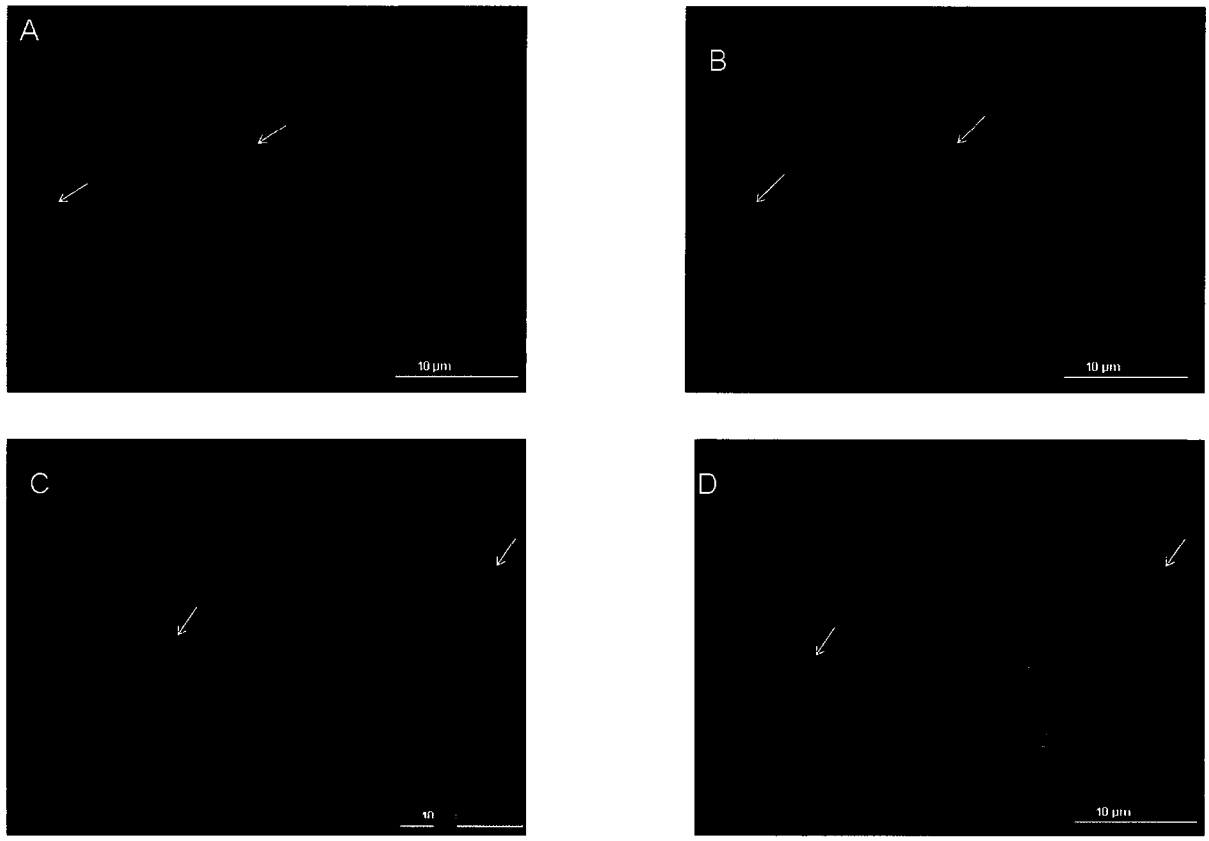
A
10 µm
B
10 µm
C
10 µm
D
10 µm

Figure 3.8: Localization of ZMAN1 in mitotic cells of young zebrafish embryos. Indirect immunoflorescent localization of ZMAN1 was performed in whole-mount embryos at the late blastula stage (4hpf, A-L) by indirect immunostaining with the polyclonal ZMAN1 serum (**A, C, E, G, I** and **K**). Cells are shown during interphase (**A, B**), prophase (**C, D**), prometaphase (**E, F**), metaphase (**G, H**), anaphase (**I, J**) and telophase (**K, L**). Counterlabelling using the DNA dye Hoechst 33258 was also done (**B, D, F, H, J** and **L**). During interphase, staining is diffuse at the nuclear periphery and in the intranuclear space as indicated by the arrows in **A**. At prophase, staining is diffuse in the cytoplasm (arrows in **C**). No staining is observed in prometaphasic and metaphasic cells (arrows in **E, G**). Staining reappears around anaphase (**I**) and immunolabelling is observed around the two daughter cells at telophase (arrows in **K**). Digital images were taken using a Zeiss Axiophot. Bars, 10μm.

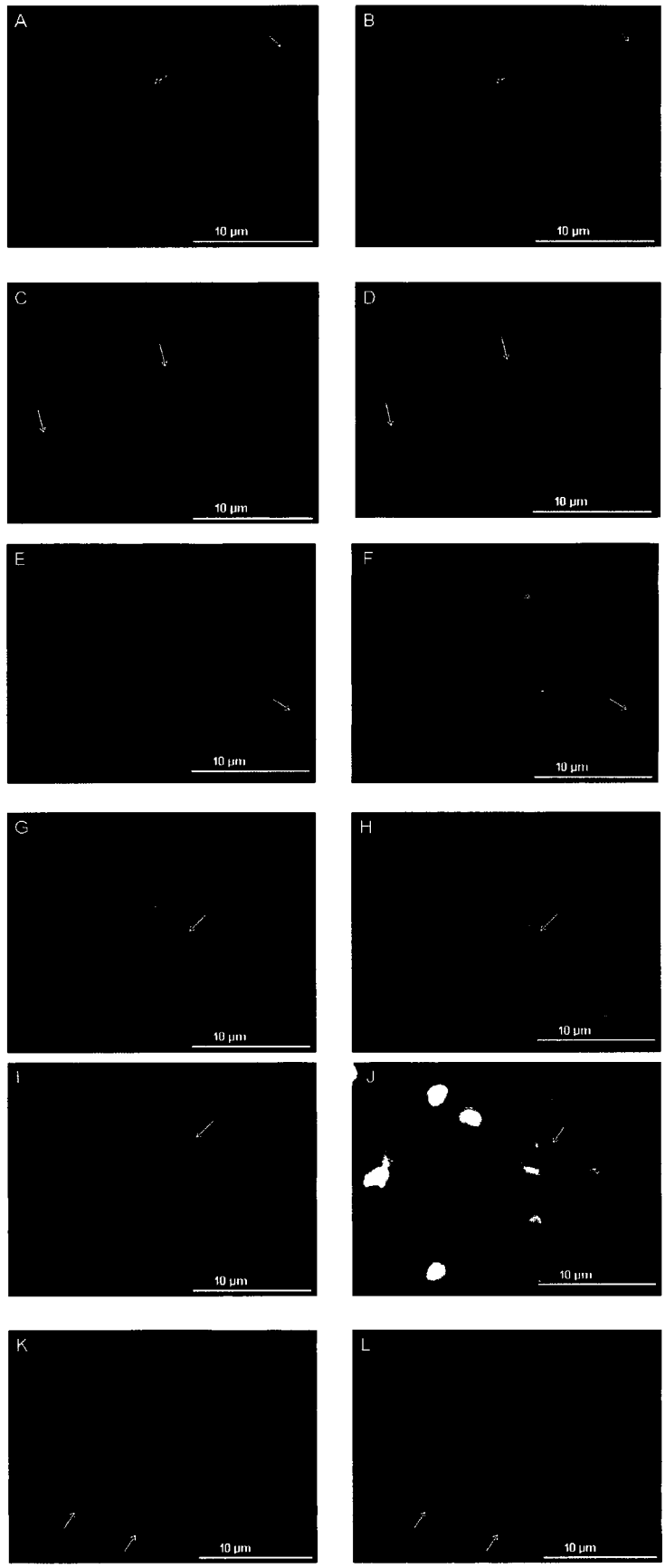
A
10 µm
B
10 µm
C
10 µm
D
10 µm
E
10 µm
F
10 µm
G
10 µm
H
10 µm
I
10 µm
J
10 µm
K
10 µm
L
10 µm

Figure 3.9: Western blot analysis of ZMAN1 in selected zebrafish adult tissues representing the three primary germ layers. Total proteins were extracted from the brain (**A** and **B**, lane **1**), the gills (**A** and **B**, lane **2**), the liver (**A** and **B**, lane **3**), the kidney (**A** and **B**, lane **4**), and the muscle (**A** and **B,** lane **5**) of seven adult zebrafish, and subsequently separated by SDS-PAGE electrophoresis. The ZMAN1 protein was detected by immunoblotting with the ZMAN1 serum (**A**). **B** shows immunoblotting with the secondary antibody serum as a negative control. Expression of the ZMAN1 protein (120kDa) is indicated by an arrow. An unknown polypeptide (150kDa, red arrow) was detectable in the brain tissue. The position of the intracellular protein GAPDH (38kDa) is also marked by an arrow. The molecular masses (in kDa) of some reference proteins of the prestained molecular weight marker are shown in **A** by black dots.

A

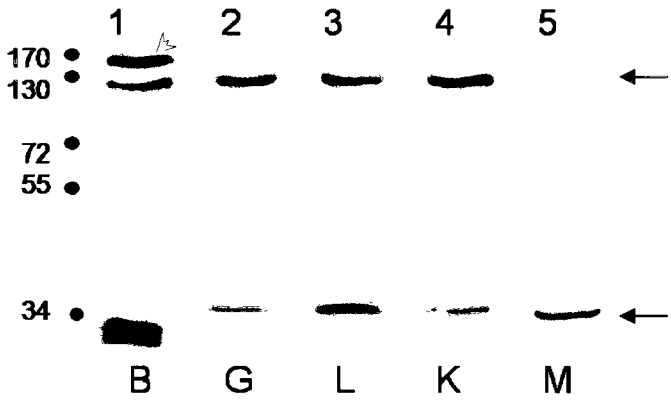

B

which represents GAPDH (Fig.3.9, panel A). The other polypeptide corresponds to the ZMAN1 predicted molecular mass of 120kDa (Fig.3.9 A). ZMAN1 was detected at similar levels in all tissues tested, although its expression was four times lower in the muscle tissue (lane 5, Fig.3.9, panel A) compared to the rest of the tissues. An additional band, of 150kDa, was also observed in the brain tissue (red arrow, lane 1, Fig.3.9 A). This unknown polypeptide could be the result of a post-translational modification of ZMAN1 in the brain or it could be an isoform of this protein, but this issue will be further discussed in chapter IV (Discussion). No band was detected in the control immunoblot (Fig.3.9, panel B). Western immunoblotting experiments were repeated five to six times, using different batches of tissues collected at different times for each experiment. Therefore, ZMAN1 protein is ubiquitously expressed in all tissues tested, although; at much lower intensity in the muscle tissue.

Furthermore, tissues from the three primary germ cell layers were selected and compared by RT-PCR. The brain, of ectodermal origin, the muscle, of mesodermal origin, and, the gills, of endodermal origin, were collected. These three tissues were selected because of their interesting protein profiles; ZMAN1 is highly expressed in the brain and gills but is present in much lower amounts in the muscle. Total RNA extraction was followed by cDNA synthesis and PCR experiments to examine and compare expression levels of ZMAN1. To be able to analyze ZMAN1 mRNA expression in these tissues, it was necessary to design primers not only against ZMAN1 but also against the housekeeping gene, elongation factor 1- alpha (EF1-α). EF1-α serves as a common denominator when comparing ZMAN1 expression levels.

A band of 165 base pairs (bp), corresponding to the size predicted for ZMAN1, was detected in each tissue (lane 2, lane 4 and lane 6 Fig.3.10), which confirmed the presence of ZMAN1 transcripts in all the samples tested. The EF1-α band of 165bp is observed in lane 3, lane 5 and lane 7 (Fig.3.10, panel B). EF1-α RNA levels seemed comparably equal in all tissues. These RT-PCR experiments were repeated at least three times using three different batches of zebrafish tissues collected at different times.

However, it is important to mention that the RT-PCR technique has several limitations that must be taken into account and other strategies may be more suitable for quantification purposes (see Discussion). Total RNA preparations from the brain (lane 1), the gills (lane 2) and the muscle (lane 3), were migrated on a 1.2% agarose gel (Fig.3.10 panel B) and examined to verify RNA quality and integrity. Hence, ZMAN1 transcripts were ubiquitously expressed in the brain, the gills and the muscle. The first two results are concordant with the Western immunoblots. Surprisingly, ZMAN1 transcript was as highly expressed in the muscle tissue as in the other two tissues, which was not the case of its protein profile in this tissue.

Northern blots were also attempted on the brain in order to determine the identity of the unknown polypeptide, of molecular mass 150kDa, detected in this tissue. I prepared a probe using zebrafish MAN1 genomic DNA that I inserted in a plasmid. This probe was also sent for sequencing to confirm the reliability of the probe. Although the method and the solutions used to detect the expression of all ZMAN1 transcripts seemed to work fine, after many different trials, I was not able to identify any specific signal. This part of the project was, therefore, not pursued.

3.5. Distribution of ZMAN1 in tissues from the three primary germ layers

To gain insights into the physiological role of the ZMAN1 proteins, I have investigated the distribution of ZMAN1 protein within the same three tissues originating from the three primary germ layers. Once each organ was extracted, frozen and sectioned, immunostaining was performed on the brain, gills and muscle tissues using primary antibodies directed against ZMAN1 and CY3 as a secondary marker (Fig.3.11, Fig.3.12 and Fig.3.13, panels A and C). Moreover, primary omissions are also presented (Fig.3.11, Fig.3.12 and Fig.3.13, panel E).

In the brain nuclei, ZMAN1 immunolabelling was clearly detected around the nuclear envelope and also some traces were seen in the nucleoplasm (arrows in Fig.3.11 panels A and B). Further analysis of specific brain parts showed that it was evenly and ubiquitously expressed throughout the brain tissue. In the gills, ZMAN1 was also detected around the nuclear envelope. However, ZMAN1 signal was not as strong and prominent as the one in the brain tissue; in fact, it was observed in most of the gills tissue but is not quite as ubiquitous (arrows in Fig.3.12 panels A and B). In comparison with the two other tissues, the muscle tissue showed very little ZMAN1 staining (arrows in Fig.3.13 panels A and B). These tissue immunostaining experiments were done at least six times and each time tissues were collected from different animals. Hence, the brain and the gills, which are of ectodermal and endodermal origins respectively, showed a very strong expression of ZMAN1 protein with a wide distribution. However, the muscle, of mesodermal origin, displayed very low expression of ZMAN1 and these results will be further discussed in chapter IV (Discussion).

Figure 3.10: Reverse transcriptase-PCR (RT-PCR) analysis of ZMAN1 expression in various zebrafish adult organs Total RNA was extracted from three zebrafish tissues originating from the three primary germ cell layers: the brain (lane **2** and **3**), of ectodermal origin, the gills (lane **4** and **5**), of endodermal origin, and the muscle (lane **6** and **7**), of mesodermal origin (**B**) 2μg of total RNA was prepared from the brain (lane **1**), the gills (lane **2**) and the muscle (lane **3**) and was examined on a 1 2% agarose gel The 28 S and 18 S rRNAs are indicated by upper and lower arrows, respectively. (**A**) RT-PCR of ZMAN1 transcripts was performed by using primers against ZMAN1 (lane **2, 4, 6**). Primers against elongation factor 1- α (EF1-α) (lane **3**, **5**, **7**) an internal housekeeping gene were also used Samples were electrophorosed on a 1.2% agarose gel An arrow indicates the molecular weight in base pairs (bp) of the detected band (**A**). The black dots correspond to the position of the DNA molecular markers (in bp) Experiments were repeated three times with similar results

A

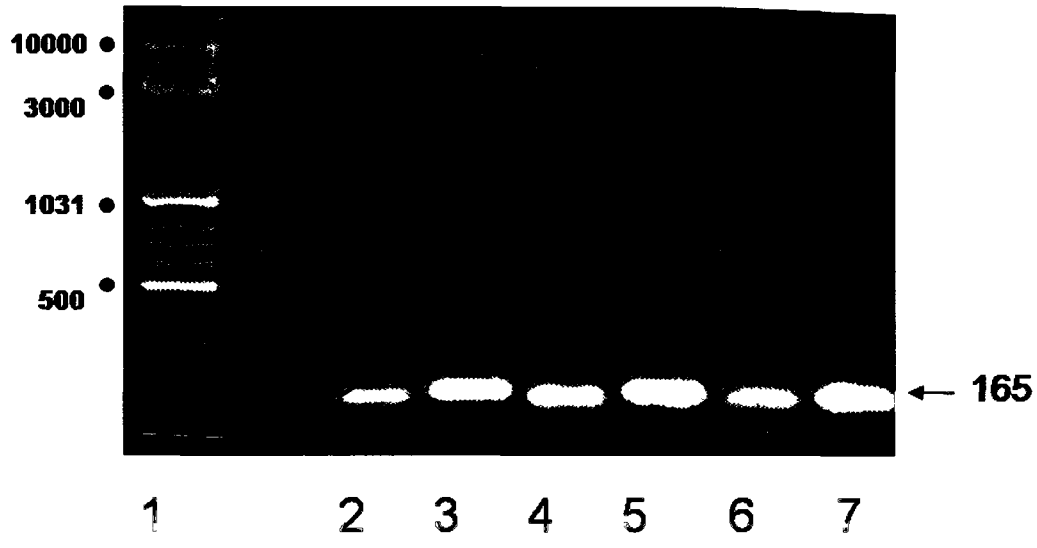

B

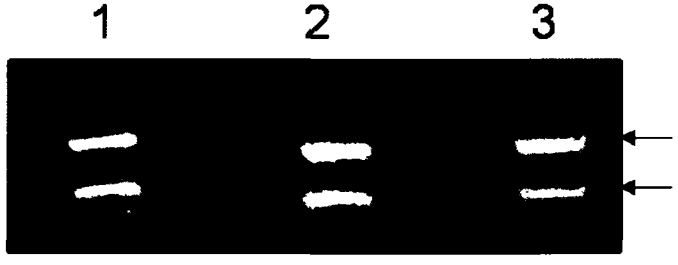

Figure 3.11: Distribution of ZMAN1 in the brain tissue in the adult zebrafish. Intact brain tissue, of ectodermal origin, was extracted, frozen and thinly sliced using a cryostat. Frozen sections were then fixed and immunostained with the ZMAN1 serum (**A**, **C**). The arrows in **A** and **C** indicate the immunolabelling at the nuclear periphery. Staining is observed ubiquitously in all the different parts of the brain tissue. Counterlabelling using Hoechst 33258 to analyze DNA was also done (**B, D**). A negative control omitting the primary antibody was performed to assess non specific binding of the detection system (**E).** Digital images were taken using a Zeiss Axiophot. Bars in **A** and **B** represent 1μm. Bars in **C**, **D** and **E** represent 10μm.

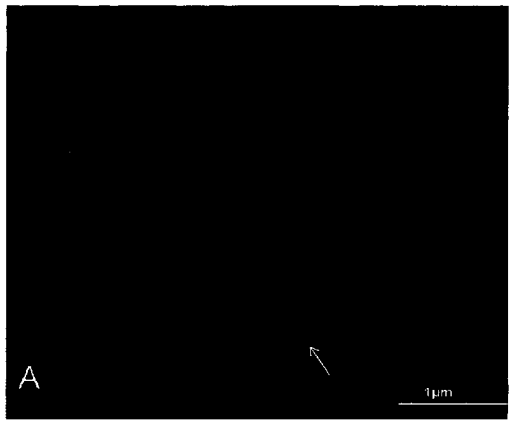
A
1 µm

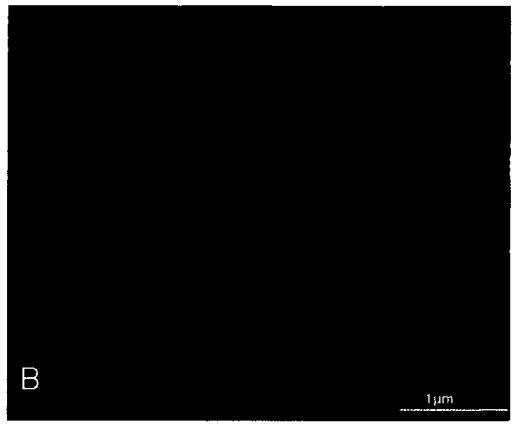
B
1 µm

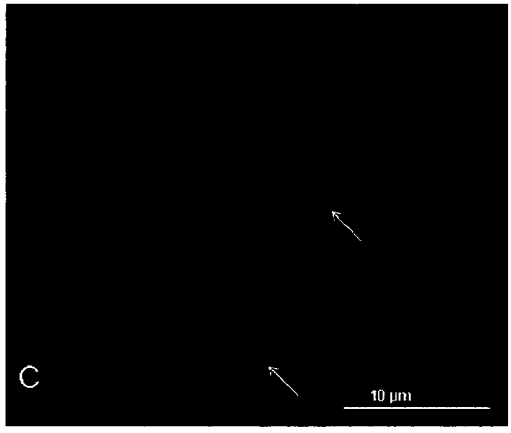
C
10 µm

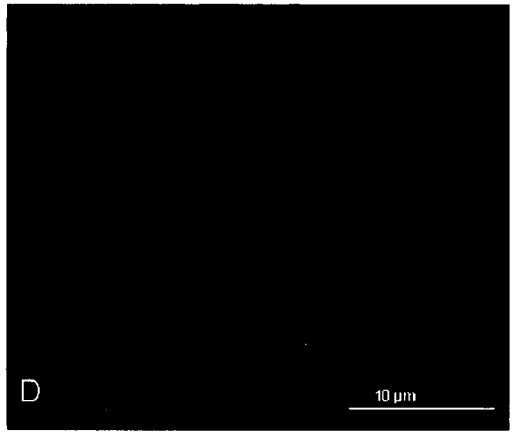
D
10 µm

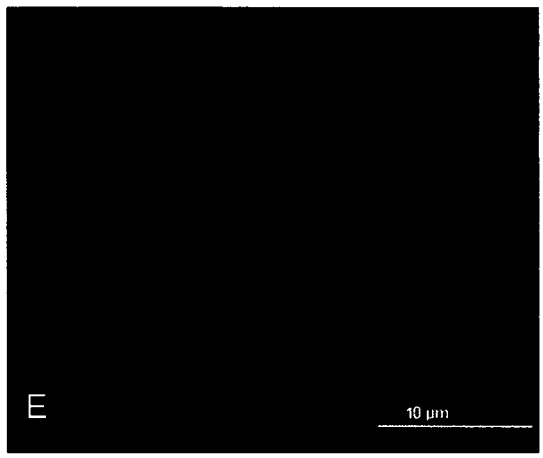
E
10 µm

Figure 3.12: Distribution of ZMAN1 in the gills tissue in the adult zebrafish. Intact gills tissue, of endodermal origin, was extracted, frozen and thinly sliced using a cryostat. Frozen sections were then fixed and immunostained with the ZMAN1 serum (**A**, **C**). The arrows in **A** and **C** indicate the immunolabelling at the nuclear periphery. Counterlabelling using Hoechst 33258 to analyze DNA was also done (**B, D**). A negative control omitting the primary antibody was performed to assess non specific binding of the detection system (**E**). Digital images were taken using a Zeiss Axiophot. Bars, 10μm.

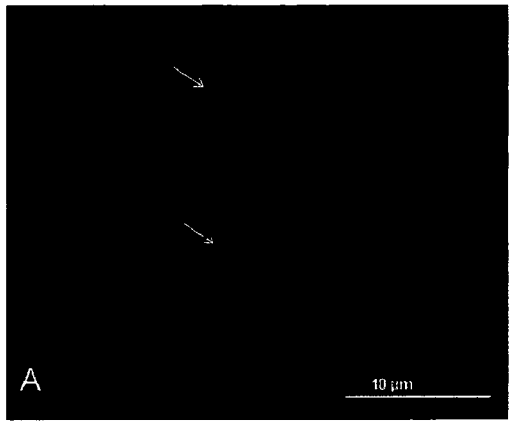
A
10 µm

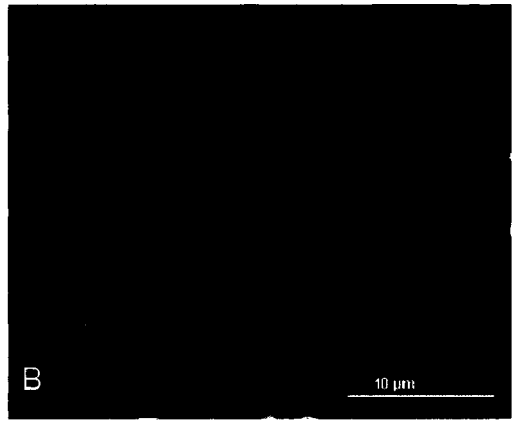
B
10 µm

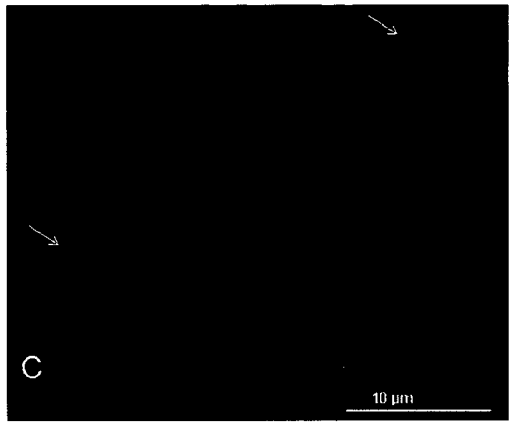
C
10 µm

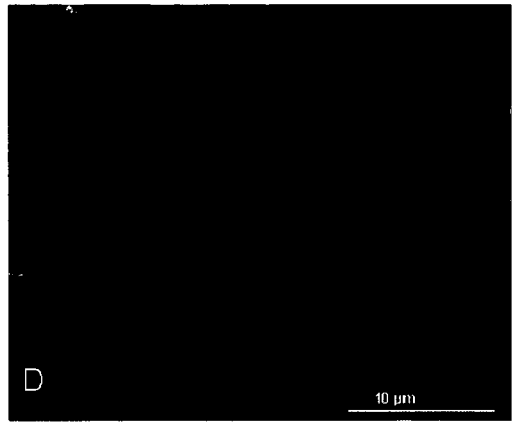
D
10 µm

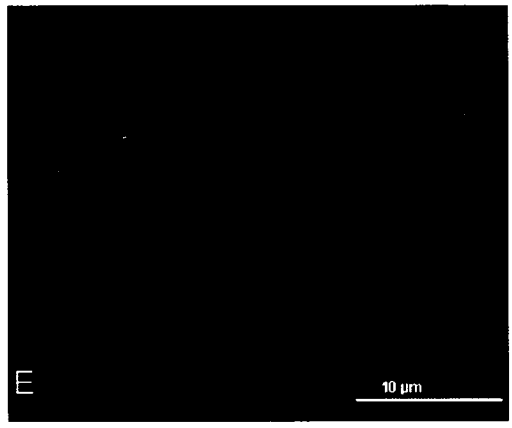
E
10 µm

Figure 3.13: Distribution of ZMAN1 in the muscle tissue in the adult zebrafish. Intact muscle tissue, of mesodermal origin, was extracted, frozen and thinly sliced using a cryostat. Frozen sections were then fixed and indirect immunofluorescence staining with the ZMAN1 serum was performed (**A**, **C**). Immunostaining showed low and/or no reactivity in most parts of the preparations (arrows in **A** and **C**). Counterlabelling using Hoechst 33258 to analyze DNA was also done (**B, D**). A negative control omitting the primary antibody was performed to assess non specific binding of the detection system (**E).** Digital images were taken using a Zeiss Axiophot. Bars in **A** and **B** represent 1μm. Bars in **C**, **D** and **E** represent 10μm.

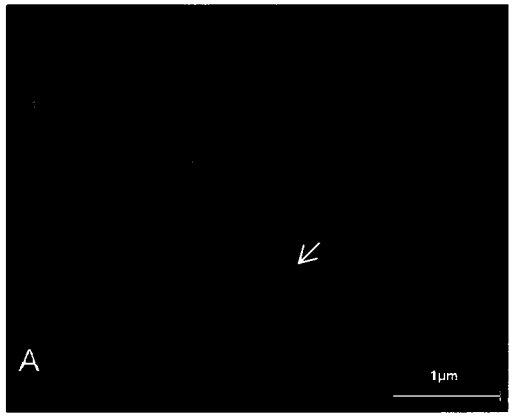
A
1µm

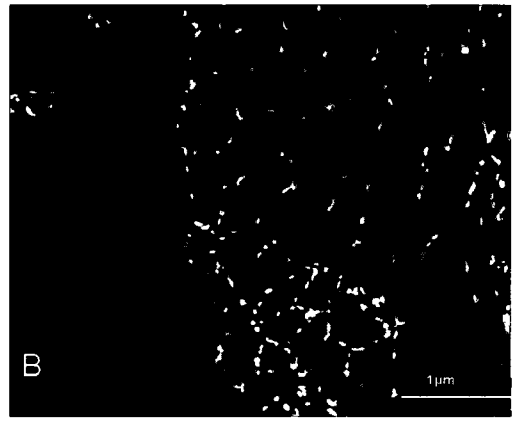
B
1µm

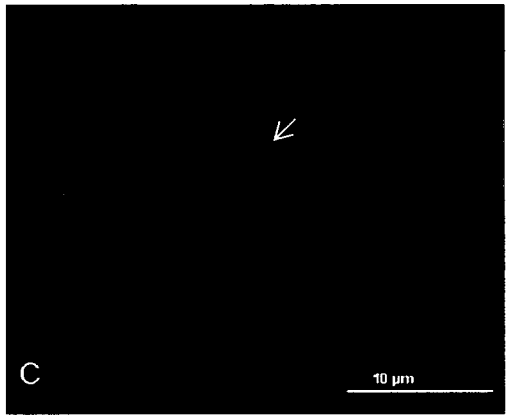
C
10 µm

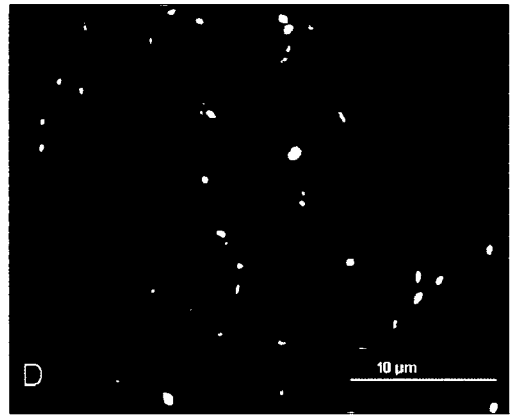
D
10 µm

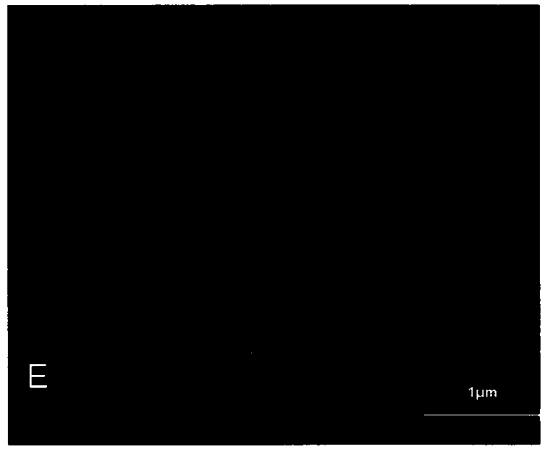
E
1µm

3.6. Microinjection of the morpholino oligonucleotide 1 in zebrafish embryos inhibits the expression of ZMAN1

To better understand the roles played by ZMAN1 in zebrafish embryogenesis, we performed a knockdown using an antisense morpholino oligonucleotide 1 (MO1) designed to block protein translation of ZMAN1. Morpholinos are chemically modified oligonucleotides that possess a morpholine ring instead of a ribose. They show strong resistance to nucleases and are effective translation blockers through steric blockage (Brent and Drapeau, 2002). This tool has been widely exploited by zebrafish users in the past years; it will be very helpful to determine the functions of ZMAN1 during embryogenesis.

The MO1 sequence was 25bp long and bound to the translation initiation site of ZMAN1 mRNA sequence (see Fig.3.14). MO1 was injected into 1 or 2-cell-stage embryos at concentrations of 4ng/nl (lane1 Fig.3.15 panel A), 8ng/nl (lane2 Fig.3.15 panel A), and 12ng/nl (lane3 Fig.3.15 panel A), which corresponded to 0.5mM, 1mM and 1.5mM respectively. Following a 48-hour incubation period, immunoblotting was performed on the injected embryos (Fig.3.15, panels A and B: lane 1, lane 2, and lane 3) and the wild-type uninjected ones (Fig.3.15, panels A and B: lane 4). Western analysis was done using primary antibodies against ZMAN1 and GAPDH. Respectively, the anti-guinea-pig and anti-mouse antibodies conjugated to HRP were used as secondary markers. On the other hand, a Coomassie blue gel was performed to verify even loading (Fig.3.15 panel B).

First, a constant and equally intense band of low molecular weight (37kDa) was observed in all lanes (Fig.3.15, panel A). This band corresponds to GAPDH protein, which is the internal control protein used in the experiment. Since GAPDH levels are

Figure 3.14: Schematic drawings of the 5'untranslated region (UTR) of ZMAN1 mRNA. The positions of morpholino oligo 1 (MO1), morpholino oligo 2 (MO2), the initiation codon ("Start", AUG) and the position of the morpholino oligo sequences complementary to my targets are shown (written from 5' to 3'). Scale bar, 2mm is equivalent to 3bp.

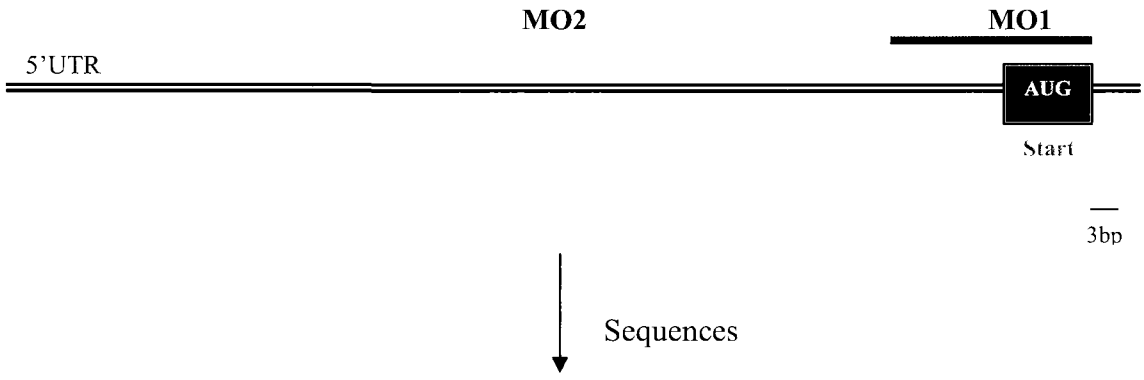

TTGTGACTTGTTTTCCTCCATATTTCTTGATTGTGTTTTGTTGTGTTGTTTAATGTTGGTCATTT

AATCACAAAAAAGGGTTTCCTGTTTCTTTCCTTTCAAGTTGGCCGTCTGTCCGCTTACTTTTAC

MO2 5'**AAAGTAAGCGGACAGACGGCCAACT** 3'

Start

GTCACTTCCGCCGTGTCTCGCTGTGTGCG[redacted]

MO1 5'**GCAGACGCCATCTTTGCACGAAAAA** 3'

Figure 3.15: Western blot analysis of ZMAN1 in 48-hour old zebrafish embryos. ZMAN1 morpholino oligonucleotide 1 (MO1) was microinjected in embryos at the one-cell or two-cell stages at three concentrations (4ng/nl, lane **1**, 8ng/nl, lane **2**, and 12ng/nl, lane **3**) at a volume of 1nl. At 48hpf, total proteins of 15 embryos were extracted from the injected embryos (lane **1**, **2** and **3**) and from wild-type embryos (lane **4**) of the same age. Proteins were loaded in each lane and separated by SDS-PAGE gel. (**A**) Immunodetection against ZMAN1 and GAPDH antibodies was subsequently performed. (**B**) A coomassie blue staining was done to confirm equal protein levels and to show the prestained molecular weight marker (**MW**). The positions of ZMAN1 (120kDa) and GAPDH (37kDa) are marked by arrows with a star. Three unknown polypeptides of molecular weights 170kDa, 150kDa and 52kDa are also indicated by arrows. The molecular masses (in kDa) of some reference proteins of the prestained molecular weight marker are shown in **A** by black dots.

A

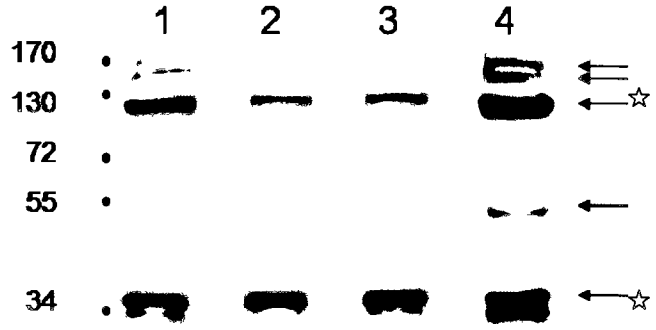

B

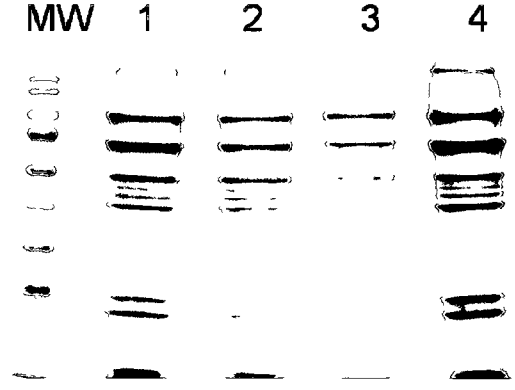

relatively constant and comparable in each lane, it is safe to assume that the expression levels of ZMAN1 in vivo are related to the expression detected through immunoblotting. Western analysis also revealed a prominent band of 120kDa present in lane 1, lane 2, lane 3 and lane 4 (panel A), which corresponds to ZMAN1 protein. Moreover, three unknown polypeptides of molecular weights 170kDa, 150kDa and 52kDa were observed. The latter seems to be a product of degradation while the two former are thought to be posttranslational modifications or possible isoforms of ZMAN1.

When comparing the injected embryos (Fig.3.15, panel A, lane 1, 2 and 3) with the uninjected wild-type ones (Fig.3.15, panel A, lane 4), one can notice a decreasing intensity of ZMAN1 expression when the injected concentration of MO1 increases. Expression of ZMAN1 in embryos injected with 1.5mM (12ng/nl) was approximately four times lower than its expression in the uninjected ones, whereas it is twice lower in embryos injected with 0.5mM (4ng/nl) and 3.5 times lower in embryos injected with 1mM (8ng/nl). MO injections followed by Western immunoblotting were performed at least three times using embryos injected and collected on different days. The same results were observed for each experiment. Therefore, these results demonstrate that the expression of ZMAN1 is successfully inhibited by microinjection of MO1. Interestingly, the expression is reduced but not completely eliminated even at high concentrations (Fig.3.15, panel A, lane 3).

3.7. Effects of injection dose of morpholino 1 on embryo survival

In order to confirm the proper concentration of morpholino 1 to be used in further experiments, three different doses were injected in embryos at the one-cell stage with approximately 1nl. At 48 hours, these embryos were collected and compared to embryos

Figure 3.16: Zebrafish embryos at 48hpf following knockdown of ZMAN1 with morpholino1 (MO1). Embryos at the 1-cell or two-cell stages were collected and microinjected with three concentrations (0.5mM: 4ng/nl, **A**; 1mM: 8ng/nl, **B;** and, 1.5mM: 12ng/nl, **C**) of MO1 at a volume of 1nl. The morphology of the morphants (MO1 injected embryos) was observed at 48 hours. (**A**) General phenotype of embryos microinjected with 4ng/nl. A twisted tail is designated by an arrow. (**B**) Phenotypical changes observed in the MO1 injected embryos with 8ng/nl are indicated by arrows. (**C**) MO1 injected embryos (injected at a dose of 12ng/nl) displayed extreme phenotypes with poor development. They did not survive past 3 days. Note at higher concentrations, ZMAN1 knockdowns have severe tail deformations. (**D**) A 48-hour old uninjected wild-type (WT) zebrafish embryo.

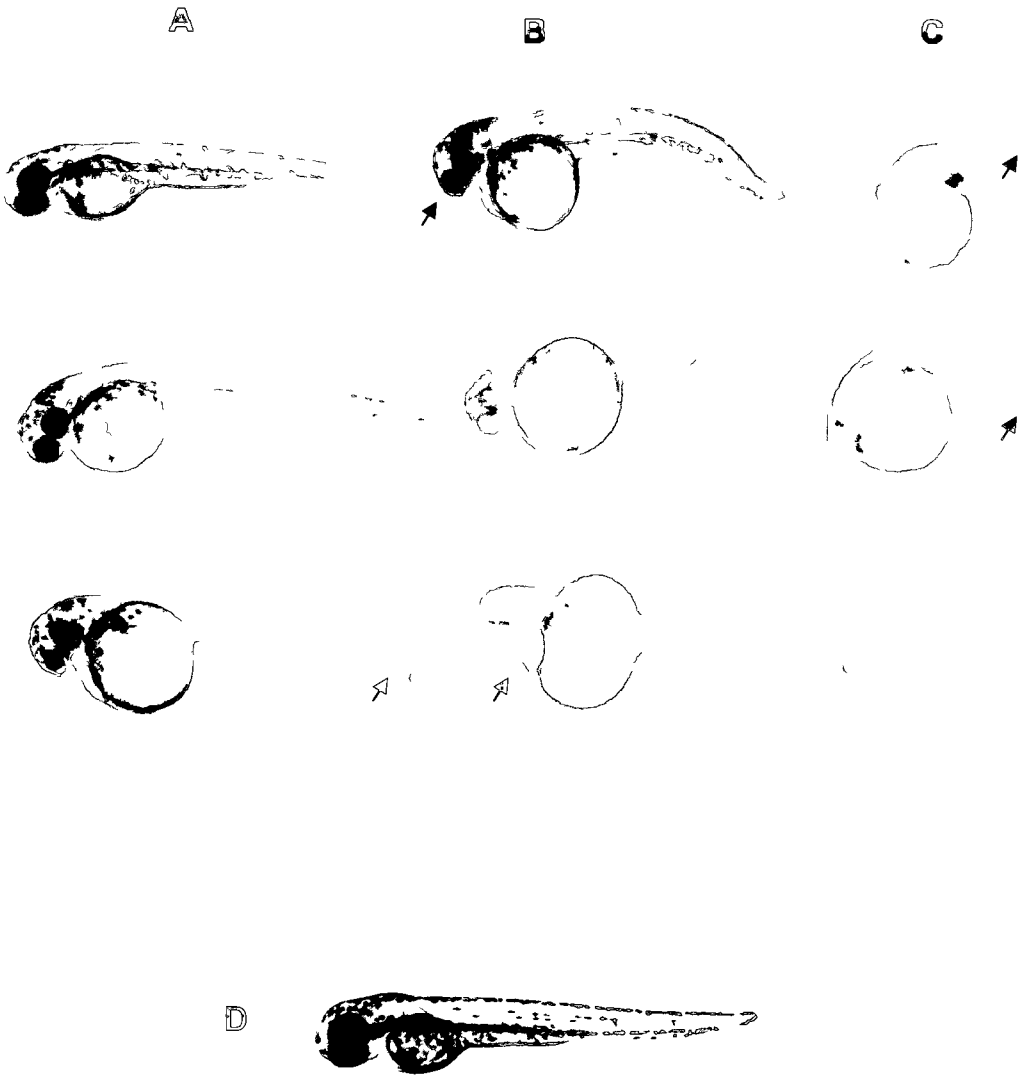
A
B
C
D

Figure 3.17: Number of survivor embryos after microinjections with MO1 and control MO. Embryos at the 1-cell or two-cell stages were collected and microinjected with three concentrations (0.5mM: 4ng/nl, 1mM: 8ng/nl, and, 1.5mM: 12ng/nl) of MO1 (**A**) and of cont. MO (**B**) at a volume of 1nl. The number of embryos which survived after 48 hours, 72 hours and 5 days is shown in the tables. "Morphotype": MO1 injected embryos displaying an abnormal phenotype. Embryos injected with a cont. MO were kept under the same conditions as the experimental ones.

A

	injection dose (ng/nl)		
	4	**8**	**12**
Total injected	42	46	43
at 2h	42	46	43
at 48h	30	33	22
at 72h	28	28	8
after 5 days	24	22	0
morphotype	7	27	21

B

	injection dose (ng/nl)		
	4	**8**	**12**
Total injected	50	51	41
at 2h	50	51	41
at 48h	45	44	29
at 72h	43	40	24
after 5 days	43	39	21

injected with the standard control morpholino oligo (cont. MO). These comparisons were not only based on the survival rates of the morphants but also on whether they presented phenotypical anomalies.

Following microinjection of 0.5mM (4ng/nl) MO1, most 48hpf zebrafish embryos displayed a normal phenotype with only a small number with an abnormal phenotype (morphotype) in each experiment (see Fig.3.16, panel A). Microinjections with higher concentrations, such as 1mM (8ng/nl) and 1.5mM (12ng/nl), resulted in approximately 50% of the surviving embryos showing distinctive morphotypes (Fig.3.16, panels B and C) compared to the uninjected embryos (Fig.3.16, panel D). Very few embryos were affected by the injection MO1 at a dose of 0.5mM (4ng/nl, see Fig.3.16, panel A). At 1mM (8ng/nl) of MO1, the surviving embryos showed several phenotypical abnormalities (Fig.3.16, panel B). Similar traits were also observed in the embryos injected with 1.5mM (12ng/nl, Fig.3.16, panel C). However, it is important to mention the major differences between these two dosages. Apart from the low survival rate observed in the embryos injected with the highest concentration of MO1 (Fig.3.17, panel A), the phenotypical defects in the latter were much more severe. Since the results obtained with these three concentrations were gradually more severe, it is possible to conclude that the observed differences are a consequence of the amount of morpholino injected.

When performing microinjections with MO1, survival rates were almost identical after 2 hours of incubation and were independent of the injection dosage (Fig.3.17 panel A). At 48 hours, survival rate became dependent on the injected concentration. The number of embryos alive was lower at a high injection dose such as 1mM but it was even

lower at the highest injection dose of 1.5mM (12ng/nl). When comparing the number of embryos displaying an abnormal phenotype, injection with 0.5mM (4ng/nl) of MO1 produced a low number of abnormal embryos. The number is higher with the highest concentration (1.5mM, 12ng/nl) but the highest number of abnormal embryos was observed with 1mM. After 3 days, the number of embryos alive continues to diminish in the 1mM dose, it is very low at 1.5mM but almost no change was observed in the 0.5mM group (Fig.3.17, panel A). Finally, after 5 days, the 1.5mM group died off while the other two groups remained alive. In the lowest injection dose group, I observed a low and steady number of deaths, whereas the 1mM group yielded progressive deaths throughout the days. Past five days, the embryos of the 0.5mM (4ng/nl) group and of the 1mM (8ng/nl) group survived. There were no survivors in the 1.5mM (12ng/nl) group (Fig.3.17, panel A).

Moreover, embryos injected with the control MO did not show a morphotype. Although, only 14% and 23% of the embryos injected with 0.5mM and 1mM of cont. MO died after 5 days, the highest injection dose, 1.5mM, showed a higher death rate of approximately 50% (Fig.3.17, panel B). Therefore, I cannot exclude the possibility that the deaths observed at 1.5mM, in the embryos injected with MO1 and cont. MO, are a consequence of the toxicity effects accompanying high injection doses. The data presented were collected from microinjection experiments performed on two separate sets of microinjected embryos but only the data from one experiment are shown. These results complement the Western blots discussed earlier.

This experiment, together with the Western analysis (Fig.3.15), allowed for the selection of an appropriate injection dosage of 1mM (8ng/nl), which seemed to

effectively reduce the activity of ZMAN1 without yielding a high number of deaths. This injection dose was used in further experiments.

3.8. Phenotypical effects of ZMAN1 knockdown on the development of zebrafish embryos

In order to test the direct role of ZMAN1 proteins during zebrafish development, the injection concentration of 1mM was used to microinject one-cell embryos and knockdown ZMAN1 early on in development. A standard control morpholino antisense oligo (cont. MO), provided by Gene Tools, was also injected at the fixed concentration of 1mM into one-cell zebrafish embryos. After microinjection, embryos were incubated at 27°C. The control MO does not compete with the experimental oligonucleotide MO1 and does not match the MO1 sequence; its sole purpose is to provide us with the non-specific effects. I also collected uninjected wild type (WT) embryos at the same stage, which were kept under the same conditions as the injected ones.

Approximately 70% of the injected embryos between cleavage (2hpf) and mid-gastrula (6hpf) appeared to be developmentally delayed (Fig.3.18, "MO") when compared to the uninjected wild-type ones (see Fig.3.18 "WT"). This delay was also observed in most embryos injected with the control MO (Fig.3.18 "Control"). This defect is due to microinjection manipulations and is non-specific. No other phenotypic abnormality was observed in the morphants compared to the control and WT during early embryogenesis, between cleavage and mid-gastrula. However, all these phenotypes were only observed by light microscopy and no investigation was carried out to determine whether cell division or other specific early developmental functions were affected.

Effects of the knockdown were more evident in later developmental stages. Injections with MO1 at a concentration of 1mM produced a wide range of abnormal phenotypes in older embryos with a small proportion of normal embryos.

By 24hpf, slow development was still observed in the majority of the embryos microinjected with MO1 (see Fig.3.19, "MO") compared to the wild type ones (Fig.3.19, "WT"). Apart from the characteristics accompanying the developmental delay, no obvious phenotypical differences were seen. At 48 hours, ZMAN1 knockdown seemed to interfere with proper formation of the trunk and the heart cavity (Fig.3.19,"MO"). The majority of embryos microinjected with MO1 displayed curved trunks or curved tail ends and, in some instances, an oversize yolk (approximately 3 times larger than the wild-type or control one), and smaller eyes than the wild-type (Fig.3.19, "WT") and the control embryos (Fig.3.19, "Control"). Contrary to the other traits, small eyes are considered to be non-specific. 3 day-old and older embryos (e.g. 5 days) still displayed curved tails and another characteristic observed in most of them was an expanded heart cavity (Fig.3.19, "MO"). Some of them had an enlarged swim bladder (Fig.3.19, "MO").

Figure 3.18: Morphological comparison between microinjected and control zebrafish embryos. Embryos at the one-cell stage were collected and microinjected with MO1 at 8ng/nl (1mM, "**MO**") or with a standard control morpholino at 4ng/nl (0.5mM, "**Control**") at a volume of 1nl and 2nl respectively. Control uninjected wild-type ("**WT**") embryos were also collected at the one-cell stage. After microinjection, the morphants and the wild-type were incubated at 27°C and observed during early embryonic development: late cleavage period (2hour-post-fertilization (hpf)), mid-blastula (4hpf), early gastrula (5hpf), and mid-gastrula (6hpf).

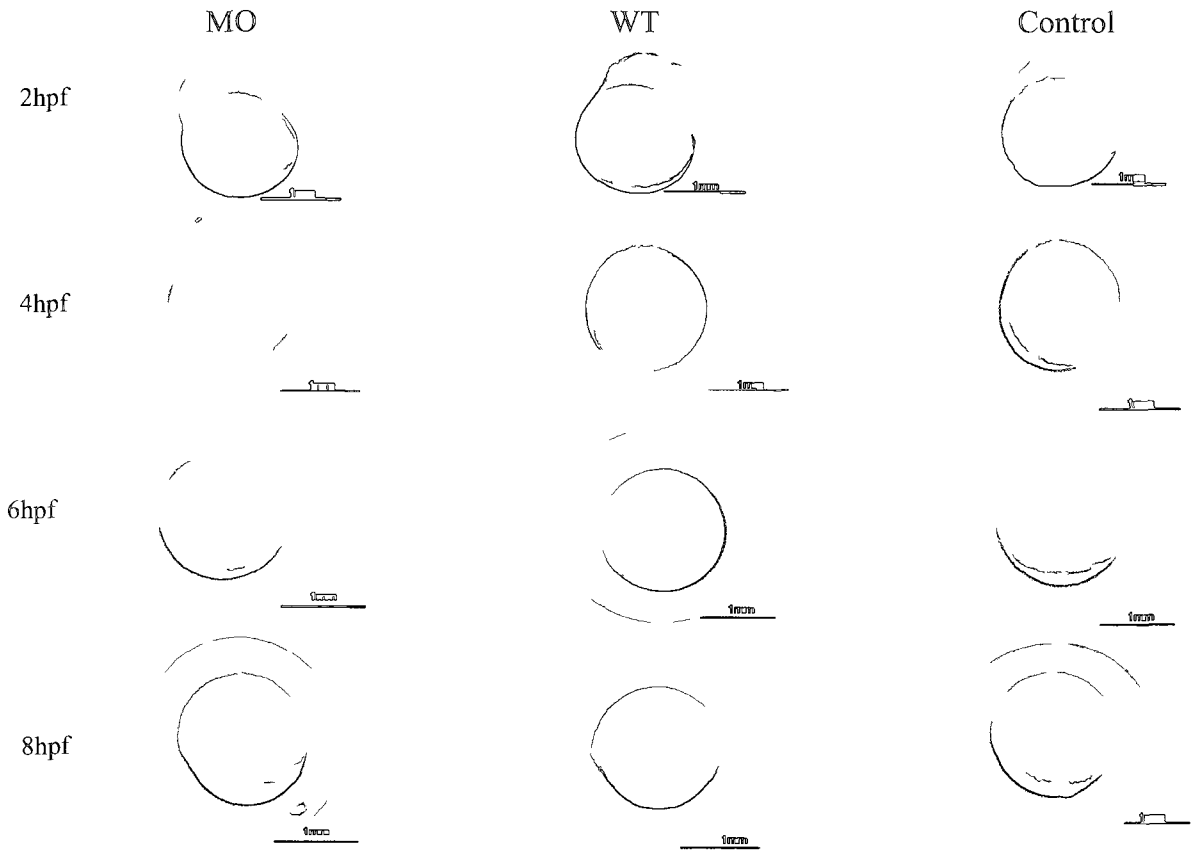
MO
WT
Control
2hpf
4hpf
6hpf
8hpf

Embryos injected with the control MO, at a concentration of 1mM (8ng/nl), did not display abnormal phenotypes, except for the delay in development and the small eyes observed in some of them. A closer look at the embryonic structures affected by the knockdown was carried out around 72 hours. When observing the specific ZMAN1 knockdown effects, approximately 70% of these embryos had curved tails or trunks (Fig.3.20 a, c and e), which impaired their movement causing them to move diagonally or not to move at all. The majority of the knockdown embryos also displayed pericardium edema and weak heart contractions, in addition to an oversize yolk (see Fig.3.20, a, c and e). Severe phenotypes showed extended intermediate cell mass (ICM) in their tails (Fig.3.20 a, red arrow) and a hunchback (Fig.3.20 a) but none of these underdeveloped embryos survived past 72 hours. Non-specific traits such as slightly smaller heads and eyes were also observed in most of the MO1 injected embryos.

In summary, the knockdown of ZMAN1 revealed several abnormalities in zebrafish late development stages, particularly in the tail region and the heart cavity including other minor defects such as body size and a head bump. From these observations and from the Western blots analysis demonstrating a knockdown of ZMAN1 at 1mM (8ng/nl) of MO1, it appears that there is a strong correlation between the knockdown of the ZMAN1 protein and the developmental problems detected. However, a more extensive evaluation of these phenotypes is necessary to determine the specific cellular functions and pathways affected by the knockdown of ZMAN1.

Figure 3.19: Morphological comparison between microinjected and control zebrafish embryos. Embryos at the one-cell stage were collected and microinjected with MO1 at 8ng/nl (1.0mM, "**MO**") or with a standard control morpholino at 4ng/nl (0.5mM, "**Control**") at a volume of 1nl and 2nl respectively. Control uninjected wild-type ("**WT**") embryos were also collected at the one-cell stage. After microinjection, embryos were incubated at 27°C and observed during late embryonic development: late segmentation (24hour-post-fertilization (hpf)), early pharyngula (48hpf), late hatching (72hpf), and 5 days post-fertilization (dpf).

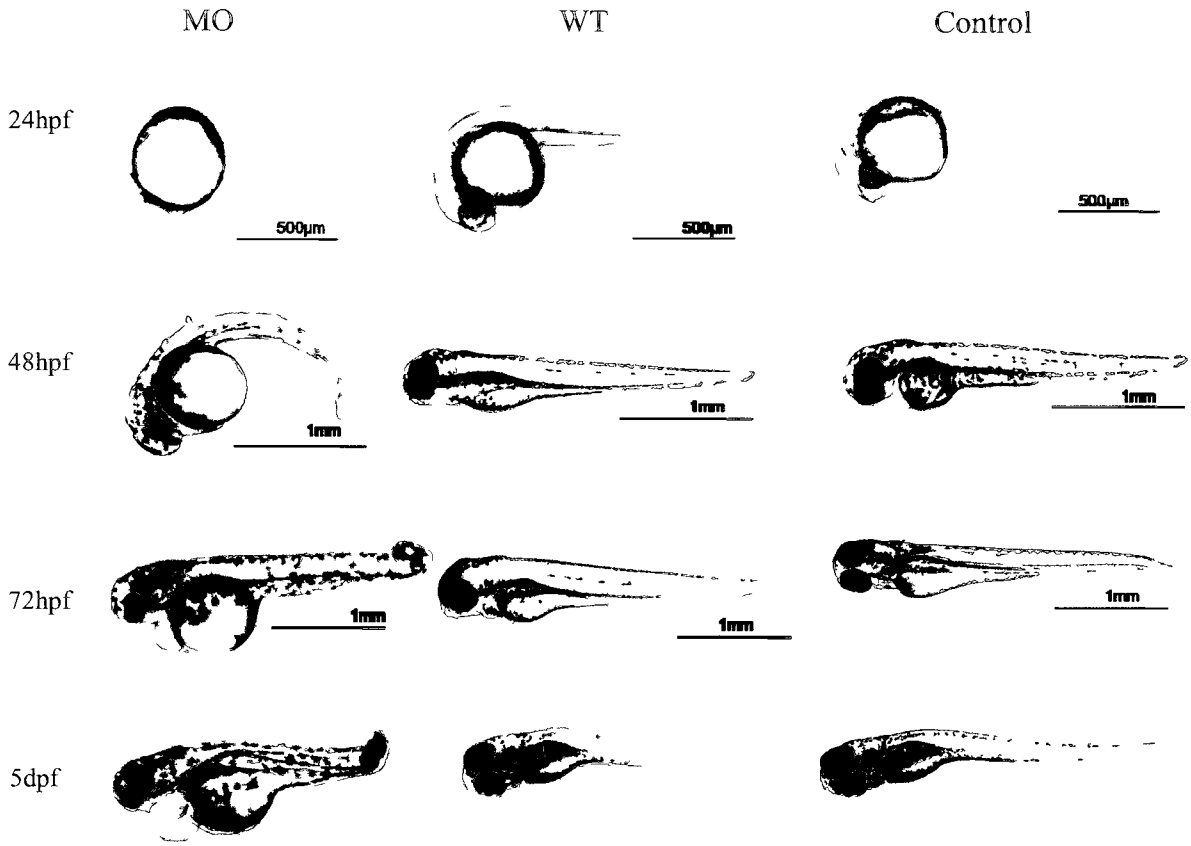
MO
WT
Control
24hpf
48hpf
72hpf
5dpf
500µm
500µm
500µm
1mm
1mm
1mm
1mm
1mm

Figure 3.20: Detailed analysis of ZMAN1 morphants. Embryos at the one-cell stage were collected and microinjected with MO1 (1mM) at a volume of 1nl. At 72 hpf, ZMAN1 injected embryos display several phenotypical defects. These are mainly: a pericardial edema (a, c and e), a twisted tail (arrows in a, c and e), a bigger yolk (arrows in c and e) and a hunchback (arrow in a). Severe phenotypes have extended intermediate cell mass (ICM) in their tail, indicated by red arrow in a. The severely affected embryos did not survive after 72 hours, while the less affected ones (c, e) survived past 5 days. (g) Image of an uninjected control wild-type embryo. Cardiac phenotypes of wild-type (h) and ZMAN1 knockdown (b, d and f) embryos are shown in detail.

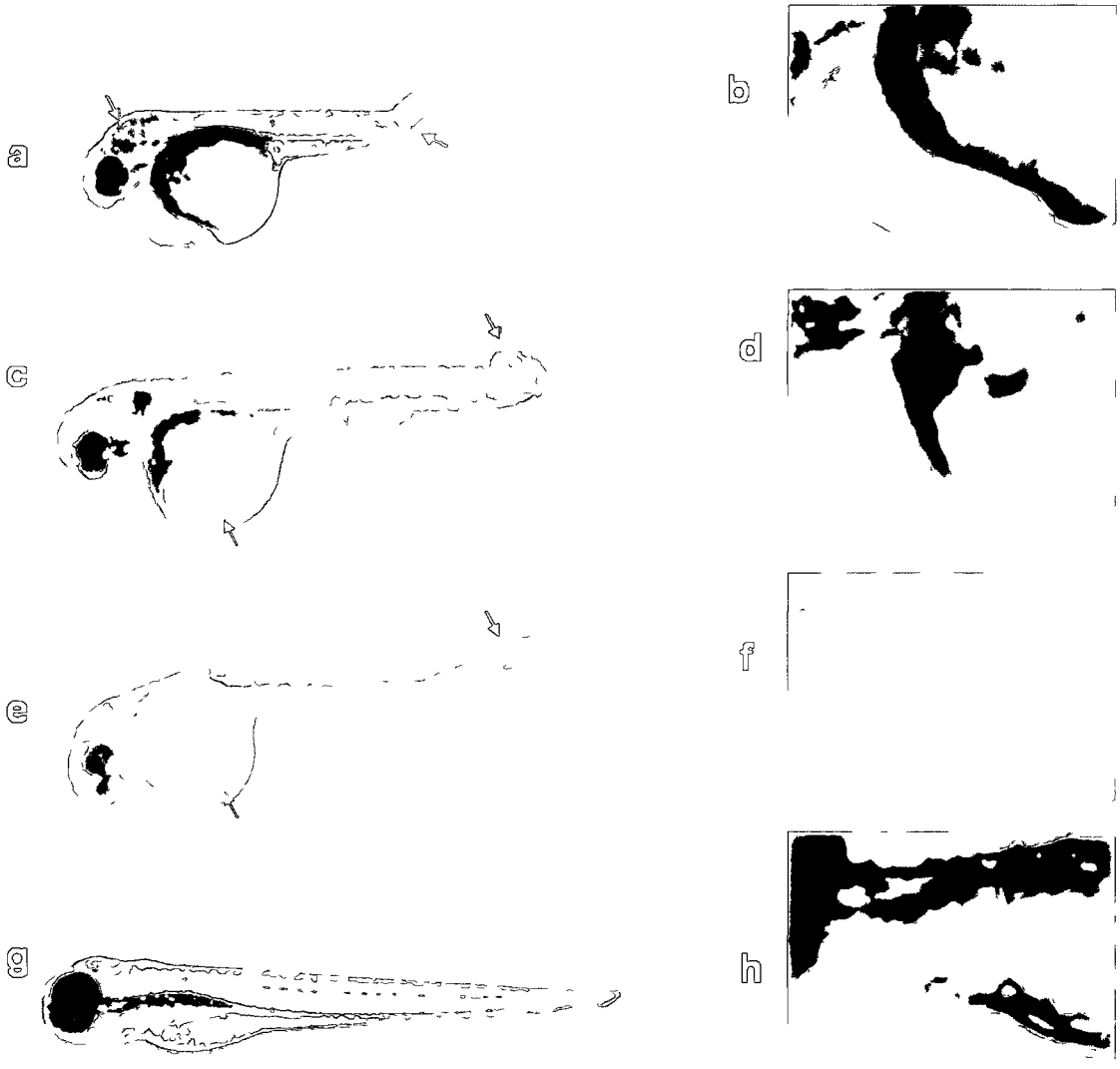
a
b
c
d
e
f
g
h

3.9. Phenotypical changes of fli-GFP transgenic zebrafish embryos after ZMAN1 knockdown

Following the identification of the phenotypical defects engendered by morpholino 1, another experiment involving microinjections of MO1 in combination with another morpholino oligonucleotide 2 (MO2) was performed. The sequence of MO2 is 25bp long and was designed to block translation by binding to the 5'untranslated region (UTR) of ZMAN1 at approximately 50bp upstream of the initiation codon (see Fig.3.14).

I also used a transgenic zebrafish line to help determine whether ZMAN1 knockdown affects the zebrafish vascular system. This transgenic line expresses the green fluorescent protein (GFP) in the vascular system. I relied on the transparency of zebrafish embryos to observe them under a fluorescent microscope in order to determine whether the blood vessels were affected by the knockdown. This transgenic fish line is called the fli-GFP transgenic line after the fli1 gene which leads GFP expression and which is expressed in the vascular endothelium of zebrafish (Ryun Cha & Weinstein, 2007).

One-cell embryos were collected and microinjected with MO1, MO2 and the control morpholino oligonucleotide (cont. MO). They were then allowed to recover at 27°C. Subsequent optical observations allowed for visualization of embryonic vascularisation in the control embryos and in the experimental ones.

At 24hpf, both morpholinos seem to produce the same effects. Embryos were under-developed and displayed a smaller body size and smaller eyes. As discussed earlier, these defects are considered off-targets and seem to be recurrent in most morpholino experiments (see Fig.3.21). However, after two and a half days, embryos

Figure 3.21: The effects of ZMAN1 knockdown on the blood vessels of zebrafish embryos. MO1, MO2, and the standard cont. MO were microinjected into transgenic zebrafish line (fli:EGFP) at a concentration of 1mM (8ng/nl) at a volume of 1nl. Embryos were examined and compared at 24hpf. Embryos injected with MO1 (**A**) and MO2 (**B**) developed slowly compared to the control ones (**C**). Bar represents 2mm.

A

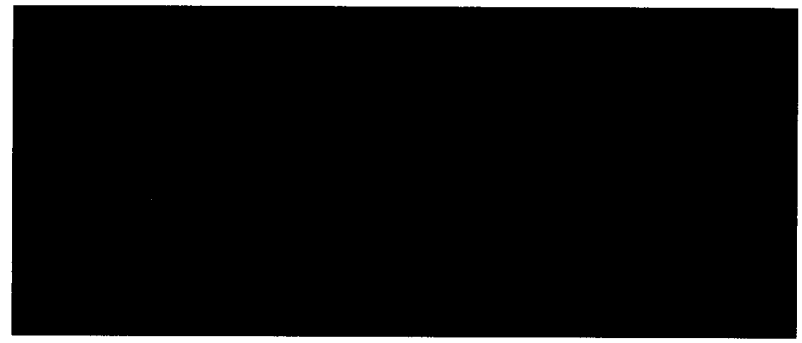

B

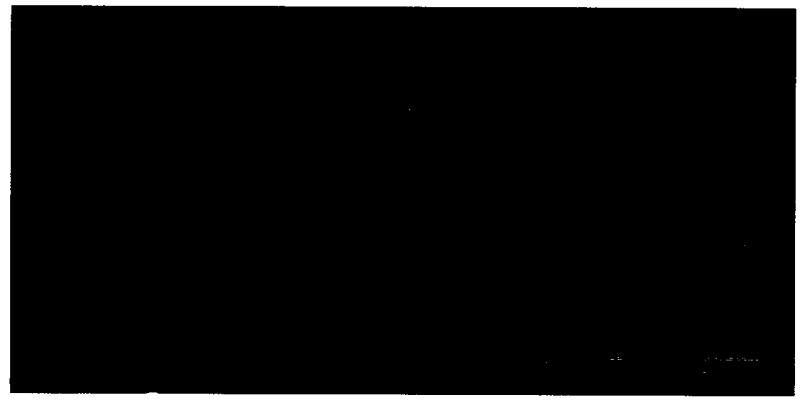

C

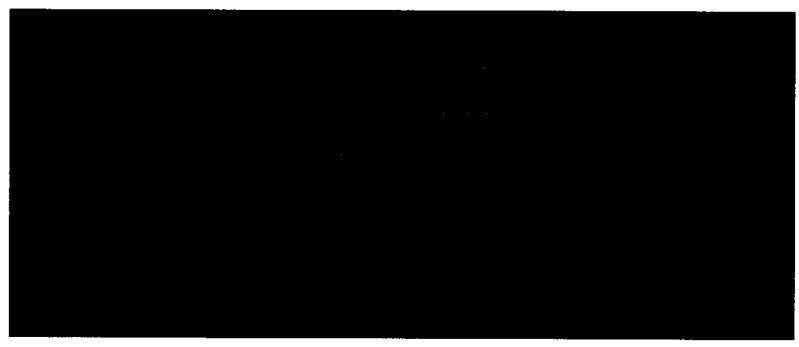

Figure 3.22: Vascular patterning of ZMAN1 knockdown zebrafish embryos. MO1 (**a**, **b**, **c**, **d**, **e** and **f**) and the standard cont. MO (**g**, **h** and **i**) were microinjected into transgenic fli:EGFP zebrafish embryos at a concentration of 1mM (8ng/nl) and a volume of 1nl. At 2.5 days, embryos were collected and examined under the fluorescent microscope. The parachordal vessels (PAV) and the dorsal longitudinal anastomotic vessel (DLAV) are poorly developed in the experimental embryos (**b**, **e**) compared to the controls (**h**). The intermediate cell mass (ICM) of the tail region is thickened and extended (arrows in **b** and **e**). The arrows in **e** and **h** point out to the intersegmental vessels (SE).

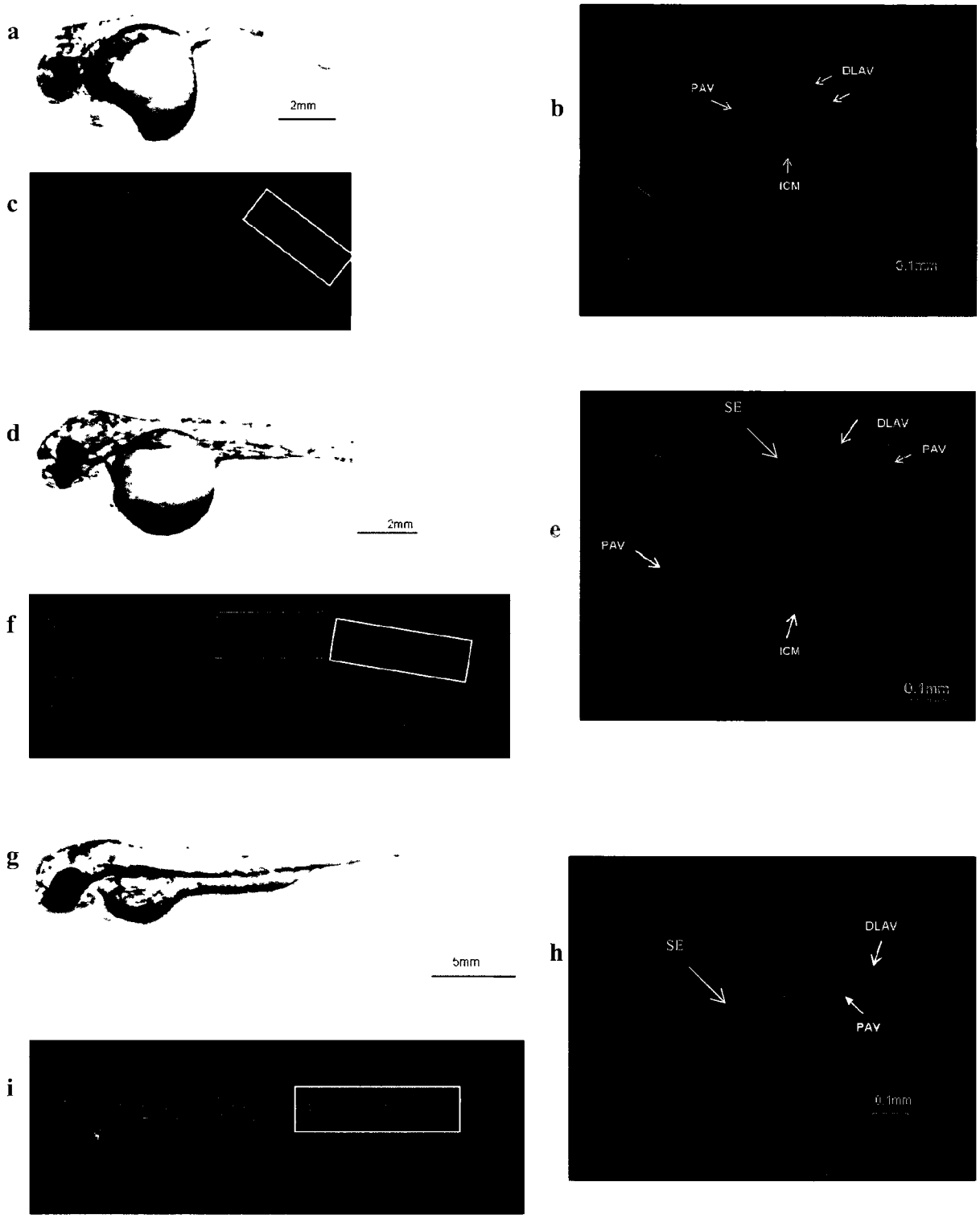
a
2mm
b
DLAV
PAV
ICM
c
d
2mm
e
SE
DLAV
PAV
PAV
ICM
f
g
5mm
h
SE
DLAV
PAV
i

Figure 3.23: Vascular patterning of ZMAN1 knockdown zebrafish embryos. MO2 (**a**, **b**, **c**, **d**, **e** and **f**) and the standard cont. MO (**g**, **h** and **i**) were microinjected into transgenic fli:EGFP zebrafish embryos at a concentration of 1mM (8ng/nl) and a volume of 1nl. At 2.5 days, embryos were collected and examined under the fluorescent microscope. The parachordal vessels (PAV) and the dorsal longitudinal anastomotic vessel (DLAV) are indicated in MO2 injected embryos compared to the controls (arrows in **h** and **e**).

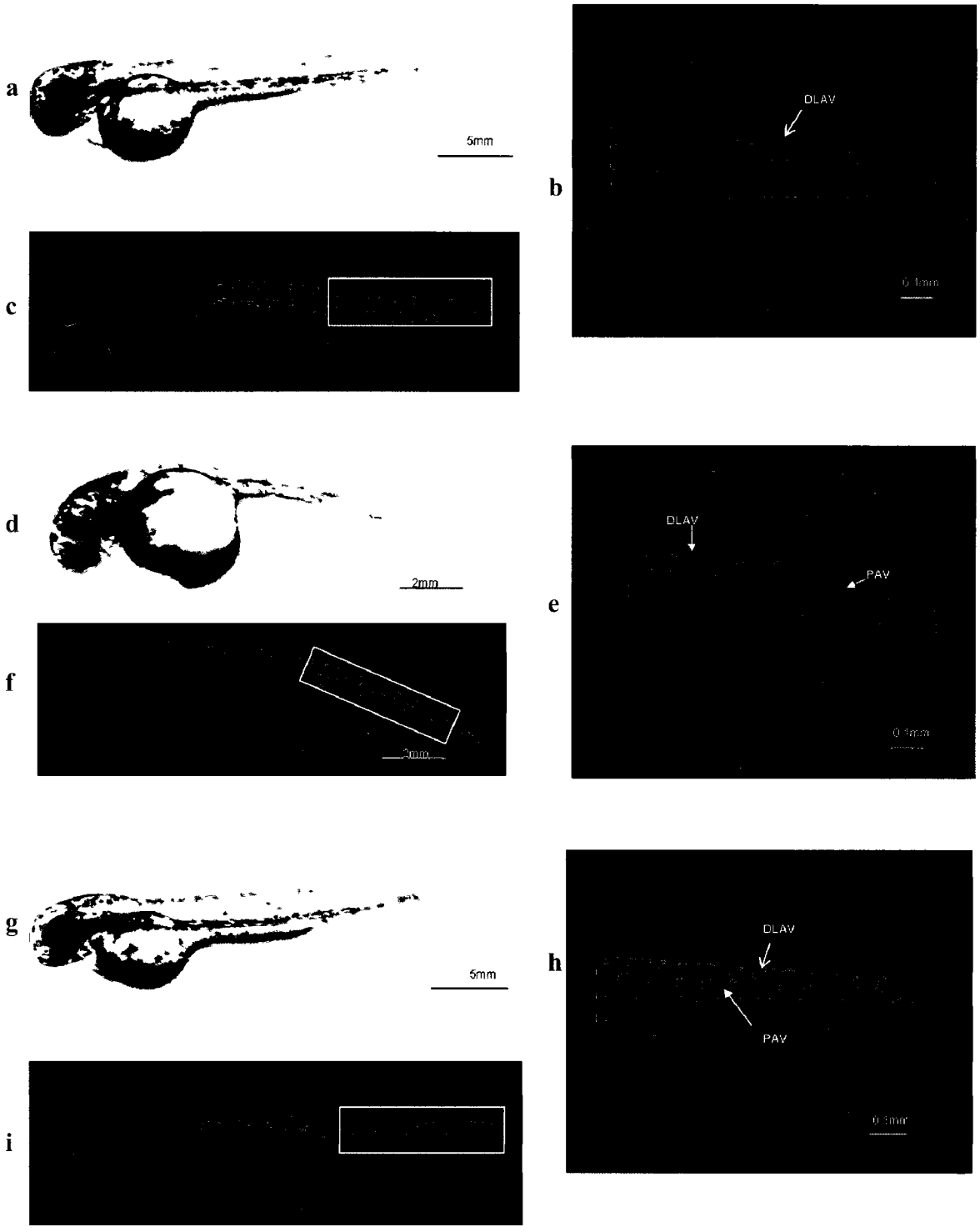
a
5mm
b
DLAV
c
d
2mm
e
DLAV
PAV
f
2mm
g
5mm
h
DLAV
PAV
i

injected with MO1 displayed vascular defects, and, in contrast with the controls, the blood vessels in the trunk region were disorganized and poorly formed.

When comparing specific structures such as the parachordal vessels (PAV) and the dorsal longitudinal anastomotic vessel (DLAV), we detected irregular and incomplete formation (Fig.3.22, panels b and e). The end of the tail region showed a thickened intermediate cell mass (ICM) (Fig.3.22, panels b and e) compared to the tails of the control embryos (Fig.3.22, panel h). Furthermore, lower GFP signalling was observed and may indicate a lower number of endothelial cells in the MO1-injected embryos. Due to the difficulty of observing the heart vessels, I was not able to determine whether these are affected by the knockdown. The same experiment using MO2 showed some vascular malformation in some embryos although the majority of these were not severely affected and about 60% had a normal phenotype (Fig.3.23, panels b and e). MO2 did not seem to work as well as MO1 in the knockdown of ZMAN1 expression and this could be due to several factors that will be discussed in Chapter IV (Discussion). The disorganized vascular patterning resulting from the knockdown of ZMAN1 with MO1 suggest a possible implication of ZMAN1 in vascular embryonic development, which will be discussed in more details in the following chapter.

4. DISCUSSION

4.1. Expression and distribution of ZMAN1 protein in adult and embryonic cells

Immunofluorescence microscopy on zebrafish AB9 somatic cells and on ZF4 embryonic cells demonstrated that ZMAN1 is targeted to the nuclear envelope periphery during interphase. This finding is consistent with previous studies and confirms that ZMAN1 is indeed an integral protein of the NE. Contrary to ZLAP2 proteins, the ZMAN1 protein relocalizes to the cytoplasm during prophase, prometaphase and late anaphase and does not appear to associate with mitotic chromosomes (Schoft *et al.,* 2003). As the cells progress into mitosis, ZMAN1 staining disappears from metaphasic cells, which confirms that ZMAN1 protein behaves differently from ZLAP2 during the cell cycle.

Previous data mentioned that zebrafish nuclear reassembly starts with the formation of karyomeres, which are vesicles with nuclear envelopes forming around a few chromosomes, and these karyomeres later merge to assemble as a single nuclear envelope (Schoft *et al.,* 2003). In the embryonic ZF4 cells, invagination of nuclei was detected with some intranuclear staining during interphase. It is generally assumed that invaginated nuclei are a feature of nuclear envelopes assembling through karyomere formation (Schoft *et al.,* 2003). Moreover, at the beginning of nuclear reassembly, small vesicles detected during late telophase in ZF4 cells might indicate that ZMAN1 is present in the membrane vesicles and that the nuclear envelope was only partially formed at this point. Furthermore, a recent study demonstrated that, MAN1, together with other integral proteins, is responsible for directing the ER membranes towards the reassembling NE by

interacting with chromatin (Anderson *et al.*, 2009). It is, therefore, possible that ZMAN1 is involved in the targeting of the membrane vesicles to the chromatin as was shown in human cells by Anderson *et al.* (2009). In the AB9 cells, vesicle formation was not detected, which might be due to the fact that it is a cell line originating from the adult zebrafish. In fact, vesicle formation during mitosis only exists during early stages of zebrafish development and does not persist in adult zebrafish (Roosen-Runge, 1939). Together, these results show that MAN1 clearly participates in nuclear organisation and occupies an important function in nuclear envelope reformation.

4.2. Expression and distribution of ZMAN1 transcripts and protein in adult zebrafish tissues

MAN1 was suspected to have an important function in tissue development. Several studies showed that MAN1 plays a key role in several laminopathies such as osteopoikilosis, Buschke-Ollendorff syndrome and melorheostosis (Lin *et al.*, 2005). It was then suggested that the loss of MAN1 is involved in tissue-specific defects (Lin *et al.*, 2005). Moreover, another recent study in *D. Melanogaster* showed that a loss of MAN1 resulted in wing malformation, sterility and locomotion difficulties (Pinto *et al.*, 2008), which also points to a relationship between the absence of MAN1 and tissue malformation. It was previously proposed that the *Xenopus* MAN1 plays a key function in the development of the central nervous system, as its transcripts were detected in the anterior central nervous system, the eyes, the otic vesicles and the bronchial arches of this species (Bengtsson, 2007). Therefore, at the beginning of my study, I based my experiments on the *Xenopus* observed expression pattern and I expected a similar expression in *D. rerio*.

When selecting tissues to visualize the distribution and expression of MAN1 protein and transcripts, I chose tissues originating from three different primary germ layers. Choosing tissues originating from three germ layers was intended to highlight the differences that may rise among them in correlation to MAN1 expression and localization or the lack thereof. Immunoblots of proteins isolated from the following tissues: brain (ectodermal); gills and liver (endodermal); and, kidney and muscle (mesodermal) demonstrated that MAN1 was detected in all these zebrafish tissues. The additional polypeptide detected in the brain tissue, which was apparently absent from the other tissues, was suspected to be either a MAN1 isoform or a posttranslational modification of this protein. The zebrafish genome is fully sequenced and available and when searching through the NCBI database there was no indication that the zebrafish MAN1 protein has an alternative isoform. Besides, no study had showed the existence of another version of MAN1. It is, therefore, very unlikely that the polypeptide detected is an isoform. Moreover, the guinea pig ZMAN1 serum used in the present study is polyclonal and another possible explanation to this additional polypeptide is that the polyclonal serum recognizes an epitope present only in the brain. Northern experiments might be the key to confirming the identity of this polypeptide.

Immunoblots also revealed that expression of MAN1 seemed ubiquitous amongst all adult tissues tested. Interestingly, a much lower protein expression was observed in the muscle tissue and this observation might indicate that the MAN1 protein may be inhibited in this tissue. Moreover, the loss of MAN1 was demonstrated to be detrimental to tissues of mesodermal origin such as skin, bone and connective tissues (Lin *et al.*, 2005). Therefore, there seems to be a link between the mesodermal tissues affected by

MAN1-related diseases and the observation that ZMAN1 shows a differential expression level in the muscle, which is also a tissue of mesodermal origin.

At the RNA level, RT-PCR analyses indicated that the transcript coding for ZMAN1 was present in all three tissues (brain, gills and muscle) selected for examination. Compared to the housekeeping gene, EF1α, the ZMAN1 transcripts seemed to be equally expressed in these tissues. In fact, it seemed that the muscle tissue possessed similar levels of ZMAN1 to the other two tissues. At first, this result seems contradictory to the previous immunoblotting analyses, yet RNA levels do not necessarily translate to similar protein levels. In fact, several factors may result in differences between RNA and protein expression levels. One must take into account post-trancriptional modifications, the half-life of the protein, and also the sensitivity of MAN1 to proteases in the muscle tissue. Moreover, because of the limitations that conventional RT-PCR presents (low sensitivity, saturated PCR cycles, etc.), the results of the present study are only semi-quantitative in nature, and, therefore, other methods such as quantitative real time PCR would be more reliable in terms of quantifying RNA expression levels (Walker *et al.*, 2003).

Localizing ZMAN1 by immunofluorescence microscopy within specific structures of the tissue tested affords a better understanding of ZMAN1 functions in these structures. Immunolabelling of brain, gills and muscle tissues from the adult zebrafish allowed visualization of ZMAN1 distribution. The staining was predominant and ubiquitous in the brain tissue where MAN1 protein clearly localized to the nuclear periphery of the brain nuclei. Also, nuclear staining was observed in the majority of the gill nuclei. These two observations confirm the previous idea that the MAN1 protein is

targeted to the nuclear envelope and is ubiquitously distributed in the brain and gills tissues. By comparison, the muscle tissue displayed very low MAN1 staining. This low expression of the MAN1 protein in the muscle tissue was expected given the previous immunoblot experiments. Immunoblotting analyses and immunolocalization results reinforce the hypothesis suggested earlier of a possible inhibition of ZMAN1 protein in the muscle of adult zebrafish.

Emerin is another protein of the LEM family. It is usually found in muscle tissues and its loss causes Emery-Dreifuss muscular dystrophy (EDMD) (Mansharamani & Wilson, 2005). MAN1 is very likely to play roles similar to emerin and may even be regulated by this protein because of its ability to interact with emerin (Mansharamani & Wilson, 2005). Therefore, based on the documented relationship between MAN1 and emerin, the low expression of MAN1 observed in the muscle may be a consequence of a regulatory effect played by emerin on MAN1 in this tissue. Emerin is essential in the muscle tissue and is also a binding partner of MAN1. As a result, emerin might have a role in inhibiting MAN1 in the muscle causing it to be downregulated in the adult. EDMD disease is a direct consequence of the loss of emerin, and it is then possible that MAN1 is overexpressed in the muscle tissue of individuals affected by this illness. According to my data and to previous studies on emerin/MAN1 interactions, I suspect a specific involvement of ZMAN1 in the muscle tissue of the adult zebrafish, and a possible indirect role of this protein in the EDMD disease. However, this speculation must be further investigated. One strategy to accomplish this could involve the knockdown of emerin and subsequent analyses of ZMAN1 expression profiles and distribution in the morphants.

4.3. Expression and distribution of ZMAN1 protein during embryonic development

There is evidence that, at the tailbud stage, *Xenopus* MAN1 expression is restricted to the anterior central nervous system and other ectodermal tissues (Osada *et al.*, 2003). Detection of MAN1 transcripts at later stages showed that in this species, MAN1 is downregulated (Osada *et al.,* 2003). These results encouraged me to investigate the expression of MAN1 protein during early embryogenesis of zebrafish.

Western immunoblots of early stages of zebrafish embryogenesis demonstrated that ZMAN1 is already present in embryos at the early blastula stage, which is one of the earliest stages of development. I therefore concluded that ZMAN1 is maternally inherited. In fact, genome activation occurs in the embryo at mid-blastula. Before this stage, the proteins and RNA transcripts detected are maternally inherited and represent the only building blocks available to the young embryo (Schier, 2007). Interestingly, ZLAP2 is also another LEM protein inherited maternally by the young embryo (Schoft *et al.*, 2003). The inherited ZMAN1 protein is probably involved in necessary cellular mechanisms early on in zebrafish development and fulfills specific functions at that stage. As previously mentioned, it was shown that LAP2, as well as MAN1, interacts with chromatin (Schoft *et al.*, 2003; Bengsston, 2007). Therefore, a possible role of these two LEM proteins is to direct nuclear reassembly during oogenesis. ZMAN1 protein was detected at similar levels in all four developmental stages (late cleavage, 2hpf; during blastula, 4hpf; during gastrula, 8hpf; and, at the early pharyngula stage, 24hpf) tested. Note that the polypeptide mentioned previously that seemed to be present exclusively in the brain tissue was not detected in these very young embryos. An explanation of this observation is that the brain starts developing just before the pharyngula period and

continues during early pharyngula (Kimmel *et al.*, 1995). Therefore, the polypeptide may not be yet expressed in the primitive embryonic brain.

By immunostaining cleavage (2hpf), mid-blastula (4hpf) and mid-pharyngula (36hpf) embryos, I aimed to determine the fate of ZMAN1 protein during embryonic mitosis. However, due to heavy background staining and difficulties staining cells in thick tissues, visualization of the behaviour of ZMAN1 protein turned out to be a challenge. As expected, ZMAN1 was detected at the nuclear envelope during interphase in cleavage, mid-blastula and pharyngula embryos. In contrast, at prophase, prometaphase and anaphase cleavage, embryonic cells showed diffused ZMAN1 staining and distribution in the cytoplasm. This observation confirms the cellular immunostaining results in which ZMAN1 displayed a cytoplasmic distribution in most mitotic stages except for interphase, late telophase and cytokinesis. For the blastula embryos, ZMAN1 was observed diffusely in the cytoplasm during prophase, anaphase and telophase. However, no staining was observed in late prometaphase, metaphase and anaphase. The lack of staining during metaphase confirms the previous cellular immunostaining experiments; however, no staining in prometaphase and anaphase does not. This finding could mean that ZMAN1 behaves differently in the animal compared to the AB9 and ZF4 cell lines, or it could simply be due to the poor immunofluorescence images I obtained at this stage. Mid-pharyngula (36hpf) is an interesting stage to analyze ZMAN1 distribution since most tissues are already formed. Unexpectedly, ZMAN1 protein was detected throughout the entire embryo but with much stronger detection in the tail region at this stage.

When comparing this result with the previous data, which demonstrate a very low expression of ZMAN1 protein in the muscle tissue, it appears that the strong expression of ZMAN1 in the tail region at the pharyngula stage contradicts the much lower expression detected later on in the adult zebrafish. Nevertheless, ZMAN1 may occupy an essential role within the tail muscle at mid-pharyngula explaining its higher levels in that region at that stage. The drop of ZMAN1 protein expression in the same region (tail muscle) noticed in the adult zebrafish could be the result of down-regulation of this protein due to a lesser need for its function in adult life. In fact, as mentioned previously, during early *Xenopus* embryogenesis, XMAN1 directs dorsal-ventral axis determination by associating with Smad1 or Smad5 and consequently antagonizing BMP signalling (Osada *et al.*, 2003). Moreover, analysis of XMAN1 transcripts showed a high mRNA expression during early embryogenesis with an expression drop around stage 45 (a late stage of embryogenesis), which corresponds with my findings. Therefore, another explanation of the high expression of MAN1 at pharyngula and the much lower expression observed later on, could involve MAN1 being upregulated to inhibit BMP or TGFβ pathway at mid-pharyngula stage, and downregulated in the adult zebrafish to allow the expression of the genes targeted by the BMP/TGFβ cascade. It is also during mid-pharyngula that the tail acquires motility and pigmentation. In addition, in zebrafish, BMP is a significant promoter of posterior tail and blood vessel formation (Holley, 2006). Therefore, ZMAN1 could be a regulator of the BMP pathway during tail and blood vessel morphogenesis. Emerin, the essential protein for proper muscle function, could also be involved in the regulation of ZMAN1 by acting as an agonist of ZMAN1 at mid-pharyngula and as an inhibitor during the adult zebrafish. It is, however, important to

mention that the regulation of BMP/TGFß by MAN1 was demonstrated in human cells, *Xenopus, Mus musculus* and *Drosophila* but was not investigated in *D. rerio*.

4.4. Effects of ZMAN1 knockdown on the development of zebrafish embryos

Microinjection of antisense morpholino oligonucleotide was the technique used to determine the structures affected by the knockdown of ZMAN1 in the zebrafish embryo, to further identify the specific roles occupied by this integral protein. By microinjecting an antisense morpholino oligonucleotide against ZMAN1 protein in 1-2 cell stage embryos, I was able to efficiently knockdown ZMAN1 expression.

Evidence for the decrease of ZMAN1 expression was obtained by Western analysis where ZMAN1 expression profiles in embryos injected with 0.5 mM (4 ng/nl), 1 mM (8 ng/nl) and 1.5 mM (12 ng/nl) were compared to the wild-type uninjected embryos. This analysis also revealed the existence of three polypeptides of molecular mass 170 kDa, 150 kDa and 52 kDa. The latter seems to be a product of degradation while the two former are probably posttranslational modifications of ZMAN1 recognized by the polyclonal serum or are isoforms of this protein, which is however a less likely hypothesis. Moreover, it appears that the polypeptide of 150 kDa mass might be the same unidentified polypeptide detected earlier in the brain tissue. Interestingly, none of these two high molecular mass polypeptides are detected at the early pharyngula stage (24 hpf). The absence of the 150 kDa polypeptide may indicate that in 24-hour old embryos several brain structures are not yet present in this tissue and may be part of the brain at 48 hours, thus detection of the high molecular weight polypeptide becomes possible.

Another interesting observation that I made from this Western blot is that even at high injection doses ZMAN1 protein was not completely eliminated and was

approximately knocked down to 25% of its initial expression. Therefore, traces of the protein remain functional in the embryo so that the knockdown effects can be visualized without an excessive number of embryonic deaths.

Moreover, additional data were collected on embryonic survival rates. When microinjecting three different concentrations of MO1 in zebrafish embryos, survival rate in these morphants could be compared to the wild type (WT) uninjected embryos and to those injected with the standard control MO. While a higher concentration of MO1 appeared to decrease ZMAN1 expression, as discussed above, it seemed that higher concentrations were also linked to embryonic deaths. I observed the highest number of deaths with the highest injection dose (12ng/nl). There could be two explanations for this observation. First, ZMAN1 knockdown could provoke these deaths given that it was found in most adult tissues and embryonic stages tested, ZMAN1 seems to have an important function and its loss could be detrimental. Another explanation to this phenomenon is that larger amounts of morpholino could be inducing the p53 pathway responsible for the off-target effects observed with morpholino injections (Robu *et al.*, 2007). Another hypothesis is that the effects are a by-product of non-specific microinjection errors. At 48hpf, in comparison with 25% mortality in the control group, approximately 30% of MO1 injected embryos were dead for the 0.5mM and the 1mM injection doses, whereas 50% did not survive in the 1.5mM group. Since mortality is similar in the control group and in the MO1 injected embryos for the 1.5mM dose, most of the deaths observed at this injection dose can be attributed to toxicity caused by high morpholino injection doses. Surprisingly, although the number of embryos displaying a morphotype was expected to be the highest with the highest injection dose (1.5mM,

12ng/nl), I observed a higher number with the 1mM (8ng/nl) injection dose Thus, the highest injection dose did not induce the highest number of abnormal embryos However, this could be explained by the excessive number of deaths observed with the 1 5mM concentration

To check whether the MO1 sequence matches another site (other than ZMAN1) in the zebrafish genome, I relied on a BLASTn search (NCBI website) BLASTn compares the sequence of interest to other sequence present in the genome not only in zebrafish but also in other species I also used an option of this algorithm to make the search less stringent so that I can detect sequences that are related but not identical to my MO1 sequence No matches were detected in zebrafish by this BLAST search, which is a good indicator that the MO1 sequence is not found elsewhere in the zebrafish genome and thus will be less likely to show non-specific binding However, since binding of morpholino oligos depends on many different factors such as temperature, pH, and other conditions, there is still a possibility that MO1 inhibits another gene *in vivo*, in addition to ZMAN1 Besides, microinjection manipulations do not guarantee a precise and reproducible injection volume, which is another challenge of this technique (Eisen & Smith, 2008) Together, Western immunoblotting and survival rates analyses seem to confirm an efficient knockdown of ZMAN1 protein by MO1 but do not exclude the possibility that MO1 also targets another gene

The two major phenotypic traits that seemed to associate with ZMAN1 knockdown were a twisted/curved tail region and an enlarged heart cavity Based on the previous data, physiological defects in the trunk region were expected, since ZMAN1 seems to be highly expressed in the tail at the pharyngula stage, which may be due to an important

function it may occupy in that structure. Moreover, since BMP is a major player in tail formation, ZMAN1 knockdown may have provoked an overexpression of the BMP pathway resulting in abnormal trunk formation. The pericardium malformation observed in the morphant could indicate an implication of ZMAN1 in heart formation. In fact, two recent studies were conducted in mice and demonstrated a role for MAN1 in heart formation (Ishimura *et al.*, 2008) as well as in blood vessel development (Ishimura et al., 2006). Therefore, the enlarged pericardium may be an indication of the role of ZMAN1 in the development of this structure.

I also disrupted ZMAN1 protein by microinjecting MO1 in a transgenic zebrafish line (fli:EGFP). This transgenic line allows for visualization of the vasculature through the green fluorescent protein (GFP). Analysis was done at the early pharyngula stage (24hpf) as well as at the end of the pharyngula (2.5dpf). The choice of the pharyngula developmental stage was based on the interesting results in the Western immunoblots and immunostaining experiments.

To reduce misinterpretation due to off-target effects, it is recommended to test the validity of the phenotypic anomalies observed when injecting MO1 by using an additional morpholino oligo (Eisen & Smith, 2008). Most morpholino injections lead to non-target phenotypes which can include cell death and other complications. Activation of the p53-mediated apoptosis pathway is one major cause for these off-target effects. Recent studies have successfully deactivated this pathway by coinjecting a morpholino against p53 (Robu *et al.,* 2007). Another antisense morpholino oligo (MO2) was microinjected in the fli fish embryos to serve this purpose. However, MO2-injected embryos did not display the drastic phenotypes observed with MO1; neither was it

apparent that the vasculature was disrupted These observations could have several explanations, thus further investigation involving techniques such as Western immunoblotting, immunofluorescence microscopy and *in situ* hybridization will be necessary to characterize the specificity of MO2

MO1 morphants displayed a developmental delay, which was observed in the controls also, at 24hpf There was no other visible trait of ZMAN1 knockdown at this early stage of pharyngula However, at 2 5 days, disorganized vasculature structures of the tail/trunk region were apparent in the MO1 injected embryos In fact, the parachordal vessels (PAV) and the dorsal longitudinal anastomotic vessel (DLAV) seemed poorly developed and the intermediate cell mass (ICM) of the tail region was thickened and extended A study involving crim1 gene, which is antagonistic to BMP signalling in zebrafish, showed that crim1 morphants have a bent tail and notochord malformation Crim1 was also implicated in the loss of the DLAV and produces an expansion of the ICM demonstrating its involvement in somitogenesis and vasculature development (Kinna *et al* , 2006) ZMAN1 knockdown could have induced poor regulation of BMP signals, causing the overexpression of the downstream BMP gene targets From these data, it is possible that the twisted tails and enlarged heart cavities observed point to an important role played by ZMAN1 in tail vasculogenesis, as well as, in the heart and trunk morphogenesis

Altogether, my results indicate that ZMAN1 seems to possess significant functions during zebrafish development Further experiments with an additional morpholino targeting ZMAN1, in addition to *in situ* hybridization and rescue microinjections, will have to be done in order to get a better grasp on the structures affected by ZMAN1 and

the implications this protein may have on the early development and the adult life of zebrafish.

CONCLUSIONS

In summary, I have demonstrated a possible developmental role for ZMAN1 in the muscle tissue of the tail region of zebrafish. ZMAN1 may play an essential function in the tail/posterior trunk of mid-pharyngula embryos based on its intense *in vivo* localization in this region at this stage. On the other hand, I have observed low expression and distribution patterns in adult muscle tissue, which suggests a down-regulation of ZMAN1 at the adult stage. Cellular localization of ZMAN1 suggests a key role for this protein during nuclear envelope reassembly. Moreover, I have provided evidence of phenotypical anomalies in ZMAN1 morphants in the trunk region and in the heart cavity, which may indicate an essential function of this protein in these structures during early embryogenesis. The analysis of the tail vasculature morphogenesis showed highly disorganized blood vessel structure, as previously demonstrated with the BMP antagonist Crim1 gene knock-down in which similar morphotypes to ZMAN1 morphants were also observed (Kinna *et al.,* 2006). Finally, there appears to be a strong correlation between the up-regulation of ZMAN1 in the tail region at mid-pharyngula, the downregulation observed in the adult muscle tissue, the abnormal curved tail phenotype and the disorganized and primitive tail vasculature structure, which suggest that ZMAN1 protein plays a key regulatory function in zebrafish adults and embryos.

REFERENCES

Anderson, D.J., J.D. Vargas, J.P. Hsiao, M.W. Hetzer. (2009). Recruitment of functionally distinct membrane proteins to chromatin mediates nuclear envelope formation in vivo. *Journal of Cell Biology* **186**: 183-91.

Bengtsson, L. (2007). What Man1 does to the Smads TGF/BMP signalling and the nuclear envelope. *The FEBS Journal* **274,** 1374–1382.

Bengtsson, L., and K. L. Wilson. (2004). Multiple and surprising new functions for Emerin, a nuclear membrane protein. *Current Opinion in Cell Biology* **16,** 73-79.

Bione, S., E. Maestrini, S. Rivella, M. Mancini, S. Regis, G. Romeo, and D. Toniolo. (1994). Identification of a novel X-linked gene responsible for Emery-Dreifuss muscular dystrophy. *Nature Genetics* **8,** 323-327.

Brachner, A., S. Reipert, R. Foisner, and J. Gotzmann. (2005). LEM2 is a novel MAN1-related inner nuclear membrane protein associated with A-type lamins. *Journal of Cell Science* **118,** 5797-5810.

Brent, L. J. N., and P. Drapeau. (2002). Targeted 'knockdown' of channel expression in vivo with an antisense morpholino oligonucleotide. *Neuroscience* **114,** 275-278.

Cai, M., Y. Huang, R. Ghirlando, K. L. Wilson, R. Craigie, and G. M. Clore. (2001). Solution structure of the constant region of nuclear envelope protein LAP2 reveals two LEM domain structures: one binds BAF and the other binds DNA. *The EMBO Journal* **20,** 4399 – 4407.

Caputo, S., J. Couprie, I. Duband-Goulet, E. Konde, F. Lin, S. Braud, M. Gondry, B. Gilquin, H. J. Worman, and S. Zinn-Justin. (2006). The carboxyl-terminal nucleoplasmic region of MAN1 exhibits a DNA binding winged helix domain. *The Journal of Biological Chemistry* **281,** 18208-18215.

Cha, Y. R., and B. M. Weinstein. (2007). Visualization and experimental analysis of blood vessel formation using transgenic zebrafish. *Birth Defects Research* Part *C: Embryo Today: Reviews* **81**, 286-296.

Cohen, T. V., O. Kosti, and C. L. Stewart. (2007). The nuclear envelope protein MAN1 regulates TGF signalling and vasculogenesis in the embryonic sac. *Development* **134**, 1385-1395.

D'Angelo, M. A., and M. W. Hetzer. (2008). Structure, dynamics and function of nuclear pore complexes. *Trends in Cell Biology* **18**, 456-466.

Denver, R.J., S. Pavgi, and Y. Shi. (1997). Thyroid Hormone-dependent Gene Expression Program for Xenopus Neural Development. *The Journal of Biological Chemistry,* **272**, 8179-8188.

Dooley, K., and L. I. Zon. (2000). Zebrafish: a model system for the study of human disease. *Current Opinion in Genetics & Development* **10,** 252-256.

Driever, W., and Z. Rangini. (1993).Characterization of a cell line derived from zebrafish (Brachydanio rerio) embryos. *In Vitro Cellular & Developmental Biology - Animal* **29**, 749-754.

Eisen, J. S., and J.C. Smith. (2008). Controlling morpholino experiments: don't stop making antisense. *Development* **135**, 1735-1743.

Foisner, R., and L. Gerace. (1993). Integral membrane proteins of the nuclear envelope interact with lamins and chromosomes, and binding is modulated by mitotic phosphorylation. *Cell* **73,** 1267-79.

Georgatos, S. D. (2001). The inner nuclear membrane: simple, or very complex? *The EMBO Journal* **20,** 2989–2994.

Gruenbaum, Y., A. Margalit, R. D. Goldman, D. K. Shumaker, and K. L. Wilson. (2005). The nuclear lamina comes of age. *Nature Reviews Molecular Cell Biology* **6,** 21-31.

Hausen, P., Y.H. Wang, C. Dreyer, and R. Stick (1985) Distribution of nuclear proteins during maturation of the Xenopus oocyte. *Journal of Embryology & Experimental Morphology*. **89,** 17-34.

Hetzer, M. W., T. C. Walther, and I. W. Mattaj. (2005). Pushing the envelope: structure, function, and dynamics of the nuclear periphery. *Annual Review of Cell and Developmental Biology* **21**, 347-380.

Hirano, Y., Y. Iwase, K. Ishii, M. Kumeta, T. Horigome, and K. Takeyasu. (2009). Cell-cycle dependent phosphorylation of MAN1. *Biochemistry* **48,** 1636-1643.

Holaska, J. M., K. K. Lee, A. K. Kowalski, and K. L. Wilson. (2003). Transcriptional repressor germ cell-less (GCL) and barrier to autointegration factor (BAF) compete for binding to emerin in vitro. *Journal of Biological Chemistry* **278,** 6969-6975.

Holley, S.A. (2006). Specification of trunk and tail somites in the zebrafish blastula Anterior-posterior differences in vertebrate segments. *Genes Dev.* **20**, 1831-1837.

Holmer, L., H. J. Worman. (2001). Inner nuclear membrane proteins: functions and targeting. *Cellular and Molecular Life Sciences* **58,** 1741-1747.

Ishimura, A., J. K. Ng, M. Taira, S. G. Young, and S. Osada. (2006). Man1, an inner nuclear membrane protein, regulates vascular remodelling by modulating transforming growth factor signalling. *Development* **133,** 3919-3928.

Ishimura, A., S. Chida, and S. Osada. (2008). Man1, an inner nuclear membrane protein, regulates left-right axis formation by controlling nodal signaling in a node-independent manner. *Developmental Dynamics* **237,** 3565-3576.

Jesuthasan, S., and U. Strähle. (1996). Dynamic microtubules and specification of the zebrafish embryonic axis. *Current Biology* **7,** 31–42.

Kane, D. A., R. M. Warga, and C. B. Kimmel. (1992). Mitotic domains in the early embryo of the zebrafish. *Nature* **360,** 735-737.

Kimmel, C. B. (1989). Genetics and early development of zebrafish. *Trends in Genetics* **5,** 283-288.

Kimmel, C. B., W. W. Ballard, S. R. Kimmel, B. Ullmann, and T. F. Schilling. (1995). Stages of embryonic development of the zebrafish. *Developmental Dynamics* **203,** 253-310.

Kinna, G., G. Kolle, A. Carter, B. Key, G. J. Lieschke, A. Perkins and M.H. Little. (2006) Knockdown of zebrafish crim1 results in a bent tail phenotype with defects in somite and vascular development *Mechanisms of Development*.**123**, 277-287.

Kvam, E., and D. S. Goldfarb. (2006). Structure and function of nucleus-vacuole junctions: outer-nuclear-membrane targeting of Nvj1p and a role in tryptophan uptake. *Journal of Cell Science* **119**, 3622-3633.

Lee, K. K., T. Haraguchi, R. S. Lee, T. Koujin, Y. Hiraoka, and K. L. Wilson. (2001). Distinct functional domains in emerin bind lamin A and DNA-bridging protein BAF. *Journal of Cell Science* **114,** 4567-4573.

Lin, F., D. L. Blake, I. Callebaut, I. S. Skerjanc, L. Holmer, M. W. McBurney, M. Paulin-Levasseur, and H. J. Worman. (2000). MAN1, an inner nuclear membrane protein that shares the LEM domain with lamina-associated polypeptide 2 and emerin. *The Journal of Biological Chemistry* **275,** 4840-4847.

Lin, F., J. M. Morrisson, W. Wu, and H. J. Worman. (2005). MAN1, an integral protein of the inner nuclear membrane, binds Smad2 and Smad3 and antagonizes transforming growth factor-beta signaling. *Human Molecular Genetics* **14,** 437–445.

Liu, J., K. K. Lee, M. Segura-Totten, E. Neufeld, K. L. Wilson, Y. Gruenbaum. (2003). MAN1 and emerin have overlapping function(s) essential for chromosome segregation and cell division in Caenorhaditis elegans. *Proceedings of the National Academy of Sciences* **100,** 4598-4603.

Mansharamani, M. and K. L. Wilson. (2005). Nuclear membrane protein MAN1: direct binding to emerin in vitro and two modes of binding to BAF. *The Journal of Biological Chemistry* **280,** 13863-13870.

Margalit, A., S. Vlcek, Y. Gruenbaum, and R. Foisner. (2005). Breaking and making of the nuclear envelope. *Journal of Cellular Biochemistry* **95,** 454–465.

Martins, S., S. Eikvar, K. Furukawa, and P. Collas. (2003). HA95 and LAP2 beta mediate a novel chromatin-nuclear envelope interaction implicated in initiation of DNA replication. *The Journal of Cell Biology* **160,** 177-188.

Milan, D. J., and C. A. Macrae. (2008). Zebrafish genetic models for arrhythmia. *Progress in Biophysics and Molecular Biology* **98,** 301-308.

Nusslein-Volhard, C., and R. Dahm. (2002). Zebrafish: a practical approach. *Oxford University Press, USA* **ISBN**-13: 9780199638086.

Osada, S., S. Y. Ohmori, and M. Taira. (2003). XMAN1, an inner nuclear membrane protein, antagonizes BMP signaling by interacting with Smad1 in Xenopus embryos. *Development* **130,** 1783–1794.

Ostlund, C., and H. J. Worman. (2003). Nuclear envelope proteins and neuromuscular diseases. *Muscle Nerve* **27,** 393-406.

Pan, D., L. D. Estévez-Salmerón, S. L. Stroschein, X. Zhu, J. He, S. Zhou, and K. Luo. (2005). The integral inner nuclear membrane protein MAN1 physically interacts with the R-Smad proteins to repress signaling by the transforming growth factor-β superfamily of cytokines. *The Journal of Biological Chemistry* **280,** 15992-16001.

Paulin-Levasseur, M., D. L. Blake, M. Julien, and L. Rouleau. (1996). The MAN antigens are non-lamin constituents of the nuclear lamina in vertebrate cells. *Chromosoma* **104,** 367-379.

Pinto, B. S., S. R. Wilmington, E. E. L. Hornick, L. L. Wallrath, and P. K. Geyer. (2008). Tissue-specific defects are caused by loss of the Drosophila MAN1 LEM domain protein. *Genetics* **180,** 133-145.

Prüfert, K., C. Winkler, M. Paulin-Levasseur, and G. Krohne. (2004). The LAP2 genes of zebrafish and chicken: no LAP2 a isoform is synthesized by non mammalian vertebrates. *European Journal of Cell Biology* **83,** 403-411.

Raju, G. P., N. Dimova, P. S. Klein, and H. C. Huang. (2003). SANE, a novel LEM domain protein, regulates bone morphogenetic protein signaling through interaction with Smad1. *Journal of Biological Chemistry* **278,** 428–437.

Robu, M.E., J.D. Larson, A. Nasevicius, S. Beiraghi, C. Brenner, S.A. Farber, S.C. Ekker. (2007) p53 activation by knockdown technologies. *PLoS Genetics* **25**, e78.

Roosen-Runge, E.C. (1939). Karyokinesis during cleavage of the zebrafish *Brachydanrio rerio*. The Biological Bulletin **77**: 79-91.

Salina, D, K. Bodoor, P. Enarson, W. H. Raharjo, and B. Burke. (2001). Nuclear envelope dynamics. *Biochemistry and Cell Biology* **79**, 533-542.

Schier, A. F. (2007). The Maternal-Zygotic Transition: Death and Birth of RNAs. *Science* **316**, 406-407.

Schmitz, B., and J. A. Campos-Ortega. (1994). Dorso-ventral polarity of the zebrafish embryo is distinguishable prior to the onset of gastrulation. *Roux's Archives* of *Developmental Biology* **203,** 374-380.

Schoft, V. K., A. J. Beauvais, C. Lang, A. Gajewski, K. Prüfert, C. Winkler, M. A. Akimenko, M. Paulin-Levasseur, and G. Krohne. (2003). The LAP2 isoforms b, y and w of zebrafish: developmental expression and behaviour during the cell cycle. *Journal of Cell Science* **116,** 2505-2517.

Segura-Totten, M., and K. L. Wilson. (2004). BAF: roles in chromatin, nuclear structure and retrovirus integration. *Trends in Cell Biology* **14,** 261-266.

Solnica-Krezel, L., and W. Driever. (1994). Microtubule arrays of the zebrafish yolk cell: organization and function during epiboly. *Development* **120,** 2443 -2455.

Somech, R., S. Shaklai, N. Amariglio, G. Rechavi, and A. J. Simon. (2005). Nuclear envelopathies--raising the nuclear veil. *Pediatric Research* **57**, 8R-15R.

Sprague, J., D. Clements, T. Conlin, P. Edwards, K. Frazer, K. Schaper, E. Segerdell, P. Song, B. Sprunger, and M. Westerfield. (2003). The Zebrafish Information Network (ZFIN): the zebrafish model organism database. *Nucleic Acids Research* **31,** 241–243.

Sprague, J., L. Bayraktaroglu, D. Clements, T. Conlin, D. Fashena, K. Frazer, M. Haendel, D. Howe, P. Mani, S. Ramachandran, K. Schaper, E. Segerdell, P. Song, B. Sprunger, S. Taylor, C. Van Slyke, and M. Westerfield. (2006). The Zebrafish Information Network (ZFIN): the zebrafish model organism database. *Nucleic Acids Research* **34,** D581-D585.

Stainier, D. Y. R. (2001). Zebrafish genetics and vertebrate heart formation. *Nature Reviews Genetics* **2,** 39-48.

Starr, D. A. (2007). Communication between the cytoskeleton and the nuclear envelope to position the nucleus. *Molecular Biosystems* **3**, 583-589.

Tokuko, H., T. Koujin, M. Segura-Totten, K. K. Lee, Y. Matsuoka,Y. Yoneda, K. L. Wilson, and Y. Hiraoka. (2001) BAF is required for emerin assembly into the reforming nuclear envelope. *Journal of Cell Science* **114**, 4575-4585.

Tsuchiya, Y. (2008). Till disassembly do us part: a happy marriage of nuclear envelope and chromatin. *Journal of Biochemistry* **143,** 155-161.

Tzfira, T., and V. Citovsky. (2005). Nuclear import and export in plants and animals. *Kluwer Academic/Plenum Publishers, London* **ISBN** 030648241X, 9780306482410.

Vlcek, S., T. Dechat, and R. Foisner. (2001). Nuclear envelope and nuclear matrix: interactions and dynamics. *Cellular and Molecular Life Sciences* **58,** 12-13.

Wagner, N., and G. Krohne. (2007). LEM domain proteins: new insights into Lamin-interacting proteins. *International Review of Cytology* **261,** 1-46.

Wagner, N., B. Kagermeier, S. Loserth, and G. Krohne. (2006). The drosophila melanogaster LEM domain protein MAN1. *European Journal of Cell Biology* **85,** 91-105.

Walker, S.J., T.J. Worst and K.E. Vrana. (2003). Drugs of Abuse. Semiquantitative Real-Time PCR for Analysis of mRNA levels. Methods in Molecular Medicine **ISBN** 978-1-58829-057-114.

Warga, R. M., and C. B. Kimmel. (1990). Cell movements during epiboly and gastrulation in zebrafish. *Development* **108,** 569-580.

Warga, R. M., and C. Nüsslein-Volhard. (1999). Origin and development of the zebrafish endoderm. *Development* **126,** 827-838.

Wilhelmsen, K., S. H. M. Litjens, I. Kuikman, N. Tshimbalanga, H. Janssen, I. Van den Bout, K. Raymond, and A. Sonnenberg. (2005). Nesprin-3, a novel outer nuclear membrane protein, associates with the cytoskeletal linker protein plectin. *The Journal of Cell Biology* **171**, 799-810.

Wilson, E. T., C. J. Cretekos, and K. A. Helde. (1995). Cell mixing during early epiboly in the zebrafish embryo. *Developmental Genetics* **17,** 6 -15.

Worman, H. J. (2005). Inner nuclear membrane and signal transduction. *Journal of Cellular Biochemistry* **96,** 1185-1192.

Worman, H. J., and J. C. Courvalin. (2000). The inner nuclear membrane. *Journal of Membrane Biology* **177**, 1-11.

Wu, W., F. Lin, and H. J. Worman. (2002). Intracellular trafficking of MAN1, an integral protein of the nuclear envelope inner membrane. *Journal of Cell Science* **115,** 1361-1371.

Xiao, H., and Y. Y. Zhang. (2008). Understanding the role of transforming growth factor-β signalling in the heart: overview of studies using genetic mouse models. *Clinical and Experimental Pharmacology and Physiology* **35,** 335-341.